University of Huddersfield Repository

Meramveliotaki, Aikaterini

Interaction of microwaves with organic and inorganic matter

Original Citation

Meramveliotaki, Aikaterini (2011) Interaction of microwaves with organic and inorganic matter. Masters thesis, University of Huddersfield.

This version is available at http://eprints.hud.ac.uk/id/eprint/17478/

Interaction of microwaves with organic and inorganic matter

Aikaterini Meramveliotaki

Thesis submitted in accordance with the requirements of the University of Huddersfield for degree of Doctor of Philosophy

July 2011

<u>Acknowledgments</u>

Many thanks to Professor Manfred Kroger for his very important advice and the corrections that he made for me throughout my PhD

Abstract

Microwaves interact with matter and they give rise to different phenomena to those induced by conventional heating. This is what gives rise to speculations about the possible existence of a "microwave effect". The objective of the work reported here has been to investigate the possibility of a microwave effect being responsible for microwave-induced solid state transformations in a variety of inorganic and bacterial materials.

This work consists of four parts. In the first part a theoretical explanation for the way in which microwaves interact with cellular materials is attempted, in which the cells are described by the Japanese model of multistratified shells. Unfortunately, the link between that model and the microwave effect is not achieved in this work.

In the second, the interaction of microwaves with bacteria is investigated experimentally, using a single mode cavity. Significantly, cases are found in the work when bacteria are quite probably killed at sub-lethal temperatures. Attempts are made to explain experimental results in which three different types of bacteria were irradiated namely *Salmonella Poona, Escherichia Coli* and *Staphylococcus Aureus*. The interactions of microwaves with bacteria are investigated through an extensive literature review. In the third, the interactions of microwaves with bacteria are investigated through an extensive literature review. In the fourth part, thermally-induced solid state transformations in which layered double hydroxides are converted to mixed metal oxides are investigated, again in a single mode cavity, in this case using a temperature/power feedback mechanism to control the sample temperature during the process. The most basic layered double hydroxide is hydrotalcite which contains magnesium (II) and aluminium (III). While hydrotalcite interacts with microwaves to some extent, it is found in this work that incorporation of certain transition metals, copper (II) for instance, enhances the interactions of the mixed hydroxides with microwaves, and, for materials incorporating these transition metal ions, significantly different transformations are induced in the microwave field compared to those induced in a conventional furnace at the same nominal temperature. These structural differences in the products of calcination of layered double hydroxides may have implications for the applications of these materials in catalysis and other fields.

CONTENTS

Part 1: Modelling of microwave interactions with bacteria

Part 2: Microwave irradiation of bacteria in rectangular waveguide

Part 3: Interaction of microwaves with bacteria and mechanisms of inactivation

Part 4: Thermal conversion of LDHs into oxides using microwaves and conventional heating

PART 1: MODELLING OF MICROWAVE INTERACTIONS WITH BACTERIA

1.1 Introduction

In this chapter the interaction of microwaves with microorganisms is investigated. The different factors that affect this interaction are examined and the different simulation techniques describing the interaction phenomena are outlined. The different geometries of cells are taken into consideration and the assumptions are made in order to describe the dependence of their relaxation spectra on frequency. The chapter also includes experimental results and modelling of the microwave sterilization process using different frequencies and different microbial samples. The different modelling techniques for simulating interactions are described and specific methods are detailed. 2-D and 3-D computational efforts are discussed using different cell shapes and sizes. In this model the cells are considered to consist of a number of stratums of different concentric shells, each of which has got its own dielectric properties. The difference in dielectric properties represents the different constituents of the cells (e.g. nucleus, organelles, etc).

The dielectric properties determine how the electric component of the field interacts with matter. Dielectric properties depend on temperature and frequency. In cases where these are well known then the electric field inside the cell should be calculated and linked with the killing effect of the microwaves.

1.2 Microwaves and food

There are several factors that influence the effect of microwaves on microorganisms in foods, like the intrinsic characteristics, i.e. pH moisture level, oxidation-reduction potential, nutrient content, antimicrobial constituents, biological structures, chemical composition of the shape and size of the bacteria carrying load, and extrinsic characteristics, i.e. temperature, humidity and gases of the environment,

frequency and intensity of the radiation, length of time of exposure, position in the effective field and other factors. Also the physical and the chemical composition of the microorganisms being irradiated and their stage of existence (moist or wet, spore, etc) and numbers present are also important factors. It was observed that microwave radiation can destroy several microorganisms including *E. Coli, Salmonella, L. Monocytogenes, S. Aureus*. This is probably due to the thermal effect induced by the microwaves. A theory that requires the bacteria to absorb electromagnetic radiation due to the difference in their dielectric properties from the medium/carrier, however this theory was proved to be wrong. The factors that affect the reduction of bacteria are: frequency, power output level, time and pulsed power.

1.3 Microbiological behaviour in electromagnetic fields

There are three major mechanisms that have been observed to modify the contribution of water to total dielectric activity, namely:

a) dissolved ions, which depress the dielectric constant and elevate the dielectric loss to values similar to water that are predicted by the Haster-Debye models.

b) displacement, where insoluble and immiscible constituents depress the dielectric constant and loss in aqueous mixtures and this is linked to lipid, protein and carbohydrate constituents in suspensions with water. The model that predicts this behaviour is Fricke model.

c) interaction, where interactive constituents such as alcohols or sugars shift the critical wavelength of the aqueous mixtures to wavelengths intermediate to those of their pure component. The predictive model is called Maxwell – Debye in this case (Mudgett and others 1974).

Grant (1957) has observed modifications to the dielectric behaviour of water by dissolved proteins, that is regions of dispersion for bound water which exist below

these for free water and may be contribute to the dielectric behaviour at microwave frequencies depending on the critical frequency and magnitude of such relaxations. The general effects of dissolved proteins are similar to those of dissolved salts.

These considerations suggest a generalized physiochemical model for the dielectric behaviour of liquid and semisolid microorganisms based on observed interactions of food constituents with water.

 When the frequencies are of the order of 10^6 to 10^8 Hz, free surface charge effects can result in relaxation of dissolved proteins to give twisting, bending and rotation of molecular segments.

   The prediction of dielectric behaviour in semisolid foods is also affected by the biological structure. Semisolid microorganisms are highly differentiated multicellular tissues with solid and liquid phases of diversity.

1.4 Numerical modelling techniques for simulating interactions

1.4a Method of Lines (MoL)

 This is a relatively new numerical method and it can be used to obtain the power density distribution in a dielectric material by solving directly for the electric field in three dimensional space. In this method, the progress of a wave is simulated as it propagates in the loaded cavity. This model uses the fact that Maxwell's equations can be solved for transmission lines (or the specific path of an energy wave). The oven cavity space and the load are represented by an assemblage of conducting wires and electrical components (simulating transmission lines) arranged in a three dimensional matrix.

If an electrical impulse is injected at a point in the network, its passage through the network can be calculated. The electric and magnetic fields described by Maxwell's equations are equivalent to the currents and voltages on each transmission line. The

reflecting surfaces are represented by short circuit connections (wires) and dielectric materials by reactive components (i.e. combinations of resistive, capacitive, or inductive components) (Lorenson 1990).

Essentially, MoL is a well known technique for solving parabolic type partial differential equations and it proceeds by leaving the derivatives along one chosen axis untouched (usually in time), while all other partial derivatives (usually in space) are discretized using well known strategies that include the finite difference, finite element, or finite volume techniques. The system is thereby reduced from its partial differential form to a system of ordinary differential equations that can be solved numerically by standard procedures (Zhao and others 1996).

1.4b Finite Element Method (FEM)

This method is applicable to solving Maxwell's equations in the frequency domain and it yields sets of linear equations from which the solution can be time-stepped, or alternatively, it provides sets of linear equations that can be solved for harmonic solutions, or sets of equations to determine the Eigenmodes of a system. A key advantage of the finite element method is that it can be applied for an unstructured grid. It also makes better approximations of material properties that vary through a computational grid cell. This method has been extended by researchers to the three-dimensional electromagnetic problems (Lorenson 1990).

In the finite element method, the solution to partial differential equations is approximated with the summation of known functions with unknown coefficients.

In the case of a microwave loaded cavity, the calculation of the electric field starts by making a finite element model of the cavity, which is a three-dimensional space that can have various sizes of shapes. For example, in regions where the wavelength is short (in food for example), the elements have to be small (<3 mm) while in other parts of the cavity the wavelength is longer (a typical dimension for the elements can

be ~ 30 mm). In most cases the elements are rectangular prisms, but different shapes can be used so as to conform to the boundaries of the bacteria/microorganisms. In principle, very small elements could be used for the entire region to be modelled.

1.4c Finite Difference Time Domain Method (FDTD)

Integral equations can deal with material and structural complexity, but their need to construct and solve systems of linear equations limits the electrical size of possible models, especially those requiring detailed treatment of geometric detail within a volume, as opposed to just surface shape. The FE-TD method gives frequency-domain integral equation solution to Maxwell's equations and it generates sparse rather than dense matrices. Even more, it is difficult to use for material and device non linearities. All these problems led to a new approach, which is the FD-TD method, introduced by Yee 1966. The main reasons for the interest in FDTD are that first of all, FDTD doesn't use any linear algebra, therefore doesn't limit the number of the electromagnetic unknowns. In the case of FE-TD this number is generally fewer than 10^6 while in the case of FDTD it can be 10^9, taking into consideration that there is no upper bound to this number.

Being a time domain technique, it can calculate the impulse response of an electromagnetic system. Therefore, a single FDTD simulation can provide either ultrawideband temporal waveforms or the sinusoidal steady-state response at any frequency within the excitation spectrum. For the same reason, FDTD can calculate the non linear response of an electromagnetic system and the specification of a new structure to be modelled is reduced to a problem of mesh generation rather than to the reformulation of a complex integral function.

In this approach a three dimensional mesh can be constructed in the volume of interest. The targeted object is "decomposed" in many small three-dimensional blocks of dielectric material with its assigned properties. Each cell has a set of

magnetic and electric field components associated with it and the propagation and scattering of the incident field is simulated by time-stepping a set of finite difference approximations of Maxwell's equations (Lorenson 1990). The FDTD method is quite versatile with respect to the choice of either the electric or magnetic field as the source of heating and the range of values of the dielectric that it can handle.

1.5 Computational modelling of electromagnetic field/bacteria interactions

Zhang and others (2001) used two separate programs together with specially written modules in order to couple the programs that solved Maxwell's and heat conduction equations. Spatial distributions of thermal time, representing sterilization were studied from combining time-temperature history and first order kinetics. In the case of microwaves as the material is heated its dielectric properties change and as a result the electric field and the heat generation at a particular location change. These spatial temperature variations give rise to the spatial variation of the time-temperature history and thus of the thermal effects on bacteria, nutrients and biochemical reactions. During sterilization there are three main concerns: destruction of pathogenic microorganisms, avoid degradation of nutrients and avoid altering the characteristics of food. The destruction and degradation rates of microorganisms are usually described as first order reactions obeying the equation:

$-\dfrac{dc}{dt} = k_b c$ where k_b is the reaction rate constant which is a function of

temperature, c is the concentration of a food component at time t.

Food technologists use the heating time, F_0, which provides the same final concentration when the temperature, T, is constant at a reference temperature, T_R (usually chosen as 121^oC). Using this definition, F_0 can be expressed as:

$$F_0^b = \frac{\ln\left(c_i/c\right)}{k_{b,T_R}} = \frac{k_0 \int\limits_0^t \exp\left(-E_{a,b}/RT\right)dt}{k_0 \exp\left(-E_{a,b}/RT_R\right)} = \int\limits_0^t \exp\left[\frac{E_{a,b}}{R}\left(\frac{1}{T_R}-\frac{1}{T}\right)\right]dt \quad (1)$$

where again $E_{a,b}$ is the activation energy for bacteria killing and R is the universal gas constant. From a food microbiological safety consideration, the lowest value of F_0^b anywhere in the targeted load of its pathogenic spore-former needs to be above a certain value. When this is true, the load is considered to be commercially sterile.

Goldblith and others (1967) exposed *E.Coli* and *B. Subtilis* spores to fixed frequency microwaves (2450 MHz). They were placed in the geometric centre of the cavity and data obtained was plotted according to the Arrhenius equation:

$$k = Ae^{-\frac{\Delta E}{RT}} \qquad\qquad (2)$$

The rate of inactivation of bacteria obeys first order kinetics according to the equation:

$$dN/dt = -kN \qquad\qquad (3)$$

when its deactivation is due only to heat. By using the method of separation of variables the above equation gives:

$$-\int\limits_{N_0}^{N}\frac{dN}{N} = \int\limits_0^t k\,dt \ . \qquad\qquad (4)$$

The graphical integration of equation (3) predicts the degree of inactivation during transient heating. Mc Ree's formula uses the temperature increase to evaluate the microwave energy absorption:

$$\Delta T = 0.185P(1 - e^{-0.01t}), \hspace{4cm} (5)$$

where ΔT is the temperature increase (degrees Celsius) of the specimen during time t; P is the incident microwave energy in units of milliwatts per centimetre squared; and t is the time of exposure in minutes. In this equation, the parameter 0.185, in units of degrees Celsius per minute per milliwatt per centimetre squared, is defined as "a measure of the absorbing characteristics of the specimen". This equation is applicable only to biological materials that contain certain quantities of water. Water has a much greater loss factor at 2450 MHz, so it absorbs most (98%) of the microwave energy. According to McRee's equation, ΔT for the experiment described is as follows: $T = 0.185 \times (10^7/10^3) (1 - e^{-0.1x0.1667}) = 30.5^{\circ}$ C. The observed values ranged from 29 to 36 $^{\circ}$C and averaged 32.5° C for 14 measurements. On the other hand, when the specimen was dry, the observed value was $\Delta T = 0$ for exactly the same time energy exposure. This clearly shows that, in the absence of water, fixed microwave energy at 2450 MHz is not absorbed, at least by biological material in the form of bacterial cells. The data presented here supports the fact that, in the absence of water, biological specimens, i.e., microbial cells are not damaged. McRee's time-temperature profiles are due to energy absorption by water in the biological specimen and not by the specimen (Vela and Fu 1979). Proteins in all living cells are surrounded by an aqueous atmosphere which is believed to be the site of specific action of electromagnetic radiation (Prausnitz and others 1951). These specific thermal effects, which for example could be the preferential localized heating, are a result of variation in relaxation frequency of water, which is determined by the structure of the water molecule. Studies have revealed that a

certain degree of water binding can shift the relaxation frequency of pure water close to 2.45 GHz. Khalil (1987), proved that microwaves at 2.45 GHz cause the membrane of Staphylococcus Aureus and Bacillus Stereothermopilus to rupture. It was this cell wall breakage after microwave heating that supported the hypothesis of inhomogeneous wave distribution in the cell's microenvironment. These high frequency fields create temperature gradients. Some of the cellular components that seem to be more vulnerable to microwave energy are the cell wall, the membrane lipids and the cell ribonucleic acid components.

Microwaves are *non-destructive* electromagnetic radiation. They are selectively absorbed by the microorganisms which reside in food and each different cell behaves like a dielectric material. A dielectric material is one that contains particles which polarize under the influence of an applied electric field. These charges are bound within the material and can only move short distances when the field is applied, the negative and positive ones moving in opposite directions to form induced dipoles.

In a uniform AC electric field of angular frequency ω, an ellipsoidal particle experiences a frequency dependent alignment torque, which tends to orient one of the principal axes with the field. Which particular axis of the particle aligns depends on the frequency. There are the two main polarisation mechanisms that are dominant in the microwave frequency spectrum: the orientational and the interfacial (Maxwell-Wagner).

The charge distribution around a particle can be described by introducing the concept of polarizability. Polarizability is defined as the measure of the ability of a material to respond to a field (polarise) but it is also a measure of the ability of a material to produce charge at interfaces. The polarizability is a complex quantity given by:

$$\mathbf{P} = \varepsilon_0 \left(\frac{\tilde{\varepsilon}}{\varepsilon_0} - 1 \right) \mathbf{E} \qquad (6)$$

Where $\tilde{\varepsilon}$ is the complex permittivity of the dielectric given by $\tilde{\varepsilon} = \varepsilon_0 \varepsilon_r - i\,{}^{\sigma}\!/\!{}_{\omega}$ (ε_r: dimensionless number referred to as relative permittivity of dielectric and ε_0 is the permittivity of free space which is 8.854 x 10^{-12} Fm^{-1}, σ is the conductivity of the dielectric). In real systems there is a suspension of spherical dielectric particles in a dielectric fluid and when a field is applied to the system surface charge accumulates at discontinuities (or interfaces) between the dielectrics due to the differences in electrical properties. Since the polarizabilities of each dielectric are frequency dependent, the magnitude of the surface charge is also frequency dependent and the total complex permittivity of the system exhibits dispersions that are due to the polarisation of the interfaces (Morgan and others 2003). This is referred to as the *Maxwell Wagner interfacial* polarisation and is true irrespective of the geometry of the system. When an electric field is applied to a dielectric particle suspended in a dielectric fluid medium, the charge of opposite sign accumulates at either side of the particle. This gives rise to a dipole around the particle. This *induced* or *effective dipole moment* depends on the properties of both the particle and the suspending medium and on the frequency of the applied field. In the simplest case, a uniform electric field is applied antiparallel to the *z*- axis, i.e. **E** = -E**z** in a homogeneous dielectric medium where a solid dielectric sphere of radius a is suspended. The applied field is a harmonic of single frequency ω and the dipole moment of the sphere and is given by:

$$\mathbf{p} = 4\pi\varepsilon_m \left(\frac{\tilde{\varepsilon}_p - \tilde{\varepsilon}_m}{\tilde{\varepsilon}_p + 2\tilde{\varepsilon}_m} \right) a^3 \mathbf{E} \tag{7}$$

This is the effective dipole of the sphere where *m* stands for medium and *p* for particle and α is the polarizability.

The relaxation time of the *effective* permittivity or polarizability of the particle is equal to:

$$\tau_{MW} = \frac{\varepsilon_p + 2\varepsilon_m}{\sigma_p + 2\sigma_m} \qquad\qquad (8)$$

The angular frequency $\omega_{MW} = 2\pi f_{MW} = 1/\tau_{MW}$ is often referred to as the Maxwell-Wagner relaxation frequency since the dispersion of the dipole moment is caused by interfacial polarisation. Clausius-Mossoti factor describes the frequency dependence of the magnitude of the polarizability of a particle and as a consequence of the effective dipole moment. The real part of the Clausius-Mossotti factor reaches a low frequency limiting value of $\left(\sigma_p - \sigma_m\right)\big/\left(\sigma_p + 2\sigma_m\right)$ i.e. depends only on the conductivity of the particle and suspending medium. Conversely, the high frequency limiting value is $\left(\varepsilon_p - \varepsilon_m\right)\big/\left(\varepsilon_p + 2\varepsilon_m\right)$ and the polarisation is dominated by the permittivity of the particle and the suspending medium. In the case of non-uniform fields, the uniform field solution of the dipole moment can still be used with the assumption that the dimensions of the sphere are small compared to the distance associated with the non-uniformity of the field, i.e. the electric field is considered to be uniform across the particle.

$$\tilde{f}_{CM}\left(\tilde{\varepsilon}_p, \tilde{\varepsilon}_m\right) = \frac{\tilde{\varepsilon}_p - \tilde{\varepsilon}_m}{\tilde{\varepsilon}_p + 2\tilde{\varepsilon}_m} \qquad\qquad \text{Clausius-Mossoti factor}$$

Each axis of the particle has an associated relaxation time, given by:

$$\tau_n = \frac{A_n \varepsilon_p + (1 - A_n)\varepsilon_m}{A_n \sigma_p + (1 - A_n)\sigma_m} \tag{9}$$

where A_n is the depolarizing factor.

1.6 Modelling of electromagnetic field interactions with bacteria cells

Kakutani and others (1992) derived theoretical expressions for the electrorotation for an ellipsoidal cell model with an arbitrary number of con-focal shells. The theory for a spherical model with an arbitrary number of shells is a special case of this model theory.

The authors consider an ellipsoidal multishell cell model immersed in a continuous medium. The complex dielectric constant of the external medium is ε_n^* and there are *n-1* shells, which have a complex dielectric constant assigned to each. The dielectric constant is given by:

$$\varepsilon_i^* = \varepsilon_i - j\left(\frac{k_i}{\omega}\right) \quad i = 1, 2, 3, ..., n \tag{10}$$

where ε_i and k_i are the dielectric constant and conductivity respectively of the *i*th phase. The following assumptions were made:

i) the cell is electrically isotropic

ii) the dielectric constant of each phase is independent of frequency

The surfaces of the cells are represented by n confocal ellipsoids therefore the thickness of each shell varies all over the surface.

$\overline{\varepsilon}_{1a}^{*}$ is the effective complex dielectric constant of the multishelled ellipsoid along the α ($\alpha = x, y$) axis. It is given by:

$$\overline{\varepsilon}_{1a}^{*} = \varepsilon_1^{*} \frac{\varepsilon_1^{*} + \left(\varepsilon_2^{*} - \varepsilon_1^{*}\right)\left[A_{ia} + v_1\left(1 - A_{0a}\right)\right]}{\varepsilon_1^{*} + \left(\varepsilon_2^{*} - \varepsilon_1^{*}\right)\left(A_{1a} - v_1 A_{0a}\right)} \qquad \alpha = x, y \qquad (11a)$$

with

$$\overline{\varepsilon}_{ia}^{*} = \varepsilon_i^{*} \frac{\varepsilon_M^{*} + \left(\varepsilon_{i+1}^{*} - \varepsilon_i^{*}\right)\left[A_{ia} + v_i\left(1 - A_{i-1,a}\right)\right]}{\varepsilon_i^{*} + \left(\varepsilon_{i+1}^{*} - \varepsilon_i^{*}\right)\left(A_{ia} - v_i A_{i-1,a}\right)} \qquad \alpha = x, y \qquad (11b)$$

$$v_i = \frac{a_i b_i c_i}{a_{i-1} b_{i-1} c_{i-1}} \qquad i = 1, 2, 3,..., \ n\text{-}1 \qquad (12)$$

In these equations A_{ix} and A_{iy} $(i = 1, 2, 3,..., \ n\text{-}1)$ are the depolarizing factors along the x and y axes respectively, and are given by (T. Kakutani, S. Shibatani and M. Sugai, 1992):

$$A_{ix} = 0.5 a_i b_i c_i \int_0^{\infty} \frac{d\xi^2}{(a_i^2 + \xi) R_i} \qquad (13)$$

$$\text{A}_{iy} = 0.5 a_i b_i c_i \int_0^\infty \frac{d\xi^2}{(b_i^2 + \xi) R_i} \tag{14}$$

with

$$R_i = \left[\left(a_i^2 + \xi \right)\left(b_i^2 + \xi \right)\left(c_i^2 + \xi \right) \right]^{1/2} \tag{15}$$

$$\xi_i = \left(r_i \big/ r_{i-1} \right)^3 \qquad \text{i = 1, 2, 3,..., n-1} \tag{16}$$

Asami and others (1980), considered a shelled ellipsoid immersed in a continuous medium and the complex dielectric constants of the outer medium, the shell phase and the interior of the ellipsoid are denoted by $\varepsilon_0^*, \varepsilon_s^*$ and ε_i^* respectively. The outer and the inner surface of the ellipsoid were represented by two confocal ellipsoids therefore the shell thickness is not necessarily uniform all over the surface. Asami and others (1980) introduce an ellipsoidal coordinate system by taking the outer surface of the shelled ellipsoid as a standard ellipsoid whose semi-axes are a_0, b_0, c_0.

The equivalent complex dielectric constant of the suspension ε^* as:

$$\frac{\varepsilon^* - \varepsilon_0^*}{\varepsilon^* + 2\varepsilon_0^*} = \frac{1}{9} \Phi \sum_{k=x,y,z} \frac{\overline{\varepsilon}_k^* - \varepsilon_0^*}{\varepsilon_0^* + \left(\overline{\varepsilon}_0^* - \varepsilon_0^* \right) A_{0k}} \tag{17}$$

where

$$\Phi = \frac{N a_0 b_0 c_0}{R^3} \qquad\qquad (18)$$

When the ellipsoid degenerates into a sphere, we have $a_0 = b_0 = c_0$ and all the factors A_{sk}'s have a value of 1/3.

Irimajiry and others (1979) presented a model of complex dielectric constant (ε^*) of suspension for "multistratified" spherical particles. That was in an attempt to interpret the complicated dielectric behaviour that suspensions of lymphoma cells displayed when measured in a frequency range of 0.01 – 100 MHz. The idea of the multistratified model is that each region of the cell (cell wall, membrane, cytoplasm, nucleic membrane, nucleus, etc) can be modelled as a shell around a sphere. Based on Maxwell's theory of interfacial polarization, a general expression which relates ε^* with the electrical and geometrical parameters of each stratum was derived.

The following assumptions were made:

i)   the cells are spherical particles
ii) the suspension of the particles is uniformly dispersed in the volume
iii) concentration is small enough so that the mutual polarization effect can be ignored
iv) the equation which gives the complex dielectric constant in heterogeneous systems holds for any suspension system in which the dispersed particles can be regarded as homogeneous but actually have a stratified structure

The main advantage of this model is that within the outer shell (i.e. the plasma membrane), another shell phase (i.e. nuclear membrane) demarcates a mass of nucleoplasm from the rest of cytoplasm in the lymphoid cell interior.

Such a "multi-stratified" system gives rise to multiple dielectric dispersions, the number of which corresponds to the number of interfaces lying between successive shell phases. Each region of the model is assigned an electrical permittivity and conductivity. The overall dielectric properties of the cell are then calculated mathematically. Since the model and indeed the cell, is made up of several regions there will be interfacial (Maxwell – Wagner) dispersions at each interface. Additionally, it is possible to add frequency dependent permittivities or conductivities to each cell if a known relaxation occurs in that part of the cell within the frequency range of interest. The dielectric dispersion can be decomposed into its "unit" dispersions characterized by the respective relaxation times τ_k's. Given a system of n shells that enwrap the central core, $n+1$ different relaxation times. Irimajiry and others (1979) combined the mathematical expression of the equivalent dielectric constant of a heterogeneous system (Maxwell 1891) with that of the homogeneous constant for any ith sphere inside the whole sphere. Their ultimate goal was to derive an equation for ε^* as a function of jω, which is, obtain a general formula of ε^* through which one can predict the frequency dependence of ε and k. That expression is:

$$\varepsilon^* = E + \sum_{k=1}^{n+1} \frac{L_k}{1 + j\omega\tau_k} + \frac{K}{j\omega\varepsilon_v} \qquad (19)$$

where:

E = limiting dielectric constant at high frequencies (ε_h)

K = limiting conductivity at low frequencies (k_1)

τ_k = relaxation time of kth "unit" dispersion

L_k = dielectric increment associated with the kth "unit" dispersion ($\Delta\varepsilon_k$)

The next step is to calculate the interaction of the bacteria with a microwave based electromagnetic field. This can be done by using the finite element method to solve Maxwell's equations in model geometry.

1.7 Effect of shape-introduction of depolarizing factor

In order to examine the *effect of the shape* of dispersed biological cells on the dielectric behaviour of suspensions, eq. (19) is calculated with phase parameters relevant to biological cells such as $\varepsilon_0 = 0$, $\varepsilon_s = 6.5$, $\varepsilon_i = 50$, $k_0 = 2.5$ ms/cm, $k_i = 2.5$ ms/cm, $\Phi = 0.1$. Assuming that the shell has uniform thickness:

$$v = \frac{(a_0 - d)(b_0 - d)(c_0 - d)}{a_0 b_0 c_0} \tag{20}$$

Where d is the thickness of the plasma membrane. Since biological cells are covered with a plasma membrane that has a negligible thickness compared with the cell diameters the axial ratio for the outer surface of the shell is nearly equal to that of the inner surface, therefore $A_{0k} = A_{1k}$. For further simplification we assume that $a_0 \neq b_0 = c_0$. For the spheroid the depolarization factors $A_{ok}'s$ reduce to the following integral forms:

$$A_{0x} = \frac{a_0 b_0^2}{3} \int_0^\infty \frac{d\xi}{\left(a_0^2 + \xi\right)^{\frac{3}{2}} \left(b_0^2 + \xi\right)} \tag{21}$$

$$A_{0y} = A_{0z} = \frac{1}{2}(1 - A_{0x})$$
(22)

For *prolate spheroids* with $a_0 > b_0 = c_0$ and $q_0 = \dfrac{a_0}{b_0}$ (q_0: axial ratio for the outer surface of the shell):

$$A_{0x} = -\frac{1}{q_0^2 - 1} + \frac{q_0}{(q_0^2 - 1)^{3/2}} \ln\left\{q_0 + (q_0^2 - 1)^{1/2}\right\}$$
(23)

And for the *oblate spheroids* with $a_0 < b_0 = c_0$,

$$A_{0x} = \frac{1}{1 - q_0^2} + \frac{q_0}{(1 - q_0^2)^{3/2}} \arccos q_0$$
(24)

A value of 50 A is assumed for the thickness d of the shell. All spheroids with a varying axial ratio q_0 have the same volume as that of the sphere of radius 5 μm.

It is predicted that the dielectric dispersion curves of biological cell suspensions is strongly influenced by varying the cell shape (Asami and others 1980). Both limiting values of dielectric constant ε_l and conductivity k_l at low frequencies are dependent particularly on the axial ratio q. Another effect of cell shape on the dielectric dispersion is broadening of the dispersion curve against frequency. This feature is visualized in complex plane plots. The plots of the suspension of spheres show a semi-circle corresponding to a system with a single relaxation time, while the plots for prolate ellipsoids show a remarkable deviation from the semicircle. Suspensions

of oblate spheroids show circular arcs with slightly depressed centres. This may be formally explained by the distribution of relaxation times, *for which the reason is not completely clear.* Numerical calculations show that the cell shape is one of the factors that cause broadening of the dielectric dispersion.

Kakutani and others (1992) derived the general expressions for multishelled ellipsoids. Here, the geometry of the cell changes. The shelled-sphere model can be modified to take into account simple non-spherical particles such as prolate and oblate ellipsoids (discs and rods). The difference in shape is catered for by the "depolarization factor" that appears in the Claussius – Mossoti factor, which, in turn, determines the dielectric properties of a particle in a suspending medium. The assumptions made in this model are:

i) the cell is electrically isotropic
ii) the dielectric constant of each phase is independent of frequency
iii) the outermost surface of the shelled ellipsoid is a standard ellipsoid
iv) the shell has uniform thickness

The surfaces of the shells are represented by *n* confocal ellipsoids.

1.8a The single shell model (Model 1)

In this model the cell is considered as a homogeneous ellipsoid surrounded by a single shell (membrane). Its effective dielectric constant of the ellipsoid along the a(a = x, y) axes and is given by:

$$\bar{\varepsilon}_{1a}^{*} = \varepsilon_{M}^{*} \frac{\varepsilon_{M}^{*} + \left(\varepsilon_{I}^{*} - \varepsilon_{M}^{*}\right)\left[A_{1a} + v_{1}\left(1 - A_{0a}\right)\right]}{\varepsilon_{M}^{*} + \left(\varepsilon_{I} - \varepsilon_{M}\right)\left(A_{1a} - vA_{0a}\right)} \qquad a = x, y \qquad (25)$$

$$v_1 = \frac{a_1 b_1 c_1}{a_0 b_0 c_0} \tag{26}$$

where the subscripts M and I indicate the membrane and intracellular phases respectively. The A_{0a} and A_{1a} are the depolarizing factors, given by :

$$A_{ix} = 0.5 a_i b_i c_i \int_0^\infty \frac{d\xi}{(a_i^2 + \xi) R_i} \tag{27}$$

$$A_{iy} = 0.5 a_i b_i c_i \int_0^\infty \frac{d\xi}{(b_i^2 + \xi) R_i} \tag{28}$$

with $R_i = \left[(a_i^2 + \xi)(b_i^2 + \xi)(c_i^2 + \xi) \right]^{1/2}$ (29)

1.8b The two-shell model (Model 2)

In this model an additional cell is assumed on the surface of the ellipsoidal single-shell model. In this case:

$$\overline{\varepsilon}_{1a}^* = \varepsilon_W^* \frac{\varepsilon_W^* + \left(\varepsilon_{2a}^* - \varepsilon_W^* \right) \left[A_{1a} + v_1 (1 - A_{0a}) \right]}{\varepsilon_W^* + \left(\varepsilon_{2a}^* - \varepsilon_W^* \right) \left(A_{1a} - v_1 A_{0a} \right)} \qquad a = x, y \tag{30}$$

$$\bar{\varepsilon}_{2a}^{*} = \varepsilon_{M}^{*} \frac{\varepsilon_{M}^{*} + \left(\varepsilon_{I}^{*} - \varepsilon_{M}^{*}\right)\left[A_{2a} + v_{2}\left(1 - A_{1a}\right)\right]}{\varepsilon_{M}^{*} + \left(\varepsilon_{I}^{*} - \varepsilon_{M}^{*}\right)\left(A_{2a} - v_{2}A_{1a}\right)} \qquad a = x, y \qquad (31)$$

$$v_{1} = \frac{a_{1}b_{1}c_{1}}{a_{0}b_{0}c_{0}} \qquad (55a) \qquad\qquad v_{2} = \frac{a_{2}b_{2}c_{2}}{a_{1}b_{1}c_{1}} \qquad (31b)$$

where the subscripts W, M and I indicate the outer cell (cell wall), the inner cell (membrane) and the internal phase respectively. This ellipsoidal two-shell model was proposed by Asami and others (1980) who interpreted the dielectric behaviour of *E. coli* suspensions using the theory based on this model and is also applicable to other bacterial cells with cell walls.

1.8c The three cell-model (Model 3)

In this model a second shell-covered confocal ellipsoid is assumed inside the single-shell ellipsoid (model 1).

$$\bar{\varepsilon}_{1a}^{*} = \varepsilon_{M}^{*} \frac{\varepsilon_{M}^{*} + \left(\varepsilon_{2a}^{*} - \varepsilon_{M}^{*}\right)\left[A_{1a} + v_{1}\left(1 - A_{0a}\right)\right]}{\varepsilon_{M}^{*} + \left(\varepsilon_{2a}^{*} - \varepsilon_{M}^{*}\right)\left(A_{1a} - v_{1}A_{0a}\right)} \qquad a = x, y \qquad (32a)$$

$$\bar{\varepsilon}_{2a}^{*} = \varepsilon_{C}^{*} \frac{\varepsilon_{C}^{*} + \left(\varepsilon_{3a}^{*} - \varepsilon_{C}^{*}\right)\left[A_{2a} + v_{2}\left(1 - A_{1a}\right)\right]}{\varepsilon_{C}^{*} + \left(\varepsilon_{3a}^{*} - \varepsilon_{C}^{*}\right)\left(A_{2a} - v_{2}A_{1a}\right)} \qquad a = x, y \qquad (32b)$$

$$\bar{\varepsilon}_{3a}^{*} = \varepsilon_{TM}^{*} \frac{\varepsilon_{TM}^{*} + \left(\varepsilon_{I}^{*} - \varepsilon_{TM}^{*}\right)\left[A_{3a} + v_{3}\left(1 - A_{2a}\right)\right]}{\varepsilon_{TM}^{*} + \left(\varepsilon_{I}^{*} - \varepsilon_{TM}^{*}\right)\left(A_{3a} - v_{3}A_{2a}\right)} \qquad a = x, y \qquad (32c)$$

$$v_i = \frac{a_i b_i c_i}{a_{i-1} b_{i-1} c_{i-1}} \qquad i = 1, 2, 3 \qquad (33)$$

where the subscripts M, C, TM and I indicate the plasma membrane, the cytoplasm the intracellular membrane and the internal medium respectively.

1.8d The four-shelled model (Model 4)

The four-shell model is a second shell-covered confocal ellipsoid assumed inside the two-shelled ellipsoid (model 2). In this model the fourth shells and the interior phase of it correspond to the cell wall, the plasmas membrane, the cytoplasm, the tonoplast membrane and the interior of vacuole respectively and are denoted by the subscripts W, M, C, TM and I. Therefore:

$$\overline{\varepsilon}^*_{1a} = \varepsilon^*_W \frac{\varepsilon^*_W + \left(\varepsilon^*_{2a} - \varepsilon^*_W\right)\left[A_{1a} + v_1\left(1 - A_{0a}\right)\right]}{\varepsilon^*_W + \left(\varepsilon^*_{2a} - \varepsilon^*_W\right)\left(A_{1a} - v_1 A_{0a}\right)} \qquad a = x, y \qquad (34a)$$

$$\overline{\varepsilon}^*_{2a} = \varepsilon^*_M \frac{\varepsilon^*_M + \left(\varepsilon^*_{3a} - \varepsilon^*_M\right)\left[A_{2a} + v_2\left(1 - A_{1a}\right)\right]}{\varepsilon^*_M + \left(\varepsilon^*_{3a} - \varepsilon^*_M\right)\left(A_{2a} - v_2 A_{1a}\right)} \qquad a = x, y \qquad (34b)$$

$$\overline{\varepsilon}^*_{3a} = \varepsilon^*_C \frac{\varepsilon^*_C + \left(\varepsilon^*_{4a} - \varepsilon^*_C\right)\left[A_{3a} + v_3\left(1 - A_{2a}\right)\right]}{\varepsilon^*_C + \left(\varepsilon^*_{4a} - \varepsilon^*_C\right)\left(A_{3a} - v_3 A_{2a}\right)} \qquad a = x, y \qquad (34c)$$

$$\overline{\varepsilon}^{*}_{4a} = \varepsilon^{*}_{TM} \frac{\varepsilon^{*}_{TM} + \left(\varepsilon^{*}_{I} - \varepsilon^{*}_{TM}\right)\left[A_{4a} + v_{4}\left(1 - A_{3a}\right)\right]}{\varepsilon^{*}_{TM} + \left(\varepsilon^{*}_{I} - \varepsilon^{*}_{TM}\right)\left(A_{4a} - v_{4}A_{3a}\right)}$$

a = x, y (34d)

$$v_{i} = \frac{a_{i}b_{i}c_{i}}{a_{i-1}b_{i-1}c_{i-1}} \qquad i = 1, 2, 3, 4$$

CONCLUSIONS

Microwaves have a killing effect on microorganisms by elevating their temperature slightly with respect to the surrounding medium. The factors that affect the bacteria reduction are: frequency, power output level, time and pulsed power. The last was shown to severely damage the cell membrane and the metabolic rate of cells at early stages of cell growth without causing temperature elevation. Therefore it is more effective when it comes to the destruction of such microorganisms.

The interactions of microwaves with living organisms were described at a cellular level by considering the cells to be multistratified ellipsoids or spheres. The case of spheres is a degeneration of the ellipsoid one. This model of cells gives rise to multiple dielectric dispersions. Both numerical modelling and computational simulation techniques are explained together with their application on different shape and sizes of 2-D and 3-D bacteria configurations.

PART 2: EXPERIMENTAL RESULTS OF MICROWAVE IRRADIATION OF BACTERIA IN RECTANGULAR WAVEGUIDE

2.1 Introduction

Food is composed of a loosely woven nest of large proteins, carbohydrates and other organic materials. Water molecules float freely among the materials, and like sub-microscopic magnets they have positive and negative ends, they are polarised). Alternating microwave fields spin the water molecules at high rates, thus causing friction. The heat of friction is transferred to the surrounding food molecules as heat and the food cooks Alcamo (1994). Microwaves have some advantages as compared to conventional conduction and convection heating processes. Microwaves offer a potential for rapid heat penetration, reduced processing times, and, hence, increased production rates, more uniform and volumetric heating (microwaves excite the water molecules throughout the food simultaneously, depending on the penetration depth) lower surface temperatures and improved nutrient and flavour retention.

Industrial production of foodstuffs requires, from harvesting of the raw materials to consumption, adopted methods for keeping the qualities during storage, dispatching and shelf-laying just before consumption. The new developments towards fresh-like and ready meals for the changing customer habits, has induced also considerable interest in electromagnetic energies for pasteurization and sterilization processes. Successful application of these energies, even in combination with the conventional energies, demand a multi-disciplinary approach: electromagnetic engineering, food technology, microbiology etc.

Electromagnetic energy (EME) is carried by wave like electric and magnetic fields which propagate from its source at the speed of light. EME of frequency 2.45 GHz (microwave frequency of the domestic oven) has a wavelength λ = 12.2 cm in free space but inside materials the EME slows down and loses its energy when the

material is lossy (like food). The wavelength in such a material is $\lambda/\sqrt{\varepsilon'}$, λ is the wavelength in free space. The power density of the microwaves decreases smoothly as the distance to its source decreases and lossy materials have a non zero ε'' therefore they absorb EME so that the power density decreases more rapidly. Microwaves spread out over large surfaces. Walter Van Loock (1996). Pasteurization can be considered as a heat treatment for making the food safe and to extend shelf life by killing the most common microorganisms. The temperature range is 60 to 100 ^{o}C and the temperature is applied for a certain period of time. Sterilization is more difficult to define. Sterilization is roughly the killing of microorganisms left over if pasteurization has been applied. Most sterilization processes are performed at T > 100 ^{o}C but more and more at T > 120 ^{o}C during short times. In conventional pasteurization and sterilization processes, the heat transfer is by conduction and convection and the processes are complicated in particular for non-liquid and heterogeneous foodstuffs. Some problems are: bad surface heat transfer, no or poor convection with solid food and solid foods in liquids and also with viscous liquids, critical time-temperature effects and unwanted effects on the quality, the nutrients, the appearance etc. Therefore in order to overcome these problems there is considerable interest in microwaves and also in high frequencies. From the foregoing it is clear that applying microwaves will be very difficult or almost impossible for non-liquid heterogeneous foodstuffs. The volumetric heating with EME has advantages, e.g. fast temperature rise, the heat deposition is controllable and so on. However, there is no selective microbe killing and if there is a cold spot then growth and reproduction may start. Also, the heating rates depend on the thermal and dielectric properties so that for heterogeneous foodstuff it is difficult to obtain the same rates Walter Van Loock (1996).

The quantum energy of microwaves is 1.2×10^{-5} eV and this energy is insufficient to break any chemical bond. But there are structures in biological materials, which may be affected at very low energies Takashima (1969) and Rosen (1972). The delicate balance of extensive hydrogen bonded structures, which determines the functions of biological structures, such as the bearers of genetic information in the cells, are possibly susceptible to disturbances by microwaves. The chromosome breaking

action of microwaves reported by some investigators Heller and Texeira Pinto (1959) *may* have such an origin.

There are increasing attempts to use microwaves in order to induce sterilization in foods. There is an open debate whether the killing effect that microwaves exert on bacteria is due to the thermal effect or to the transfer of the microwave energy to the DNA rotational energy (athermal or non thermal effect). In the last case the bacteria are killed at temperatures below the lethal ones. The difficulties in temperature measurement in the microwave cavity or waveguide make this debate which is still open even more complicating.

2.2 Dielectric Properties of Foods

In terms of interacting with electromagnetic field, biological materials can be treated as lossy capacitors. The heating in a microwave applicator is caused mainly by the electric field and it depends on both the thermal and dielectric properties of the material Cheng (1989). The last are described by the use of permittivity. The permittivity is a complex quantity with real and imaginary components.

The real component of the permittivity, also known as the dielectric constant (ε'), is related to the capacitance of a substance and its ability to store electrical energy. The real permittivity, ε', affects the electric field of a propagating wave, thereby changing the ratio between the electric and magnetic field strengths, this ratio being the wave impedance. The imaginary component, the dielectric loss factor (ε''), is related to the various absorption mechanisms of energy dissipation and is always positive and usually much smaller than ε'. It is approximately proportional to the attenuation of a propagating wave. In the presence of an external electric field, induction and orientation of dipoles to the field occurs within a dielectric material. Transmission properties related to energy transmitted, reflected and coupled by the product and attenuated internally are also determined by these properties. It has long been known that an insulating material (dielectric) can be heated by applying

energy to it in the form of high frequency electromagnetic waves. The origin of this heating lies in the ability of the electric field to polarize the charges in the material and the inability of this polarisation to follow extremely rapid reversals of the electric field. The response of normal materials to external fields generally depends on the frequency of the field (ω). This frequency dependence reflects the fact that a material's polarization does not respond instantaneously to an applied field. At low applied *AC* field frequencies, the dipoles have sufficient time to align with the field. As the frequency increases, the period of time that the dipole moment has to "relax" in and then follow the field decreases. With increasing frequencies, the dielectric constant (ratio of the capacitance of a capacitor filled with a given dielectric to that of the same capacitor having only a vacuum as a dielectric) decreases as energy applied to the material is not completely used to orient the dipoles. This region is defined as the dispersion region. In the region of dispersion, energy is increasingly dissipated within the material by Brownian motion (random thermal motion). Thus, dielectric loss, essentially negligible in the static region, begins to rise rapidly in the region of dispersion. This is a relaxation phenomenon resulting from molecular polarisation and is characterised by relaxation time, τ, defined as the time for the order of maximally aligned state to be reduced to 1/e of its value, upon sudden removal of the applied field, through Brownian motion.

2.3 Microwave Generators

The microwave radiation is produced by a device called magnetron (*Fig. 2.1*). The magnetron is a "cross-field" device because both magnetic and electric fields are employed in this operation and they are produced in perpendicular operations so that they cross. The applied magnetic field is constant **http://hyperphysics.phyastr.gsu.edu/hbase/waves/magnetron.html** and applied along the axis of the circular device illustrated.

Hot cathode emits electrons which travel outward

Stable magnetic field B

Electrons from a hot filament would travel radially to the outside ring if it were not for the magnetic field. The magnetic force deflects them in the sense shown and they tend to sweep around the circle. In so doing, they "pump" the natural resonant frequency of the cavities. The currents around the resonant cavities cause them to radiate electromagnetic energy at that resonant frequency.

Fig. 2.1: Magnetron

The power to the device is applied to the centre cathode which is heated to supply energetic electrons which could, in the absence of the magnetic field, tend to move radially outward to the ring anode which surrounds it. Electrons are released at the centre by a hot cathode by the process of thermionic emission and have an accelerating field which moves them outward toward the anode. The axial magnetic field exerts a magnetic force on these charges which is perpendicular to their initially radial motion, and they tend to be swept around the circle. In this way, work is done on the charges and therefore the energy from the power supply is given to them. As these electrons sweep toward a point where there is excess negative charge that charge tends to be pushed back around the cavity, imparting energy to the oscillation as the natural frequency of the cavity. This driven oscillation of the charges around the cavities leads to radiation of electromagnetic waves, the output of the magnetron.

**2.4 General Wave Behaviour along Rectangular Waveguide**
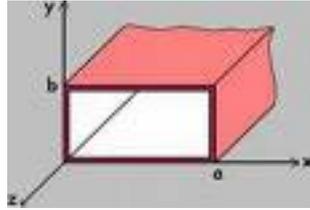
Fig. 2.2: Cross – section of a rectangular waveguide similar to the one used in the following experiments

In this *series of experiments a rectangular waveguide was used, where dimension a >
b (Fig.* 2.2). In such a waveguide structure, the *TE$_{10}$* mode is dominant (*fig. 2.3a,b
and c*). The *TE$_{10}$* mode has a longitudinal magnetic field component and a
characteristics cut-off frequency. Waves of frequencies below this frequency cannot
propagate and power and signal transmission at that mode is possible only for
frequencies higher than that cut-off frequency. Thus waveguides operating in TE
modes are like high-pass filters. This mode has the lowest attenuation of all modes in
a rectangular waveguide.
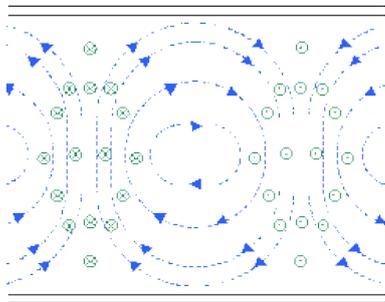
Fig. 2.3a*:* TE$_{10}$ mode, top view (blue lines, magnetic field, green lines, electric field)
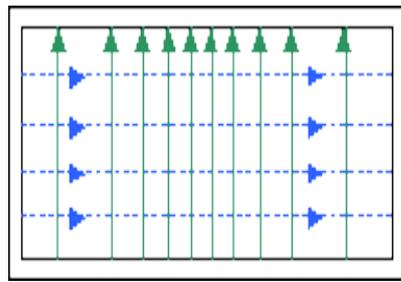
Fig. 2.3b: TE$_{10}$ mode, end view
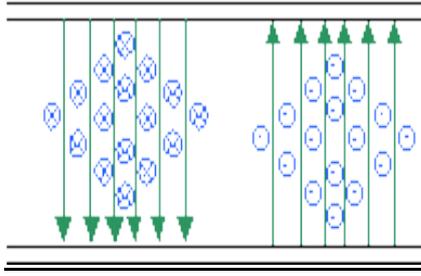
Fig. 2.3c: TE_{10} mode, side view

2.5 Experimental Methods and Set-Up

In these experiments the microwave generator used was form Sairem. The microwave generator consists of a boxed high voltage power supply and control unit (thyristor) with a separate microwave head (magnetron). This family of generator is based on switch mode power supply technology, offering excellent power stability, low ripple and narrow output spectrum. The maximum output power is 60 W. The microwaves have a frequency of 2.45 GHz and two forms of radiation were used: continuous and pulsed. The pulses had the form of a square and their frequency varied from 28 to 79 Hz. The microwave generator was connected to the waveguide with a coaxial connector as seen in *Fig. 2.4*. This experimental configuration is supposed to give more uniform heating. In order to achieve zero reflected power, the stub tuners in conjunction with the metal plate at the end of the plate were used and this lead to the optimization of the field.

stub tunners

| Microwave Generator | → | Coaxial connector | → | Rectangular Waveguide | → | Metal Plate to minimize microwave reflection (coarse tunner) |

Turntable in which the Petri dish is placed
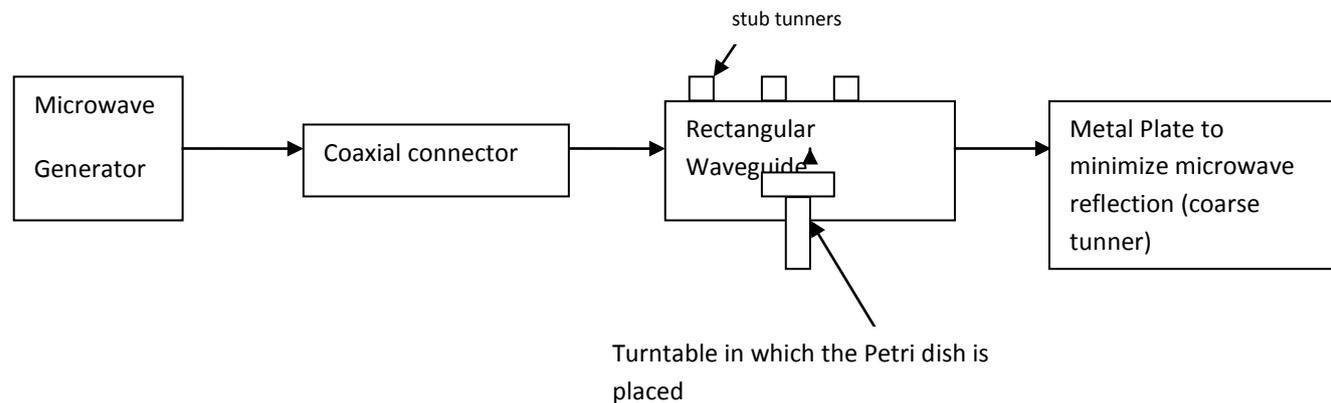
T

Fig. 2.4: Experimental set - up

2.6 A Standardized Methodology for Growing and Work with Enterobacteriaceae Organisms

2.6a Summary of Work Undertaken

In this work samples of *Staphylococcus aurous* (ATCC 22213) *Salmonella Poona* (NTCT4840) and *Escherichia coli* (ATCC25922) were cultured and maintained. These three species were subjected to microwave irradiation within the microwave suite at The University of Bolton. The culturing took place on bench top work space, with due diligence being paid to keeping the working environment clean and sterile at all times. Storage and growth took place in the $37^{o}C$ incubator (Swallow Incubator $37^{o}C$ $\pm0.5^{o}C$) available in the laboratory. Stock cultures of low pathogen city and low virility were purchased from LGC Promote, TCS or VMR. A Bench top Flow Pyrometer or ATP (adenosine triphosphate) Meter (Aquacheck-) was used to determine Light Forming Units (LFUs) of the bacterial cells, indicative of the killing effect of microwaves. This method is based on the theory which states that all cells contain ATP as an energy source and only viable cells will be able to produce it and conversely if the cell is non-viable it will not produce the it. Therefore, by comparing

the levels of ATP between standard and test samples it will be possible to make an estimation of the lethal effect of microwaves. It is known that bioluminescence results from the direct conversion of chemical energy to light energy. The chemical energy is derived from adenosine ATP, as luciferase reacts with luciferin in the presence of oxygen. The method works in the following way:

2.7 ATP (Adenosine Triphosphate) Bioluminescence Reaction Mechanism

ATP + D-LUCIFERIN + LUCIFERASE + Mg++

$$\downarrow$$

AMP + CO_2 + OXYLUCIFERIN + INORGANIC PYROPHOSFATE + **LIGHT**

Studies of bacteria reveal a somewhat different process, in which the role of ATP is still uncertain, but it is clear that oxygen is a prerequisite for the process. The light emitted from the cells is proportional to the presence of ATP. Since all life forms contain ATP, applications in microbiology are based on capturing the micro-organisms, releasing the ATP from within the cell, and measuring the amount of bioluminescence generated. A high loss of relative light units (RLUs) or LFU (Light Forming Units) indicates that a sample contains a smaller number of living microorganisms.

2.8 Growing the Bacteria from Scratch

Test Organisms acquired from TCS Bioscience Ltd:

The organisms that were cultivated and grown were the following:

(1). *Escherichia Coli* ATCC 25922, MM 33

(2). *Staphylococcus Aureus* ATCC 22213, MM14

(3*). Salmonella Poona* NTCT 4840, MM89.

The method for growth from disk was as follows: a Bunsen was used to sterilize a pair of forceps, the screw cap of the bacterial culture was opened, the forceps were flamed until they grew red and then allowed to cool. The Bacteria were grown in nutrient broth, which was sterilized by autoclaving (9ml in Universal bottles) and the bottles were sterilized by flaming the mouths of the bottles to prevent airborne contamination. The disk was taken from the vial and placed in the Universal. It was then vortexed to mix and suspended the bacterial disk in the nutrient agar. This routine was repeated for each of the *E.coli*, *Salmonella poona* and *Staph. aureus*.

The bacterial suspensions were then be incubated in The Swallow Incubator at 37°C ± 0.5°C for 24 hours. The sterility of the samples was checked using the API20e test kit system. From the Nutrient Broth populations could be calculated via serial dilutions:

2.9 Serial Dilutions - Purpose

This procedure was used to identify the number of viable micro-organisms in a fixed amount of a liquid.

2.9a Background

Serial dilution involved repeatedly mixing known amounts of source culture with (sterilised) liquid. 1 ml added to 9 ml gives a 10-fold dilution; 1 ml added to 99ml gives a 100-fold dilution. When fixed, amounts of this dilution series are mixed with

an appropriate agar and incubated, then different numbers of colonies were obtained. By working back from an easily counted plate and using the appropriate dilution factor, the number of micro-organisms in the original source culture was then calculated.

2.9b Procedure

The label the tubes were laid out and (empty) Petri dishes as shown in *Fig. 2.5a*.
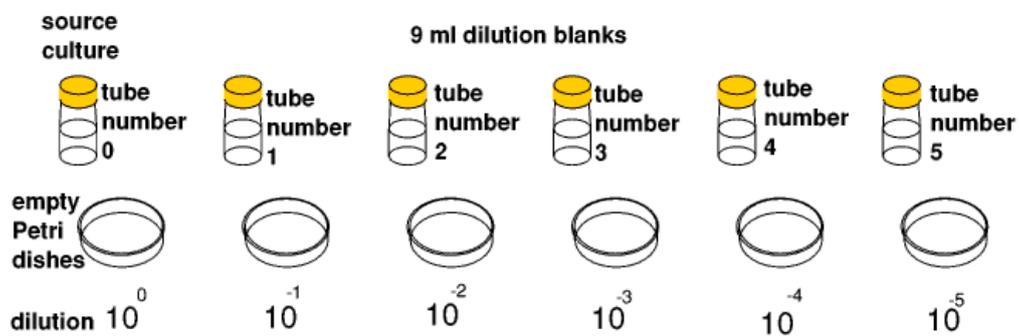
Fig. 2.5a

The lids of tubes 0 and 1 were flamed. Their total volume is 10ml, which is the volume of the irradiated sample. Using a sterile pipette 1 ml of liquid from tube 0 to plate 1 was transferred, and using the same pipette, 1 ml of liquid was again transferred from the source culture (tube 0) to tube 1 (*Fig. 2.5b*).
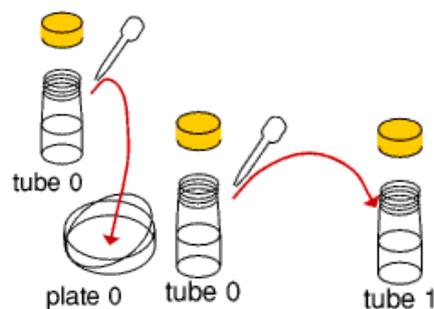

Fig. 2.5b

Then the pipette was discarded and the edge of tube 1 was flamed. The contents were sealed and mixed gently. The process was repeated with the next tube and plate: The lids of tubes 1 and 2 were flamed and loosened. Then 1 ml of liquid was transferred from tube 1 to plate -1, and also into tube 2 and the pipette was discarded. Tube 2 was flamed at the edge and the contents were sealed and mixed. The same steps were repeated, 5 or 6 times, moving along the chain as shown in *Fig. 2.5c*.
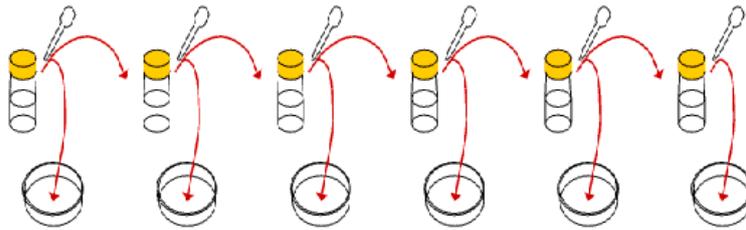
Fig. 2.5c

At the end of this process, a bottle of sterilised agar was taken from the 45 °C water bath, where it has been kept just above setting temperature. The outside of the bottle was dried, and the top and neck area were flamed. Then each Petri dish lid was opened only slightly, in order to pour nutrient agar into the dilution liquid already in the Petri dish, until it covered about two thirds of the area . The agar was mixed with the dilution liquid by a gentle swirling action, then the mouth of the bottle was flamed and moved on to pour another Petri dish. When the bottle is empty, it was washed out with hot water and the dishes were left undisturbed flat on the bench to set - at least 10 minutes. The Petri dishes were sealed and inverted, and placed in the incubator at an appropriate temperature. Then they are ready for the microwave irradiation and they are transferred in the waveguide.

2.10 Experimental Results and Discussion

The ATP meter gave an estimate of the viable cells in the petridish before and after the microwave irradiation. The results that are presented in this report are the average of the three readings that were taken before the irradiation and the three that were taken after.

2.10a Continuous Radiation

Salmonella Poona

Salmonellosis is one of the major food-borne and waterborne diseases. It currently ranks as the most reported of all food-borne diseases in the U.S. with almost 40,000 cases occurring annually. The %ATP Loss is estimated from: ((initial population – final population)/initial population)*100. When the ATP loss is negative, a multiplication of the bacteria occurs. In order to make the killing effect of the microwaves clearer, it was necessary to remove the default readings (99999) of the ATPmeter. The same was done in all the experiments and for the other bacteria as well and as a result a lot of experimental data could not be used. All the experimental results are in APPENDIX 1. *Salmonella Poona* exhibited the highest %ATP loss in 5 min and 5 W exposure (*Fig.2.6, 2.7*). At these exposure conditions *salmonella* had a maximum %ATP Loss which was 85.3. Unfortunately the reproducibility of the experiment was poor with the %ATP Loss ranging from

-112.3 to 85.3%, under the same exposure conditions. Most of the times (in seven out of nine experiments) microwaves killed a percentage of the *Salmonella Poona* (APPENDIX 1).

In these experiments the temperature of the petri dish was the same as the room temperature, i.e. 22 $^{\circ}$C. So this is probably a manifestation of the microwave athermal effect. At 40 min exposure and 7W there was some substantial %ATP loss, the maximum being 56.5 but again the same problem of reproducibility manifested itself. The 10 min of exposure time at 4 W gave a satisfactory result and this

experiment must be performed at least twice again. From these experiments it becomes obvious that low power seems to be more lethal on the *salmonella.*

The lack of reproducibility in microwave experiments is usually due to the formation of standing waves and also the hot and cold spots, something which should not happen in this waveguide. The stub tuners and the metal plate helped to the optimization of the field and there was no reflected power. But still, the distribution of the electromagnetic field inside the waveguide is probably unknown. The same is true for the possible formation of hot and cold spots in the petri dish with the nutrient broth and the bacteria. The dielectric properties of the food and the tangent loss are responsible for the absorbance of the microwaves but these remained the same throughout the experiments. The participation of electrolytes (e.g. salt) can decrease the penetration of microwaves and as a result create a cold core but the nutrient broth has no salt. The temperature of optimum growth for bacteria is around 37 ^{o}C and it can be seen from the experimental data that around this temperature the growth of *Salmonella* is the greatest. The killing temperature of this microorganism is 60 ^{o}C (**http://www.hi-tm.com/RFA/food-path-summ.pdf**). When this temperature was approached there didn't seem to be any ATP loss, however at 61 ^{o}C the readings of the ATP meter were at the default value (APPENDIX 1), therefore no safe conclusions can be drawn. The experiments must be repeated. As mentioned before, the %ATP Loss is greater at 5 W, therefore the effect of time was examined by keeping the power constant and increasing the time at steps of 5 min. Each experiment was performed a minimum of three times. In these experiments, the mean ATP Loss is negative, the standard deviation is big so the data points are spread out and the range is very large as well. The big standard deviation indicates a big spread of the data points around the mean and big experimental uncertainty. From *Fig. 2.6* it can be seen that the effect of the increasing time to the %ATP Loss is negative. When the exposure time is more than 5 min, *Salmonella Poona* multiplies. Twice when the exposure time was 5 min the bacteria multiplied as well. The reproducibility of the microwave experiments is very difficult to achieve, the temperature inside the broth with the bacteria is unknown throughout the experiments and bacteria have the ability to survive and reproduce in the cold spots

therefore the sterilization is impossible in that case. The temperature measurements were taken using a mercury thermometer, therefore they are not reliable. Apart from that, the temperature measurements were taken when the petri dish was removed from the waveguide, something that increases the experimental error even more. In the case of microwave experiments, volumetric recording of the temperature is necessary and the measurement should occur during the microwave heating or immediately after the termination of the experiment and before the petri dish is removed from the waveguide. The best way to measure temperature in such a case is with the use of enzyme inactivation or optical fibre, both the ways give volumetric reading of the temperature. It is not possible to clearly estimate if the killing of the bacteria does indeed occur in sub lethal temperatures or if their growth occurs in their optimum growth temperature, therefore experiments must be repeated with a different way to monitor the temperature which is a very important parameter in these experiments. Other parameters that influence the microbial kill and must be examined is the initial population, the volume of the nutrient broth before and after the irradiation, the exposure time and of course the power.
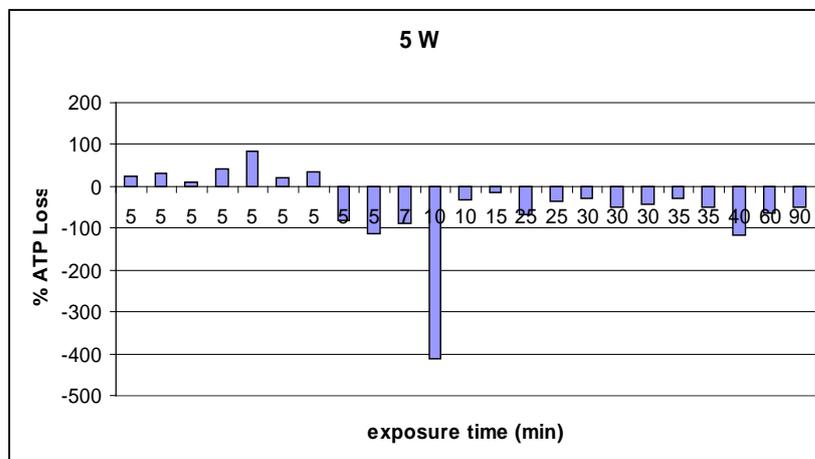
Fig.2.6: Bar chart of the %ATP Loss at 5 W for salmonella and varying exposure time.

Again at 5 min the microwaves seemed to exert a killing effect on the bacteria. Therefore, in order to examine the effect of power when the time is constant, the

time was kept at 5 min and there was an effort to increase the power, at steps of 5 W each time. The generator was terminating the experiments due to a fault in the fan. That was fixed but in some cases it was not possible to increase the power at steps of 5 W.
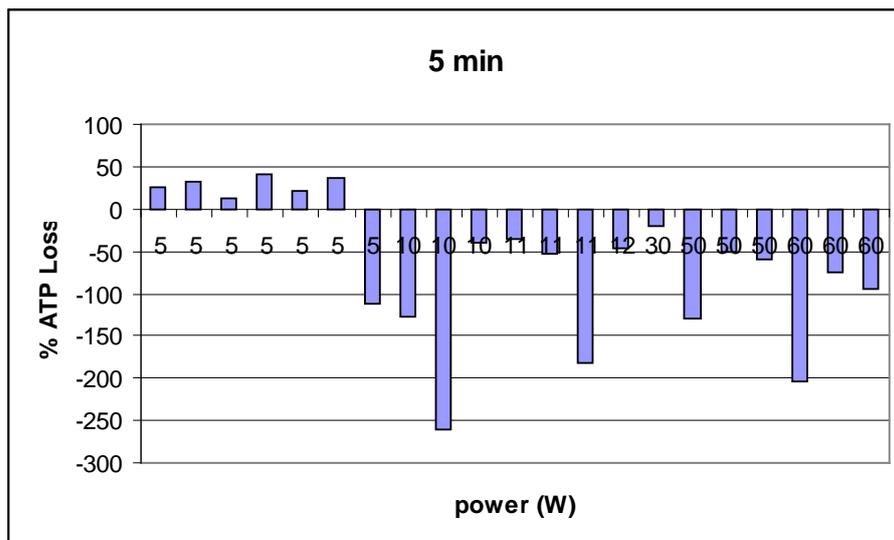
Fig. 2.7: Bar chart for 5 min exposure for salmonella and varying power

It is remarkable again to see from the *Fig. 2.7* that increasing power doesn't mean increasing killing effect. Conclusively *salmonella* was killed at low power and low exposure time.

Staphylococcus Aureus

A bacterial sphere is known as a **coccus** a term derived from the Greek *kokkos*, for berry. Cocci are approximately 0.5 μm in diameter. They are usually round (e.g. *staph. aureus*) but they may also be oval, elongated, or indented on one side. Certain

cocci divide randomly and form an irregular grapelike cluster of cells called a **staphylococcus**, from *staphyle*, the Greek word for grape. *Staphylococcus aureus* is a widespread cause of food poisoning, as well toxic shock syndrome and numerous skin infections. The latter are known in the modern vernacular as "staph" infections. Years ago it was common for people to complain of ptomaine poisoning shortly after eating contaminated food. Modern microbiologists have exonerated the ptomains and placed the blame for most food poisonings on the Gram-positive bacterium *Staphylococcus aureus.* Today, staphylococcal food poisoning ranks as the second most reported of all food disease.

A common problem with the experiments with *Staphylococcus aureus* was that the ATP-meter gave many default readings. The full data obtained for all the bacteria can be seen in APPENDIX 2.

The lethal temperature for this microorganism is 55 – 60 ^{o}C (http://www.hi-tm.com/RFA/food-path-summ.pdf). The problem of temperature monitoring was more obvious in these experiments because at 5 min and 50 W there was a difference of 10 ^{o}C in the temperatures readings that were obtained, something that might be considered to be the temperature difference between hot and cold spots. *Staphylococcus aureus* gave the mean that was closer to positive than the other two bacteria. It is the higher power that kills *Staphylococcus aureus*, and this is different to what was observed in the case of *Salmonella Poona* and *E. Coli* where low power was more lethal. The highest %ATP Loss was at 30 sec and 50 W and that was 81.3. This experiment must be repeated at least twice and the temperature must be monitored. The standard deviation was smaller than in the other two bacteria, something that indicates a smaller spread around the mean.

There seemed to be a kill at 5 min exposure time, therefore more experiments were performed at the same exposure time, *Fig. 2.8*. The results showed that if the power increases, that doesn't mean that more bacteria get killed.

Fig. 2.8: Bar chart for 5 min exposure time for Staph. aureus and varying power

Escherichia Coli

For generations, there was so much *Escherichia Coli* contamination in milk that the fecal flavour of milk was thought to be normal. Obviously this is not true in modern era, but contamination by microorganisms remains an ongoing problem for milk manufacturers. The proteins, fats, and carbohydrates in milk support the growth of numerous microorganisms and many forms of spoilage may develop.

Again, like in *Salmonella Poona* low power is more lethal for *E.Coli*, especially the 4 W. The maximum %ATP Loss, ~83, appears in this power and at 20 min exposure time. At 4 W and 15 min exposure there was a %ATP Loss of ~87 at the temperature of 29 ^{o}C, which is below the lethal one for this bacterium (55 ^{o}C, http://www.hi-tm.com/RFA/food-path-summ.pdf). At 5 min and 20 W there was a big difference in the temperature measurements , in one measurement the temperature was 33 ^{o}C and in another 44 ^{o}C. Again, this is probably an indication of the existence of hot and cold spots. Simply because the 4 W gave relatively high %ATP Loss, more experiments were performed by keeping the power constant and increasing time, *Fig. 2.9* (Results in APPENDIX 3)*.*
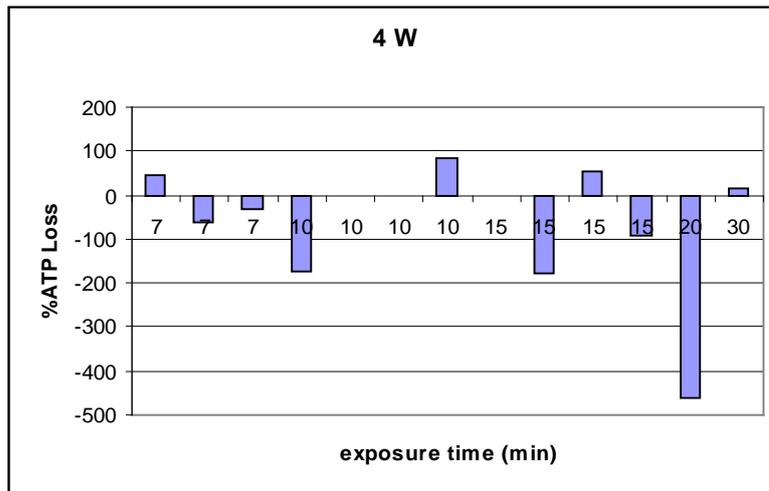
Fig. 2.9: Increasing time doesn't imply increasing killing effect for *E. Coli* at 4 W

2.11 Multiple Linear Regression

The multiple linear regression was performed by Professor Grootveld. Multiple linear regression attempts to model the relationship between two or more explanatory variables (independent variables) and a response variable (dependent variable) by fitting a linear equation to the observed data. Every value of the independent variable *x* is associated with a value of the dependent variable *y*. Like in the case of the formula of McRee, what is attempted here is to find the mathematical expression that relates the bacterial killing (expressed as %ATP Loss) with the resultant temperature and power. The population regression line for *p* explanatory variables *x₁, x₂, …,xₚ* is defined to be $y = y_i + b_1 x_1 + b_2 x_2 + ... + b_p x_p$.

 For my experiments where there are two independent variables:

$y_{ATPLoss} = y_i + b_1 x_1 + b_2 x_2$, where *x₁* represents power (W) and *x₂* the exposure time (min).

The *yᵢ* represents the intercept and the b's are the regression coefficients, representing the amount of dependent variable y changes when the corresponding independent changes 1 unit. The intercept represents the amount the dependent y

will be when all the independent variables are 0. The standardised version of the b coefficients are the beta weights and the ratio of the b coefficients is the ratio of the relative predictive power of the independent variables. In Table 1 are presented the results of the multiple linear analysis. It is obvious that only *Staph. Aureus* gives results that are close to being satisfactory. The confidence intervals (CI) in all the three cases of bacteria sweep zero something that is very unsatisfactory. The *p* value for the whole regression is very big, again only in *staph. aureus* is closer to the desirable value which is *p < 0.05*. The *p* value is the probability of the particular value of the coefficient arising by chance. The %ATP Loss when plotted against the predicted value it doesn't give any linear dependence. It comes close to this only in *staph. aureus* again but I recommend that the extreme value is removed in order to get a better graph. The %ATP Loss gives a normal distribution in all the three experiments (Table 1). However, standard distribution doesn't imply anything in particular, it is a distribution that all the experimental results exhibit when they are repeated many times, i.e. when the sample is bigger than 30. A way to improve the results of multiple linear regression is to remove the points with extreme values, something that will probably bring the relationship between the variables closer to linear. Another alternative is to increase the number of experiments hoping that eventually a linear relationship between the variables will be revealed. If the relationship between the variables is not linear then polynomial regression can be used.

Table 1

Test	Regression - Linear
	%ATP loss v Salmonella Power(W), Exposure time (min)
Performed by	MartinG

Date	29 October 2007

n	66
R^2	0.01
Adjusted R^2	-0.02
SE	###########

Term	Coefficient	95% CI	SE	t statistic	DF	p
y_1 Intercept	-114.5	-401.3 to 172.3	143.50	-0.80	63	0.4279
b_1 Salmonella Power(W)	0.06633	-9.33931 to 9.47198	4.706726	0.01	63	0.9888
b_2 Exposure time (min)	-4.226	-13.760 to 5.308	4.7710	-0.89	63	0.3792

Source of variation	Sum squares	DF	Mean square	F statistic	p
Model	###########	2	###########	0.47	0.6302
Residual	###########	63	###########		
Total	###########	65			

Fig. 2.10: Confidence Interval sweeps zero in the case of *Salmonella Poona*. *The p*

value is too large.
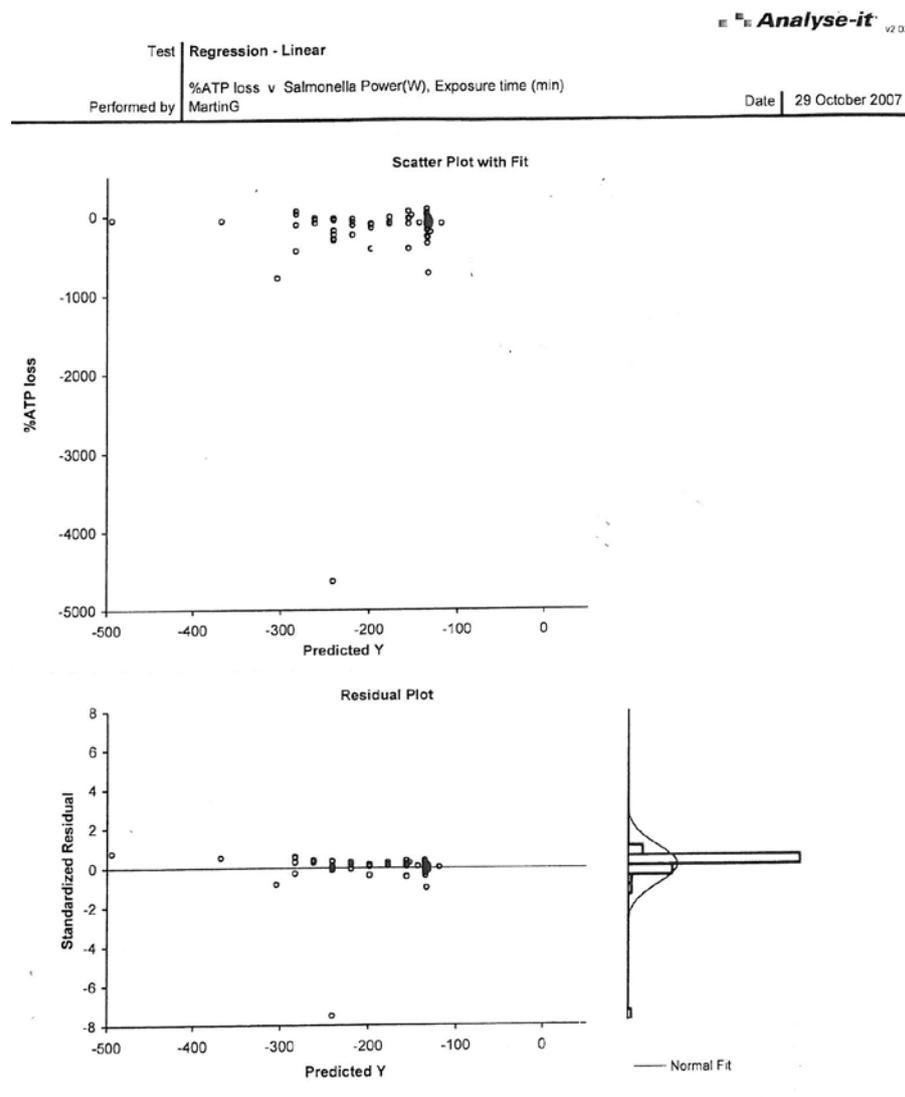
Fig. 2.11: Plot of %ATP Loss vs the predicted value and the standard distribution that the experiments exhibit.

Fig. 2.12: **Fig. 2.10:** Confidence Interval sweeps zero in the case of *Staphylococcus Aureus*. The *p* value is also too large, however *St. Aureus* gave the best possible *p* value.
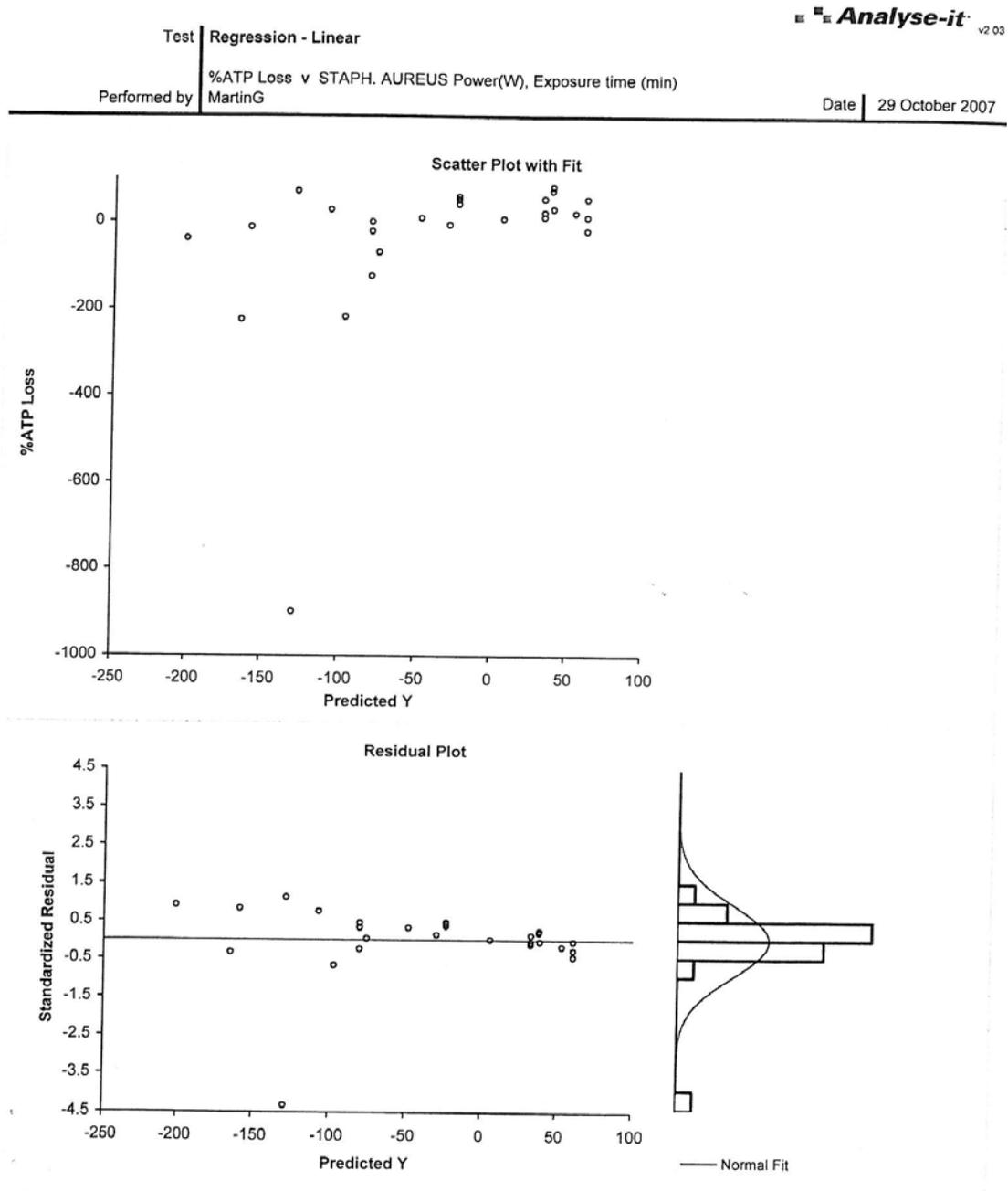
Fig. 2.13: Plot of %ATP Loss vs the predicted value and the standard distribution that the experiments exhibit.

| Test	Regression - Linear
	%ATP Loss v E.COLI Power(W), Exposure time(min)
Performed by	MartinG

Analyse-it v2 03

Date	29 October 2007

n	47

R^2	0.03
Adjusted R^2	-0.02
SE	###########

Term	Coefficient	95% CI	SE	t statistic	DF	p
Intercept	-79.54	-193.39 to 34.31	56.489	-1.41	44	0.1661
E.COLI Power(W)	-1.596	-4.635 to 1.442	1.5078	-1.06	44	0.2955
Exposure time(min)	-0.06531	-6.42692 to 6.29629	3.156549	-0.02	44	0.9836

Source of variation	Sum squares	DF	Mean square	F statistic	p
Model	###########	2	###########	0.63	0.5379
Residual	###########	44	###########		
Total	###########	46			

Fig. 2.14: Plot of %ATP Loss vs the predicted value and the standard distribution that the experiments exhibit.
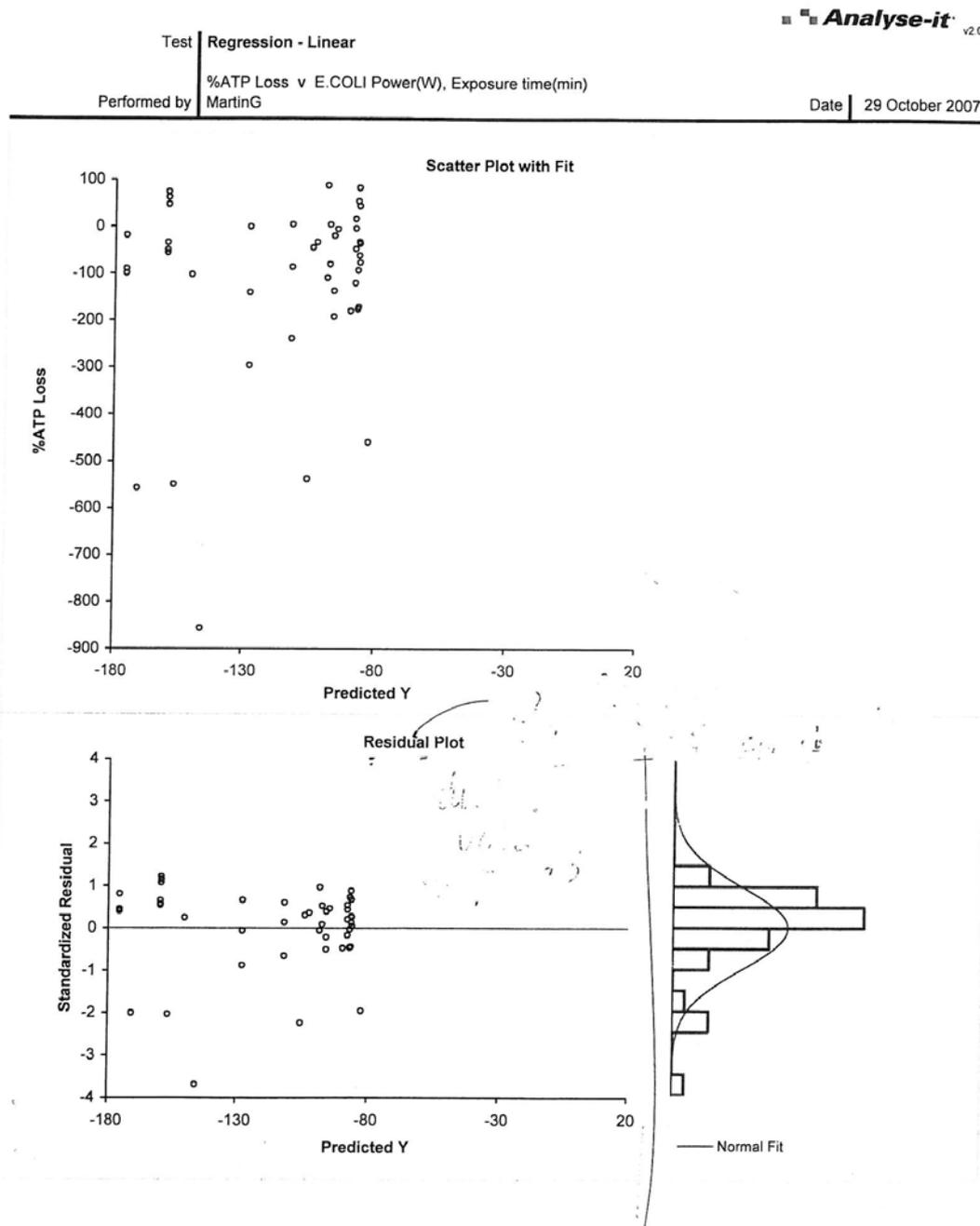
Fig. 2.15: Plot of %ATP Loss vs the predicted value and the standard distribution that the experiments exhibit.

2.12 Pulsed Radiation

Pulsed radiation was used in an attempt to increase the killing effect of microwaves. The pulses were squares but other shapes can be used as well, like triangles and saw tooth. In square pulses there is a sudden voltage change, something that according to literature is the cause of membrane rupture, that is when the intracellular material leaks and results to the lethality of the cell. There is one more parameter that participates to the killing of the microorganisms when pulsed radiation is used and this is the pulsing frequency. The pulsed radiation is the only one that gave a positive mean in the %ATP Loss, excluding the *E. Coli* (where the mean was negative again). There is a net killing effect exerted by microwaves on *Salmonella Poona* and *Staph. Aureus* (Results for all bacteria in Table 2).

Table 2

Salmonella Poona

time (min)	Max. Power (W)	before (LFU)	after (LFU)	%ATP Loss	Temp. (C)	Pulsing Freq. (Hz)	Volts
5	30	5360	9797	-82.779851		35.33	5
5	49	8563	13555	-58.297326		35.46	8
5	49	18038	8860	50.881472	58.6	60.24	8
5	60	9797	7961	18.740431		25.5	10
5	60	4984	8563	-71.809791	44.1	28.2	10
5	60	620	340	45.16129		60.42	10
5	60	28505	5248	81.589195	57.4	60.24	10
15	60	10476	6200	40.817106		60.24	10
15	60	6200	3772	39.16129		79.36	10
25	49	13555	1777	86.890446		28.3	8

St. aureus

time (min)	Max Power (W	before (LFU)	after (LFU)	%ATP Loss	Temp. (C)	Pulsing Fr. (Hz)	Volts
10	60	25115	18787	25.1960979		67.54	10
10	60	1632	43847	-2586.7034		45.87	10
12	49	18787	23373	-24.410497		50.5	8
13	60	23373	5602	76.0321739		46.72	10
13	60	89746	87606	2.38450739	38.8	46.72	10
13	60	53789	10723	80.0646972	45.6	46.72	10
15	49	72706	22982	68.3905042	46.9	45.04	8
15	49	49882	7864	84.2347941	46.4	45.04	8

E. Coli

time (min)	Max. Power (W)	before (LFU)	after (LFU)	%ATP Loss	Temp. (C)	Pulsing Fr. (Hz)	Volts
3.5	60	13042	26587	-103.85677		45.24	10
5	36	43897	56751	-29.282183		35.77	6
5	49	1547	50499	-3164.318		75.75	8
10	49	41858	23696	43.389555	43.4	35.71	8
10	60	23696	6192	73.869007		45.04	10
10	60	5391	12376	-129.5678	50.3	45.04	10
10	60	1758	41858	-2281.0011		60.24	10
15	49	44286	7645	82.737208		45.87	8
15	49	4005	20564	-413.45818	44.1	45.87	8
15	49	7335	1034	85.903204	41.8	45.87	8
15	49	4984	14731	-195.56581	44.3	45.87	8

Salmonella Poona

Salmonella is the only microorganism that didn't show a big range in the readings of the %ATP Loss. Indeed, it seems that the other two bacteria grow a lot when their temperature is the optimum and they are radiated with pulsed microwaves. In fact the biggest growth in them occurs when the radiation is pulsed and their temperature is their optimum (37 $^{\circ}$C).

Pulsed exposure is more effective in giving rise to microorganism destruction than continuous radiation of the same SAR (specific absorption rate, mW/mm^2) value. The temperature changes occur so fast and therefore modelling is the only way to determine temperature as a function of time and position (Laurence and others 2000). The temperature of the sample returns quickly to normal after the application of the pulse. This large transient increase in temperature may result in the alteration of protein conformation. The time scale is of the same order of magnitude as that of the dynamics of protein conformational change demonstrated for the interaction of nuclease with DNA (Ha and others 1999).

Staph. aureus

 Just like in the continuous radiation, *Staph. aureus* exhibited higher %ATP Loss than the other two bacteria. The mean %ATP Loss is positive again and the standard deviation was the smallest among the three bacteria. In all the cases where there was %ATP Loss the temperature was sub lethal or so it seems because when the radiation is pulsed, the temperature decreases to normal immediately after the pulse is applied. Therefore, the microorganisms probably get killed at temperatures that are above their lethal one, but this cannot be measured. It is interesting to notice that when pulsed radiation is used, all the three bacteria have their biggest growth, the %ATP Loss is more negative than in any of the CW experiments. This is probably due to an experimental error, because these readings where %ATP was very negative, were an exception and non reproducible. Therefore it was a good choice to remove them from the graphs.

E. Coli

E. Coli proved again to be more resistant to the killing effect of the microwaves. Even in pulsed radiation experiments, the mean is negative and the bacteria increased twice at such a large rate that two of the measurements had to be removed. The killing effect of pulsed microwaves in *E.* Coli was bigger than in CW, but still in four out of 9 experiments there was multiplication. *E. Coli* is definitely much more resistant than the other two bacteria.

2.13 Non Thermal Microwave Biological Effect: Are the Non Linearities a Possible Explanation?

Taylor (1981) raised the question if there are any physical models that can prove the existence of athermal microwave biological effect. In a lattice, nonlinear interactions guarantee ergodicity and thermalization of energy. Therefore, it is expected that the microwave energy irradiated on a biological specimen can be quickly thermalized and distributed among the oscillatory modes of the molecular

structure. Fermi and others (1955) proved, after a series of computer experiments, that the thermalization assumption is incorrect. Their results showed that one-dimensional nonlinear lattice exhibited recurrence phenomena. Instead of a continuous redistribution of energy from an excited lower order mode to the higher modes, the first few modes exchanged energy regularly among themselves.

In the Froehlich (1968) model it was assumed that energy is channelled strongly into the lowest polar mode, a phenomenon similar to the Bose-Einstein condensation. This phenomenon appears to depend on the assumption of a high-transition probability for the second-order process.

All biological membranes have remarkably high polarizations, of the order of 10^5 (amp)(sec)/m^2, and they are identified experimentally by some researchers as the locus of athermal microwave interactions. Materials with high polarizability have strongly polarized metastable states. Thus, Froehlich was led to conjecture that metabolic processes are pumping energy into dipolar modes of sections of macromolecules such as DNA. Oscillating systems of this type can experience long-range interactions in which each individual oscillator exhibits the phase required to minimize the interaction energy. Microwave energy that is absorbed by the system by excitation of a specific mode can be selectively channelled into the dipolar mode by nonlinear interactions and thus trigger the presumed biological actions that accompany these long-range interactions without being the principal source of energy to the entire system. This process would be strongly frequency-dependent and characterized by the existence of both time and amplitude thresholds (Wu and Austin 1979).

Strongly influenced by the Froehlich (1968) theory, Grundler and Keilman (1978) undertook a series of experiments to demonstrate a biological response to weak irradiation by electromagnetic waves at frequencies around 42 GHz. The millimeter wave region was chosen because, according to Froehlich, the periods correspond to the period of elastic vibration of a macromolecule. Using absorbed powers of the order of 20 mW, it was found that the growth rate was affected in a frequency dependent manner. Variations in growth rate of ±30% were observed

over bandwidths of 0.01 GHz. The existence of these narrow resonances was also confirmed with greater precision by Froehlich (1977).

The dielectric properties of the micro-organisms are of big importance as already stated because one of the current explanations for research findings of enhanced microbial kill under microwave heating is that of selective absorption of microwave energy within the microorganism. Results show that because of the microscopic size of bacteria, the surface area to volume ratios of these organisms is extremely high, resulting in rapid heat loss to the surrounding environment. Thus, the microorganisms have to possess extremely high dielectric loss factors to maintain even small temperature differences. Sastry and others (1991) showed analytically that if a microorganism within a liquid medium, like in our series of experiments, is to maintain a temperature of 1 ^{o}C higher than the medium, the rate of energy generation within a microorganism would have to be many times higher than that within the liquid. Since the rate of energy generation depends on the dielectric properties of the microbial contents, impedance matching and size in relation to microwave wavelength a number of arguments exist against the possibility of such large energy generation rates within the individual microbes. This gives an opportunity for the non-thermal or athermal origin of the lethality that microwaves exert on the bacteria, something that should be taken to a serious consideration. When a microwave beam falls in on a food surface, part of it will be reflected, part absorbed and part transmitted. The reflection factor will vary greatly for the dielectric properties of the food and the angle of incidence (Ohlsson and Risman, 1991). The influence of the food packaging material was shown to be dramatic both on temperature distribution and required heating time.

CONCLUSIONS

No sterilization killing level has been achieved so far, that includes my work and the literature. However the pulsed radiation experiments seem to be promising.

The main problem with microwave experiments is to find a way to measure the temperature and create a time-temperature profile. It is not possible with today's technology to measure the temperature at microscale, the dimensions of the bacteria vary from $0.5 - 15$ μm. Their temperature is unknown during the microwave process and therefore there is no clear way to determine if they actually get killed at sub-lethal temperatures. Selective microwave absorption is excluded.

The TE_{10} mode couples with the cells and its impact on the cell membrane must be examined. Theories suggest that electromagnetic fields cause ion shift on the membrane and they cause rupture. Another theory suggests that the internal part of the cell is liquid it gets heated more quickly and it expands, therefore the cell bursts. None of them has ever been verified. Simulations will help us see what happens on the cellular level. There is so far only one model developed that describes the cells in terms of their permittivity. The different geometries of cells were taken into consideration and the assumptions were made in order to describe the dependence of their relaxation spectra on frequency. Different geometries of the cells were described in this model and it is the multistratified model developed by Japanese scientists, can describe the interactions of microwaves with the cells. The factors that affect the bacteria reduction are: frequency, power output level, time and pulsed power. The latest was shown to severely damage the cell membrane and the metabolic rate of cells at early stages of cell growth without causing temperature elevation. Therefore it is more effective when it comes to the destruction of such microorganisms.

The interactions of microwaves with living organisms were described at a cellular level by considering the cells to be multistratified ellipsoids or spheres. The case of spheres is a degeneration of the ellipsoid one. This model of cells gives rise to multiple dielectric dispersions. Both numerical modelling and computational simulation techniques are explained together with their application on different shape and sizes of 2-D and 3-D bacteria configurations.

PART 3: INTERACTION OF MICROWAVES WITH BACTERIA AND MECHANISMS OF INACTIVATION

3.1 Introduction

Microwave radiation exerts a 'broad spectrum' killing effect towards microorganisms. This review is a comprehensive one of experimental set-ups and process input parameters employed, and the results acquired indeed prove a killing effect on bacteria and the inactivation of spores. Furthermore, claims of the effect of microwaves on the conformational status DNA and RNA are also examined. DNA and RNA interact with microwaves which induce conformational changes on them, the results of this interactions are not well understood. The majority of the literature findings are based on experiments conducted using conventional microwave ovens at the fixed frequency of 2.45 GHz and relatively high power levels, although some have utilised pulsed waves and apparatus operating at higher frequencies (towards the mm wavelength spectral region and relatively low power levels). The mechanisms of such processes are discussed in terms of both thermal and athermal effects of microwave radiation, and the evidence available for them is discussed in detail. Developmental investigations are required (through experimentation, modelling, and simulation) in order to provide an improved and more unified explanation of the interaction phenomena at the cellular level. The potential use of microwaves to induce killing effect on bacteria has a got a lot of advantages. Massive sterilization and savings in energy and time are a few.

3.2 Effects of microwave energy on bacteria in food matrices

There are 3 main categories of phenomena that can explain how microwaves interact with living tissues. According to an Expert Panel Report, Royal Society of Canada for Health (1999):

i) *Thermal effects* often occur when sufficient energy is deposited to cause a measurable increase in temperature of the sample in question. (for example, more than 1 ^{o}C)

ii) *Athermal effects* are those occurring when sufficient energy is deposited to nominally cause an increase in the temperature of the sample but no change in temperature is observed due to endogenous temperature regulation or exogenous temperature control.

iii) *Non-thermal effects* are those occurring when the energy deposited in the sample is less than that associated with normal temperature fluctuations of the biological system being studied.

Dielectric properties and thermal kinetics of food

Microwaves are defined as electromagnetic radiation in the frequency range between 1 – 100 GHz (wavelength between 0.3 and 30 cm); however there are no sharp boundaries distinguishing microwaves from infrared and radio waves (McGraw-Hill dictionary of scientific and technical terms). Metaxas (1983) places the microwaves in the frequency range of 300 MHz to 300 GHz (wavelength ranging from 1 cm to 1 m). Microwaves are an alternating electromagnetic field. The interaction of an electric field has its origin in the response of charge particles to the applied field. Dipoles are induced which then respond to the electric field or in the case of polar dielectrics, dipoles already exist (like in water) which re-orientate under the influence of a changing electric field. Finally another polarization source is from charge build-up at interface, the so called Maxwell-Wagner polarization. These last 2 mechanisms together with d.c. conductivity (free charge carriers like salt) give rise to high frequency heating (Metaxas 1983). During high frequency heating, many

variables in the food affect the heating performance, the most important being the permittivity of food. It is a complex quantity that describes how well a material interacts with microwaves. The equation for complex permittivity is:

$$\varepsilon = \varepsilon' - j\varepsilon''$$
(1)

where the real component ε', also named dielectric constant, is related to the capacitance of a substance and its ability to store electrical energy and the imaginary part is the loss factor. The dielectric constant and the loss factor are frequency dependent (Metaxas 1983), in particular the last:

$$\varepsilon''_{eff}(\omega) = \varepsilon''(\omega) + \sigma/\varepsilon_0\omega$$
(2)

σ is the d.c. conductivity of the medium.

An approximation of the penetration depth of microwaves is given by:

$$d_p = \frac{\lambda_o \sqrt{\varepsilon'}}{2\pi\varepsilon''_{eff}}$$
(3)

where λ_0 is the free space wavelength. Since ε' decreases the two media with different ε' values (Nyfors and Vainikainen 1989). It can also be observed from (3) that microwaves of longer wavelength have higher penetration depth and in the case of foodstuff this equation gives only an approximation. A general rule is that the penetration depths are higher when temperature and frequency are lower.

The dielectric properties of food are determined mainly by their chemical composition (mainly water and salt) and to a much lesser extent by their physical structure (Ryynanen 1995). The influence of water and salt contents depends to a large extent on the manner in which they are bound or restricted in their movement by the other food components. Binding of free water molecules by counter-ions of dissolved salts results in the depression of ε' and elevation of ε'' (addition of conductive charge carriers). These properties complicate the prediction based on data for single ingredients of the dielectric properties of a mixture. Heating characteristics also vary with particle size, homogeneity, and distribution. The calculation of dielectric properties of food is not enough to predict heating patterns, since they depend on other factors as well, like, for example, oven design, geometry parameters, internal focusing effects, or edge heating effects caused by diffraction, and so on.

The rate of heat generation per unit volume Q at a particular location in the food during microwave and radio-frequency heating is given by (Buffler 1993; Datta 2000):

$$Q = 2\pi f \varepsilon_0 \varepsilon'' E_{rms}^2 \qquad (4)$$

where E_{rms} is the root mean square value of the electric field, f is the frequency of the microwaves or the radio-frequency waves, ε_0 the permittivity of free space, and ε'' is the dielectric loss factor (a material property called dielectric property) representing the material's ability to absorb the wave. Even though it is not apparent from that equation, ε' affects the strength of the electric field inside the food. Time-temperature history at the coldest point determines the microbiological safety of the process as in other thermal processing. Once temperature is known at the coldest point as a function of time, accumulated lethality can be calculated following the well-known equation:

$$F_0 = \int_0^{t_f} 10^{(T-250)/z} \, dt \qquad (5)$$

where T is the cold point temperature at any time t, z is the z-value in -18 °C, and t_f is the total duration of heating. Two terms are used to evaluate heat resistance of a microorganism: D value, which is the time required at a given temperature to reduce the organism population by 90% (one log cycle) and z value, which is the temperature required to reduce the D value by 90% (one log cycle). In microwave heating, even for a solid food, the coldest point is less straightforward to predict and can change during the heating process, depending on a number of food and oven factors (Fleischman 1996; Zhang and Datta 1999).

2.45 GHz

The standard frequency used by domestic microwave ovens is 2450 MHz (wavelength in free space 12.2 cm). In the following series of experiments, multi-mode cavities (domestic ovens) were used. In such cavities the distribution of the electromagnetic field is unknown. Due to the reflections of the electric field in the cavity walls, there is formation of standing waves, leading to the formation of nodes and anti-nodes which then results in hot and cold spots inside the food. It is hard to predict the heating pattern inside the food and this is even more pronounced in the case of a multi-component food. Many different factors influence the heating pattern and what follows is an attempt to investigate how each of these factors, or several of them together, plays a part in temperature distribution inside the food and the killing of the bacteria in it. The experiments that follow cannot give a conclusive answer about the killing effect of microwaves, because the repeatability of the experiments is under question and, even more, the results cannot be scaled up. In some cases, as described by Kozempel and others (1998), tanks were used instead of cavities. However, there was no mention of the dominant electromagnetic mode.

Effect of chemical composition and food properties on mw-heating and bacterial lethality

 The chemical composition of food (e.g. salt and moisture content, pH) plays an important role to how much well it is heated. According to Heddleson and others (1996), the heat resistance of *Salmonella, Staphylococcus aureus, and Listeria monocytogenes* is greater at their optimum growth pH value: when it was in the range of 6.8 – 7.0, there were no significant difference in the survival of *Salmonella* species.

Increased moisture content increases the penetration depth of incident microwave energy and products are heated more efficiently. Increased salt content suppresses microbial killing by decreasing the penetration depth and high surface temperature, Fujikawa and others (1992), Heddleson and others (1996). Heddleson and others (1991) developed a model system by adding variable combinations of sucrose, sodium chloride, caseinate, and corn oil, [all in 1.0% (w/v) concentrations to 0.30 mmole·dm^{-3} phosphate buffer (pH 6.80)], in a total volume of 100 mL. Then the samples were microwaved for 47 s in a 700 W oven and the temperature was measured using a fluorescent fibre optic and mercury thermometer immediately after heating. The results showed that sodium chloride provides protection with 37.6% of the *Salmonella* population surviving, whilst in the absence of salt only 0.22% of the population survived.

Chipley (1980) noted that staphylococci recovered after microwave-heating under the same conditions throughout a range of 35 to 92 ^{o}C was showed data suggesting inadequate thermal treatment in cavities. The results indicated that the extent of destruction of *Salmonella, L. monocytogenes,* and *S. aureus* within foods varied significantly, another factor affecting microbial killing being the species involved. The influence of food composition on bacterial inactivation differs and it is more pronounced for *Salmonella* and less so for *L. monocytogenes*. However, this phenomenon also depends on other factors. Although specific heat is an often-neglected parameter in microwave heating, it is one which can have an overriding

influence on heating (Schiffmann 1986): it is this property that can cause a material which has relatively low dielectric loss (such as edible oil) to heat well in a microwave field. When the specific heat capacity is lower, less heat is required to raise a unit mass of homogeneous material one degree in temperature (assuming that during the process no phase or chemical change occurs). One of the major advantages of microwave heating is selective heating (Schiffmann 1986). In this process, microwaves couple selectively with materials which are more absorptive of energy (mainly water and carbon), a process which can lead to greater heating efficiency, although it can also give rise to unusual temperature profiles in multicomponent food systems (van Loock 1996).

Fruin and Gutherz (1982) studied *Clostridium perfringens*, *E. coli, S. faecalis,* and *S. aureus* in a 25-g meat loaf test portion which was microwaved in an oven of 700 W. The final mean temperature and temperature range were 70 and 63-81 ^{o}C, respectively (measured at different locations immediately after cooking to obtain minimum, maximum, and mean temperatures for each loaf). There was a wide temperature variation and, consequently, the correlation coefficient of decreasing microbial survival over increasing temperature cooking was only 0.35. Another contribution to this low linear correlation coefficient stems from the failure to obtain uniform microbial dispersal in view of the highly viscous and fatty consistency of the raw meatloaf. There was also failure to obtain a representative sample by coring. Cooking by microwaves resulted in a reduction in the number of microorganisms present by 90% when the heating time was 10.0 min. The most dramatic reduction observed was for *Clostridium perfringens*, *S. faecalis,* and *S. aureus,* which appeared to be the most heat-resistant.

Heddleson and others (1994) concluded that there are several factors affecting the survival of *Salmonella*. When the mixed final temperature of 100 g of milk was 57 ^{o}C or lower, there was a significantly lower bacterial elimination level (about 85%) compared to a temperature of 60 ^{o}C (95%), with the experiments being performed in a 700 W oven. When milk was heated for a constant time of 45 s at high, medium, and low power settings, samples heated at the highest levels resulted in a high percentage bacterial destruction, from 92.7 to 99.9% (less destruction was observed

in ovens of lower setting, such as 450 W). These experimental results were probably due to the uneven temperature distribution. Mixed mean final temperature cannot be employed as an indicator for bacterial destruction. Heating to end-point temperatures (EPTs) represents a more effective means of achieving consistent destruction rather than heating to a mixed mean final temperature. EPT is taken from only one point in each sample (for example, the centre), and hence is not being representative of the entire product temperature range (Lin and Sawyer 1988). However, when the coldest point's location is known, the EPT temperature can give a better indication of bacterial destruction; while in the case of mixed mean final temperature there might be cold spots in which the microorganisms survive and reproduce. Another method for temperature measurement is the use of fluoroptic probes which allow the measurement of a focused area within the menstruum during microwave heating and can pinpoint temperatures within small distances of each other. This can show if the appropriate temperatures for killing were reached.

The fate of *S. aureus* in microwave-heated food cannot be readily predicted by traditional temperature measurements in a microwave field. Indeed, Baldwin and others (1971) suggested that research with microwave energy must specify cooking power, a method to minimize the uneven heating patterns, and make allowance for post-heating temperature rise. It should be added that the factors that affect reductions observed in food bacteria levels are: frequency, power output level, time, and pulsed heating, rather than only traditional measurements of time and temperature.

Knutson and others (1988) utilized a microwave oven (700 W) for the heat treatment of milk (453.6 g or 604.8 g), in high-temperature, short-time (HTST) and low-temperature, long-time (LTLT) pasteurization (71.1 $^{\circ}$C for 15 s and 62.8 $^{\circ}$C for 30 min, respectively). They investigated the heat resistance of *Coxiella burnettii, S. Typhimurium, E. coli,* and *P. fluorescens* and this was conducted by first determining the temperature of inoculated milk subjected to microwave heating for various times. Un-inoculated steamed milk (76 mL) was heated, and the initial and final temperatures were recorded (the values of time and temperature were regressed linearly and the relationship had a correlation, r value of 0.998); the time required to

reach the desired end temperature of 71.7 $^{\circ}$C was 59 s. Taking into consideration this estimated value, the authors conducted several trials at 60 s, a time corresponding to a final temperature of 72.8 $^{\circ}$C. Again, microorganisms were recovered from the microwaved milk. Similarly, samples of 125 mL of inoculated milk were microwave-heated, and a linear relationship between temperature and time was observed with a correlation coefficient of 0.999. The HTST pasteurization temperature was reached in 76 s. However, when milk was heated for time periods in excess of that necessary to reach 71.7 $^{\circ}$C, inoculated organisms survived and a non-uniform distribution of heat throughout the food was observed.

Raw milk is one of the main causes of gastroenteritis-associated bacterial infection (Thompson and Thompson 1990) and LTLT pasteurization is defined as holding milk at 62.8 $^{\circ}$C for a period of 30 min. In an investigation performed by Thompson and Thompson (1990), milk was inoculated with *S. faecalis* which is more heat-resistant than *C.burnettii*. When *S .faecalis* was heated conventionally at 62.8 $^{\circ}$C, *S. faecalis* levels decreased by 3 orders of magnitude. Thus, if microwave heating were to simulate LTLT pasteurization, the same decrease in the number of *S. faecalis* would be expected, but 1 of 5 trials did not meet this goal. The volume of milk microwave-processed was approximately 2600 mL. Again, as with the simulation of HTST pasteurization, however in this study microwave heating of inoculated milk was found to produce sufficiently high final temperatures, yet the test microorganism survived in greater numbers than when milk was heated conventionally, probably because of non-uniform distribution of heat in the mass of the sample. Villamiel and others (1996) used a 532-W oven to heat raw cow and goat milk, the residence time was 35 s and the temperatures ranged from 73.1 to 96.7 $^{\circ}$C (temperatures were monitored continuously using digital thermometers outside the cavity). All the treatments applied to the cow and goat milk gave effective pasteurization and reduced the microbial populations satisfactorily. Moreover, the authors stated that the design of microwave pasteurization processes should not only involve studies of microbial lethalities, but also additional research into associated chemical modifications. In these treatments conducted under several temperature/time combinations, the researchers achieved low bacteria counts together with low

degrees of whey protein denaturation. Therefore, this study demonstrated that a domestic microwave oven can be employed to effectively reduce the aerobic plate counts in a raw goat milk up to six log cycles, without any influence on its organoleptic quality. The volume of the samples that the authors used varied from 2.0 to 3.0 dm^{-3}, a value representing the daily consumption of milk in a household. This method is equivalent to the legally accepted pasteurization procedures required for pathogenic bacteria such as *Salmonella spp., Listeria monocytogenes,* and the pasteurization standard *coxiella burnettii* (the authors inserted a temperature probe inside the milk, approximately 8-10 cm depth, the oven was 450 W, and the set-point temperature was 60 ^{o}C was maintained for 30 min). In a further investigation focused on the killing activity of microwaves towards milk pathogens, Kindle and others (1996) used a 600-W oven to kill *Pseudomonas aeruginosa, E. coli, Enterobacter sazakii, Klebsiella pneumoniae, S. aureus, Candida albicans, Mycobacterium terra,* and *M. poliomyelitis*. Samples were brought to a boil in 85-100 s (a value depending on the milk type) and reached an average temperature of 82-93 ^{o}C. Most of the vegetative organisms were killed with there being at least a 5,000-fold reduction in their viability.

It was the temperature increase and not the time that induced the killing effect. Probably, sufficiently high temperature induces more killing by eliminating the hot and cold spots.

Food geometry and effect of packaging

The main difficulty in microwave experiments stems from the inability to accurately measure the temperature inside a cavity without disrupting the electric field. Many researchers have tried to overcome this problem by altering the geometry of the food or the oven (as by using single-mode waveguides or directional waves) or by doing different packaging or altering the location of food inside the cavities. Some others tried to remove heat.

Fujikawa and others (1992) studied the kinetics of destruction of *E. coli* in solution using a microwave oven operating at powers of 100, 200, 300, and 500 W; the authors used beaker and petri dish. Their samples were irradiated at several power levels for various periods of time ranging from 1.0 to 4.0 min. The temperature was measured with a digital thermometer. These investigators found that the pH of the phosphate buffer (PB) solution employed exerted an influence on bacterial destruction (the volume of the solution exposed to microwaves was 100.0 mL).The bacterial lethality was maximum at pH range of 5.0-9.0 at 200 W. As expected, the quantity of microwave radiation absorption in PB was affected by the location of the beaker on the rotating plate and the exposure time. In particular, when placed at the edge of the plate, the rate of increasing temperature in ^{o}C/s (*A* value) was 96% of that of PB located at the centre of the plate for each power level applied. The container shape had an effect on bacterial destruction: when a flat Petri-dish was used instead of a beaker, the bacterial destruction was suppressed compared to the control (beaker), again at 200 W. From the relationship between *A* value and the rate of bacterial destruction (*k*), the authors were able to predict the bacteria survival level to a certain extent from the *A* value of a given solution. When microwave treatment was compared to a conventional thermal treatment with the same *A* value, the killing rate was almost the same, a result that implies that the killing of microwaves is attributable to thermal effects alone.

Lin and Sawyer (1988) investigated the effects of wrapping food in polyvinylidene chloride (PVDC) film at microwave oven power outputs of 350 and 713W. They examined the survival of *S. aureus* and *E. coli* inoculated in ground beef assembled into a loaf in order to distribute the pathogens throughout the mass; the wrapping of the beef loaf in PVDC film, load size, microwave output power, and processing time were chosen as experimental variables for this study. The authors introduced the concept of exposed microwave dose (EMD), defined as watt x minutes processed per gram of food. In this manner, they correlated wattage output, time of microwave processing, and load size. Immediately after exposure, the post-processing temperature rise (PPTR) of the beef was measured using a potentiometer connected to 16 iron-constantan thermocouples. The thermocouples were inserted half-depth

into the beef loaf, and temperature readings were continuously taken every 20 s until PPTR was no longer observed. The results acquired demonstrated that the survival percentages of 3 classes of bacteria were lower after they had been wrapped in PVDC film than those that were unwrapped. Moreover, it was observed that *S. aureus* was more resistant than *E. coli*. The effect of the PVDC wrap was less pronounced in the case of a greater food load, but neither of the bacteria survived in the PVDC wrap after the longest exposure time period. When the bacteria were inoculated only onto the surface of food products and exposed to sufficient energy to be killed, the PVDC film wrapping exerted no significant effect.

The use of 50% power (356 W) rather than 100%, did not affect the survival level of *S. aureus* and *E. coli* when subjected to the same EMD. As expected, the number of surviving bacteria exhibited an inverse relationship to PT (processing time) and exposed microwave dose (EMD), but was directly related to end-point temperature (EPT) of the centre of the beef loaf and microwave processing temperature rise (MPTR). However, it should be noted that it is almost impossible to accurately locate and measure the point of lowest temperature in food products processed by microwave energy, although the relationship between EMD and EPT can be used to predict bacterial survival in microwaved beef loaf. Since PVDC wraps, like most of the coverings, are moisture barriers preventing evaporative cooling and also provide insulation, they can save energy and improve the microbial quality of food which can be further enhanced if a standard EMD is considered for microbial safety (which depends on the variable electrical properties and device configurations).

In a similar manner, Aleixo and others (1985) wrapped whole stuffed and unstuffed turkeys in 'brown-in' bags and their results revealed that the destruction of *C. perfingens* was increased. The whole turkeys were cooked for 30-45 min in a 600 W oven, and their temperature was monitored using two microwave thermometers inserted in the turkey breasts and almost in contact with the bones. The hens were cooked to an internal temperature of 68.3 $^{\circ}$C, and the cooking time was almost half that required for turkeys cooked without 'brown-in' bags. In the case of unstuffed turkeys there was a one to two log reduction in the number of bacterial cells, and the lethality increased when the hens were unstuffed. When the stuffed hens were

cooked to an end temperature of 76.6 ^{o}C the reduction in *S.Typhimurium* was from four to seven log cycles. Turkeys were cooked at an end-temperature of 85°C to examine if complete destruction of *S.aureus* and *S. Typhimurium* was possible, but results obtained showed that this was unsuccessful. The authors concluded that their experiments confirm previous observations that microwave cooking is not as effective as conventional cooking with regard to the destruction of microorganisms. If the turkeys were held longer at such elevated temperature settings, the microorganisms would had been completely destroyed. Furthermore, in oxidation products arising from the thermal stressing of lipids, in the case of stuffed turkeys the lipids have bactericidal effects, and therefore part of the lethality of *S. aureus* in these hens is attributed to this process.

The effect of food shape on microbial survival and thermal response however remains unclear, but it is possible that a standard shape of microwaveable food products can provide an optimal control of bacteria destruction. Huang and Sites (2007) used a 550-W microwave oven equipped with a proportional-integral-differential (PID) device for in-package pasteurization of ready-to-eat (RDE) meats. Frankfurters (2.2 cm diameter x 13.3 cm length), inoculated with *Listeria monocytogenes* and vacuum sealed in plastic packages, were microwave-heated in bags, with the package surface temperature increased and maintained at 65, 75, or 85 ^{o}C for increasing periods of time (ranging from 2.0 to 19.0 min). During microwave-heating, the surface temperature of frankfurter packages increased linearly with the heating time until it reached a limit point, whilst the concentration of *L. monocytogenes* was assumed to be decreased linearly with time. The surface temperature was measured with the use of an infrared sensor that was properly shielded from electromagnetic interference. The sensor was placed approximately 30 cm above the sample at the centre of the microwave oven, and a turntable was utilized. In order to allow the surface temperature to increase as rapidly as possible and reach the set-point, full power was supplied to the magnetron, a process accomplished by the PID controller. The experimental results revealed that the surface temperature did not rise immediately to the set point, but, instead, this parameter increased linearly and then stabilized at values close to the set-points.

The inactivation rate of *L. monocytogenes* was found to be 30 – 75% faster than that observed in conventional heating.

Zimmermann and Beach (1982) investigated the efficacy of microwave-cooking for devitalizing *Trichinella spiralis* in pork roasts and chops. This parasite was detected in 9 out of 51 microwave-cooked pork products, the authors using 6 different microwave power settings ranging from 625 to 700 W (a mode-stirrer was employed to ensure homogeneous distribution of the microwaves). The 1.3-cm chops were cooked for a period of seven min and the 1.9-and 3.2-cm ones were cooked for 12 min. The mass of the chops ranged from 1.8-3.4 kg. Roasts were cooked at W x min/kg combinations, and 5 of these were exposed in this manner with a sequence of single wattages varying from 312.5 to 625 W, whilst one was cooked only at 625 W. Standing times varied and some of the roasts were tented with foil for a standing time of 5.0 to 15.0 min in order to allow for heat movement within the product. The temperature measurements were taken at the centre and ends of each roast, using microwave meat thermometers, prior to cooking, immediately after cooking, and after standing. Standing time after cooking with the roast tented with foil was found to reduce the infectivity. The authors also observed a temperature shift in tented roasts which were allowed a standing time and 'cold spots' were most noticeable near the rib bones. In view of these observations, it was speculated that microwaves were reflected off the bones and that this process contributed to an uneven temperature distribution, a phenomenon favouring the survival of bacteria (the bones also produced a 'shading' effect). In the case of fatty surfaces, a 'crust' usually develops during heating, and the muscle tissue below it occasionally develops 'hot spots'; many of the roasts contained red or pink meat after cooking, but *Trichinella spiralis* was not always detected.

Anaya and others (2006) explored the survivability of *Salmonella* cells in popcorn after microwave oven cooking was explored in a 700-W oven. The inoculated product was mixed for 5.0 min to ensure a homogeneous distribution of the bacteria and then the popcorn bag was resealed and stored at room temperature for 2.0 h to ensure uniform temperature. The popcorn bags were exposed at full power for 3.0 min, reaching a temperature of 130 ± 0.5 $^{\circ}$C in the centre (temperature was

measured by plunging a thermometer to the sample immediately after irradiation). The results showed a 6-fold reduction in *Salmonella* viability after the microwave treatment, with recoveries only from initial populations of 2×10^6 cells/g or greater.

Equipment modifications to counter-act inherent microwave problems

Most outbreaks involving *E. coli* O157:H7 and *S. enterica* have occurred in apple and orange juices (Gentry and others 2004). In 1991, *E.coli* was confirmed as the unclear epidemiological agent in apple juice and it has since been suspected in earlier outbreaks involving apple cider. Gentry and others (2004) attempted to overcome the inherent problem of unevenness in microwave-heating by adding helical coils in a microwave oven in which they heated apple cider. In this manner they managed to produce a uniform and reproducible heating, (fibre optic probes were used to measure the time-temperature data). The flow rates were adjusted so that the fluid exiting the cavity was at 73 ^{o}C, while the input power was 2,000 W; and a 7 dm^{-3} volume of cider was used. The pasteurization process resulted in a 5-log reduction in *E.coli*.

 In order to overcome the difficulty of uneven temperature distribution, Lechowich and others (1969) circulated kerosene at 25 ^{o}C through the jacket of a condenser during the microwave exposure permitting the microwaves to reach the microbial suspension (10^8 to 10^9 *Streptococcus faecalis* or *Saccharomyces cerevisiae* per mL). The authors modified a commercial 2,450-MHz oven (1,500 W) in a way such that 6 mL in a Liebig condenser could be exposed to microwaves for various times. The suspension was positioned at the centre of the oven and the temperature of the suspension varied from 25 to 55 ^{o}C. Water has a high dielectric constant, therefore it absorbs microwaves and converts them into heat even when the suspension is cooled by kerosene. Therefore, the maximum temperature attained in the suspension during microwave exposure is an important parameter. The temperature was measured by a thermocouple relay system and the measurements were taken immediately after the magnetron was switched off. No other lethal effects apart from the thermal one were observed by the authors.

Lakins and others (2008) modified a domestic microwave oven in order to prove that directional microwaves are able to destroy pathogens at lower temperatures without affecting the quality of food. The authors exposed eggs to microwaves of varying power for 20 s, and cooled them with CO_2 for 30 s, to observe a maximum of 2 log reduction in *Salmonella enteriditis*. The temperature in the egg interior reached 45 t o 50 ^{o}C. The oven was modified by the authors so that there was horizontal and rotary movement of the food heated and several microwave sources of directional microwaves (horizontal and vertical, varying power) so that there was more uniform field distribution. The reduction of *Salmonella enteriditis* was depending on the position of the sample inside the oven. The same equipment of directional microwaves was used to extend the shelf-life of white enriched bread up to two months with minimal mould growth and again without detrimental effect on quality. The bread was treated inside cryovac bags for 10 s and the mould reduction was 99.9%.

Kozempel and others (1998) developed a pilot-plant non-thermal flow process (*Fig. 3.1*) using microwave energy to inactivate *Pediococcus sp.* NRRL 2354. The process consisted of multiple passes through the microwave generator, and each passed material went to a receiving tank for subsequent passes. The flow rate was 0.96 to 1.26 kg/min and the dwell time per pass was 1.1 to 1.5 min (5.0 to 5.4 kW) and the length of the tunnel was 86 cm. The temperature in hot spots did not exceed 40 ^{o}C. The thermal energy was removed using a cooling tube. There was significant decrease in microorganisms in water, 10% glucose solution, and apple juice, and also in yeast in beer. There was no effect in skimmed milk.
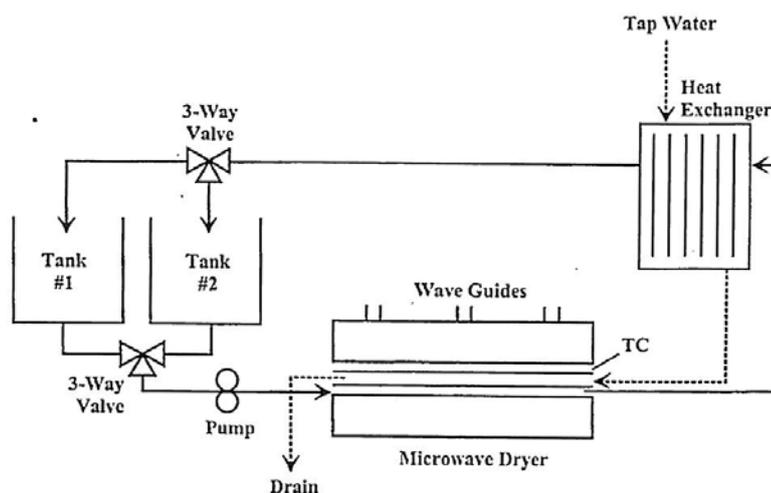
Fig. 3.1: Modified experimental process flow sheet. (Kozempel and others 1998)

915 MHz

The main advantage of this frequency is that the microwaves have a greater penetration depth. Especially for the case of highly inhomogeneous food, the greater wavelength offers the advantage of greater penetration depth: it is 3 cm as compared to 1 cm for 2,450 MHz. Therefore this provides more uniform heating, (Mudgett 1989).

Cunningham (1978) designed an experiment to test the influence of microwaves (700 W) on bacterial numbers in raw chicken patties which were exposed for periods of 0, 10, 20, and 40 s. In all cases there was substantial decrease in the total number of microorganisms (*E. Coli, SalmonellaTyphimurium, and Clostridium Perfringens).* Although there was no temperature rise in the patties that were treated for 10 s, those treated for 40 s reached approximately 56 $^{\circ}$C, measured in the middle of the patty, while the surface temperature reached only 40 $^{\circ}$C. The author concluded that microwaves can be utilized to pasteurize products by sub-cooking them without alteration in flavour or appearance.

In their research the authors Tang and others (2008) investigated the use of a single-mode 915-MHz tunnel and how microbial killing (*Clostridium sporogenes* PA 3679

spores) for a highly nonhomogeneous, pre-packaged (in polymeric trays) food can be achieved. The microwave power output was 2.7 kW. The weight of each tray was 180 ± 1 g. Five of them were processed each time and the fibre in optic sensor for the temperature measurement was inserted in the second tray. The authors additionally used a single-mode waveguide which provides predictable electromagnetic field distribution, resulting in predictable and repeatable heating patterns in food. A single-mode resonant heat allows a sample to be placed at positions of much higher electric field strengths than can be obtained in a multi-mode oven. After the placement of the sample inside the waveguide, the cavity changes the resonant frequency and in order to remain tuned the plunger must be adjusted (Mingos and Bughurst 1991). The trays were heated until they reached the desirable F_0 value; in this case it was 3 min. In particular, the sample trays were preheated to 60 ^{o}C at the cold spot with 122 ^{o}C water, then moved at an adequate speed through the microwave tunnels for the cold spot of the food (located at the centre) to reach 121 ^{o}C by the combination of 2.7 kW power and hot water, then held to make F_0 around 1 min, and finally cooled to 75 ^{o}C by tap water to gain additional F_0 of about 2 min. A four log reduction was observed when F_0 was 3 and in the cases of F_0 = 6 min the reduction was 8 log and, finally, when F_0 = 12 min there was a 12 log reduction, all of these values according to the D value of samples. The coldest spot is placed in the centre of the sample and this is due to the limitations of microwave penetration and heat conduction. In these series of experiments the heating patterns were repeated. The heating pattern and cold spot inside the packaged real food is difficult to detect when using the real food itself. The authors used a computer vision system to verify that the coldest spot was indeed at the centre of the sample.

In another attempt to reduce heating time, Lau M H and others (2002), explored the application of short-time microwave pasteurization for pickled asparagus in glass bottles of 1.8 kg weight. The result was uniform heating and reduced process time of at least one-half when compared to water-bath heating and an additional advantage was that the thermal degradation of the product was significantly reduced. Uniformity of microwaves in the cavity was enhanced with the use of a stirrer and the authors observed that the microwaves passing through the glass wall over the

head space of the glass bottle focused on the top portion of the brine causing localized heating. Therefore, they covered the top one-third of the bottle with aluminium foil. The authors used 2 microwave output powers, 1 kW and 2 kW. The 1 kW output power gave more uniform heating, even though the time required to reach 88 ^{o}C was 30 min for conventional hot water heating, 15 min for 1 kW microwaves, and 9 min for 2 kW. The uniformity observed at 1 kW power output was attributed to convective movement of the brine.

Pulsed radiation

Pulsed radiation is more effective in giving rise to microorganism destruction than continuous radiation of the same SAR (Laurence and others 2000). The large transient increase in temperature may result in alteration of protein conformation. The time scale is of the same order of magnitude as that of the dynamics of protein conformational change demonstrated for the interaction of nuclease with DNA (Ha and others 1999).

Shin and Pyun (1997) investigated the effects of pulsed microwave radiation (PW) on cell suspensions of *L. plantarum* (this test organism was isolated from fermented kimchi) and 2 or 3 loopfuls of growth from the slant were inoculated into a 100 mL flask containing 50 mL of lactobacilli MRS broth dehydrated, and then incubated at 37 ^{o}C for 24 h. An activated pre-culture (volume of 3 mL) was again inoculated into a 500-mL flask containing 200 mL of MRS broth followed by incubation for 24 h, and the final culture broth was subjected to various microwave treatments, The PW irradiation system consisted of a 2.45-GHz microwave source (650 W), a pulse generator, and a pulse driver. The authors used a generator that was adjusted to deliver repetitive rectangular pulse trains at 500 pulses/s and the duty ratio was 1/10, equivalent to a pulse width of 0.2 ms and a period or time-base of 2 ms. The use of PW was proposed for pasteurizing foods with reduced heat, even though its biological effects were not fully understood by the investigators. When the shortest

pulse generatable was employed, it resulted in a very high power peak. For short pulses with low repetition rate, the average power can be very low, although the peak power may be in the Megawatt or Gigawatt ranges, depending on the power output of the magnetron. Microwave pulses are described by the duty cycle, which is defined as the ratio of pulse width to the period. The average power is given by the product of peak power duty cycle. Pulse-modulated radiation may penetrate more deeply than continuous wave irradiation with the same frequency (Lin and Sawyer 1988).

Experimental results obtained by the researchers showed that there was a 4 log cycle reduction of viable cells when exposed to a sub-lethal temperature of 50 $^{\circ}$C by continuous microwave irradiation (CW); at the same temperature, PW irradiation yielded lower viable counts by 2 or 3 orders of magnitude and such findings indicate that PW is more effective. An indication of heat damage to cells is the leakage of cell components into the heating medium. Under the influence of sub-lethal stress, cells experience a loss in membrane integrity, so that amino acids, peptides, membrane lipids, and ions increase in the extracellular environment as a response to injury (Moat 1961; Smith and others 1982). The injury of the *L. plantarum* cell membrane was more severe when PW was used, and hence the non-thermal effects of microwave-irradiation could result in shifts of ions across membranes and the re-orientation of macromolecules. The absorption of high-power PW radiation probably produces thermoelastic waves in biological tissues and such pressure and displacement may cause physical damage to cell membranes and cytoplasm (Lin and Sawyer 1988).

Dardanoni and Toregrossa (1985) exposed *Candida albicans* cells to 1 kHz square-wave modulated microwaves at 72 GHz and found a significantly reduced number of CFU when expressed relative to those with non-irradiated controls, as well as those monitored with continuous-wave (CW) radiation. A 1.0 mL volume of cell suspension (4.5 x 10^7 CFU cells) was inserted into Teflon holders of 11 cm internal diameter and 1 mm bottom thickness, the holder being centrifuged to obtain cell sediment close to the plane of incidence of microwave power. The exposure time was 3.0 h and the microwave power was divided by means of the hybrid tee and sent to irradiators

consisting of 2 opened-flanged waveguides; the peak power incident at the base of the sample holders was 0.2 mW. After 26 experiments, CW radiations caused a mean increase of 24% (standard deviation ±0.28) in the number of colonies when expressed relative to the non-irradiated controls, whereas the modulated-waves microwaves caused a significant reduction (mean value of decrease 16%, standard deviation 0.18). However, the authors found a remarkable variability in the results, in some experiments both increases (more than 50%) of CFU with CW and decreases were observed. In the case of modulated waves, there was always an inhibitory effect on growth rate, an observation that cannot be attributed to a MW-temperature increase caused by microwave absorption, since the mean incident power was halved in comparison with CW radiation. The variability of the results obtained in repeated experiments is not simply explicable, although it should be noted that different cultures contain sub-populations which have different sensitivities.

In an attempt to optimize-pulsed microwave heating, Gunasekaran and Yang (2007) simulated the heating of pre-cooked mashed potato for a period of 30 s using a model developed based on Maxwell's equations. The mashed potato was transferred to 4.0- and 2.4-cm-radius glass beakers to a height of 7.0 cm and covered with waxed paper to prevent water loss; subsequently, samples were stored in a refrigerator at 4 ^{o}C for 16 h to ensure uniform temperature distribution which was measured across the horizontal mid-plane at radial distances of 1, 2, 3, and 4 cm from the sample centre (a fine wire of 0.82 mm diameter type-T thermocouple was used for temperature measurement after 1.0 min of heating). The experimental variables were sample radius, temperature rise, temperature drop, total processing time (< 1,000 s), and average sample temperature (60 ^{o}C). A laboratory microwave oven was used at 2.45 GHz and 250 and 500 W. Pulsed heating is advantageous when deep and rapid penetration of energy is to be accomplished whilst constraining the maximum temperature at the surface. Additionally, it results in a greater depth of heating than continuous heating for the same total heat input; indeed, penetration of microwave energy inside a material depends on its dielectric properties, which alter the temperature distribution. With increasing sample size, the centre does not

heat satisfactorily in view of the exponential decay of the microwave energy. For samples that are small compared to the microwave penetration depth, there is core overheating caused by the accumulation of microwave energy, although pulsed heating can eliminate these phenomena. It is most effective when 'hot' and 'cold' spots are present in the light of the equalization of thermal energy at the power-off periods ascribable to conduction. Pulsed microwave heating is most effective when the sample radius is $\leq 2.5D_p$.

Tong and others (1993) modified a domestic microwave oven (2.45 GHz, 720 W) so the field intensity in the cavity could be continuously modified and a feedback temperature controller was fitted for controlling the product temperatures during heating by cycling the magnetron to an on and off status. The temperature controller consisted of a fibre optic temperature sensing system, a computer, an optocoupler, and a mechanical relay. In controlled-temperature microwave heating the computer reads the temperature and then compares it with the upper limit entered by the user. However when the temperature is above this limit it switches off the magnetron. In such a case, the sample temperature decreases as a result of heat conduction, heat convection, and evaporative cooling (the rate of cooling depends on sample size and porosity). In these experiments the authors heated a bread sample and the set point was 60 ^{o}C when the lower and upper limits were 59.8 and 60.2 ^{o}C (according to authors, the degree of overheating is time-dependent, something that is probably because the electric field intensity at the same location is also time-dependent). Variable power microwave cavities are important because the sample in such a case reaches the set-point temperature more rapidly. The effect of microwaves modulated with square waves of different pulse repetition frequencies on physiological behaviour of the cyanobacterium *Anabaena Doliolum* was investigated by Samarketou and others (1996). For direct exposure, 21 cotton-plugged conical flasks each containing 200 mL sterile BG_{11} nutrient solution were inoculated with a known amount of 0.50 ml bacterial cells. Of these, 18 samples were microwaved and the remaining served as control. The organism was exposed for 1.0 h by inoculating a nutrient solution at 9.575 GHz of different pulsed repetition frequencies at an incident power density of 0.658 mW/cm^2. This study revealed that

microwaves induce athermal biological effects by differentially partitioning the ions and, hence, altering the rates and/or directions of biochemical reactions. The different biological effects that microwaves caused depended on field strength, frequencies, waveforms, modulations, and duration of exposures. These effects are attributed to microwave heating; however, there is no precise information on the causes or bio-effects of microwaves. This is mainly because of the lack of precise temperature measurement.

Inactivation of spores using microwaves (2.45 GHz)

Spores, like *staphylococci*, *Gram-negative* organisms, and anaerobes (including spores of the genus *Clostridium*) are highly resistant to both chemical and physical microbiocidal agents. They are the cause of many infections acquired in hospitals (Russel 1982). Indeed, Warth (1978) pointed out that the core is a normal cell in terms of its macromolecular constituents, and Setlow (1975) and Setlow and Waites (1976) found that the spores of *B. megaterium* and *Cl. bifermentens* contain a substantial amount of low-molecular-weight proteins which are rapidly degraded during germination. In the core are also included deoxyribonucleic acid (DNA) and ribonucleic acid (RNA) and proteins also present in the core are associated with the spore DNA (Setlow and Setlow 1979). Murrell (1969) showed that most of the DPA (dipicolinic acid) is associated in a chelated form with calcium ions and this finding provides indirect evidence that the dipicolinic acid (DPA) is located in the core.

Murrell and Warth (1965) found that the heat resistance of spores is directly related to their Ca^{2+} and inversely related to their Mg^{2+} contents. The $Mg^{2+}:Ca^{2+}$ ratio was related to thermal resistance varying from 0.3 in the least resistant spores to 0.05 in the most resistant ones.

The DNA of spores is well protected against thermal damage and this appears to be the result of the high level of Ca^{2+}-dipicolinic acid in spores. Many factors contribute to spore resistance and long-term survival, the main being DNA repair (Setlow 2007). However, in the same paper Setlow also comments that the protection of DNA

against heat damage is primarily caused as a result of the saturation of spore DNA with a group of small, acid-soluble spore proteins (SASP), which are synthesized in the developing spore and degraded after completion of spore termination.

The possibility of sterilizing heat-sensitive products at relatively low temperatures for a short period of time makes the use of microwaves very intriguing according to Jeng and others (1987) who inactivated spores by exposing them to 4 kW at 2.45 GHz. The total exposure times required to reduce 10^5 spores in glass vials were 75 and 48 min at 130 and 137 ^{o}C, respectively. If microwave treatment can sterilize dry products more efficiently at low temperatures and low exposure times than conventional heating, then it can, at least in principle be attributed to their non-thermal effects. However, Jeng and others (1987) discovered that microwave-heating, at temperatures below 117 ^{o}C was not effective, and this suggests that the sporicidal activities of microwaves are ascribable to their thermal effects.

Vaid and Bishop (1998) provided a further explanation in experiments involving the microwaving of *Bacillus megaterium* NCIMB 7581, *B. stearothermophilus* NCIMB 8922, *Clostridium sporogenes* NCIBM 8053, and *Thermoanaerobacterium thermosaccharolyticum* NCIMB 9385. The microwaving was performed with a 600-W microwave oven and two conditions: (i) 14 bar, 140 ^{o}C for 2 – 14 min with increasing durations of 2 min, or (ii) 14 bar for 8 min at temperatures of 60 – 200 ^{o}C with increments of 20 ^{o}C. The authors also boiled the spores for varying lengths of time, but even after the maximum duration of boiling (14 min) no breakage of the spores was observed. On the contrary, when spores were microwaved, they collapsed after 8 min when their final temperature reached 100 ^{o}C. When they were microwaved at 140 ^{o}C for increasing periods of time, a maximal release of Ca^{2+} and biomolecules absorbing at 260 nm were found above about 9 min of exposure. For the spores of all species, the release of Ca^{2+} occurred more rapidly than did the release of material absorbing biomolecules at 260 nm. It is the latter indicator that the authors presumed should give a measure of the release of core components such DNA, DPA, or nucleotides. In order to liberate DNA, the heating for at least 8 min at 160 ^{o}C was required. Finally, it was observed that the profile of amplification products observed

for each organism remained the same, even when the spores had been microwaved at the highest temperature employed (200 ^{o}C).

The heating effect of microwaves is attributable to the excitation of small polar molecules such as water; however, the spore protoplast is in a dry state, and therefore another molecule is excited rather than water. The authors tested if DPA could fulfil this role or supplement the effect of water by examining suspensions of identical cell densities of spores of *B. sphaericus* NCTC 9602 and the deficient mutant CW6 for DPA. It was found that the parent contained nearly 3 times as much DPA as CW6. The profiles of time- and temperature-dependent release of components absorbing at 260 nm and Ca^{2+} releases were almost identical, and these results indicated that DPA does not play a significant role in the microwave-induced destruction of bacterial spores.

The authors concluded that with respect to the disruption of spores at a given temperature, microwave radiation exerts a more significant effect than conventional heating. For example, spores of *Cl. sporogenes* heated by microwaves at 100 ^{o}C for 8 min showed clear signs of disruption to their structure, but a similar exposure to boiling water left them unchanged. Conventional heating, even when prolonged, does not result in the fragmentation of spores produced by microwaves, and thus a different mechanism is involved in each case. A possible explanation for the fragmentation of spores observed under these conditions is an 'explosion' ascribable to internal pressure generated within the core (Vaid and Bishop 1998).

Celandroni and others (2004) used a microwave waveguide (100 W output power) as an applicator to generate a uniform and measurable distribution of the microwave electric field; the authors considered that this experimental apparatus also gave a measurable temperature distribution. Spore suspension aliquots (0.25 mL) were irradiated for different time intervals up to 20 min and the waveguide fibre optic was used to measure the temperature. This temperature reached the set-point of 101 ^{o}C in 45 s. Exposure of *Bacillus subtilis* spores to microwave irradiation did not modify the cortex, and extracellular DPA was not detectable by observation, although complete spore destruction was seen at 20 min of irradiation. The authors suspected

that microwaves promote the formation of stable complexes between DPA and selected spore components, particularly Ca^{2+} ions, a process blocking the release of DPA (or its chemical modification). Finally, they showed that DPA depends on calcium concentration. The authors recommended that microwave sterilization can substitute the conventional methods and they related, for the first time, the inactivation of spores to the well-defined electric field rather than to microwave source. Additionally, the lack of cortex swelling indicated a marked effect exerted by the electric field on spores. 'Dark-spots' were observed in the protoplasts of conventionally- and microwave-heated spores, most likely attributable to the aggregation of core proteins. Salvatorelli and others (1996) showed that the ability of *Bacillus subtilis* spores (when kept in tryptic agar to generate colonies) declined when exposed to microwaves. The authors used 250 mL of brain heart infusion agar that they then inserted in a microwave sterilizer (600 W), and radiation was applied until the boiling point was reached. The microwaves caused a distinct progressive drop in spore viability as a function of exposure time, and total inactivation was achieved after 5 min which the authors attributed not solely to the effects of heat.

Mechanisms for the interaction of microwaves with bacterial cells and its effect on DNA and RNA

Microwave energy is of course insufficient to break an O-H bond of the water molecule. The energy of microwaves (with a typical wavelength of 10 cm in free space) is around $1.2 \cdot 10^{-5}$ eV and the bond strength of the water molecule is 5.2 eV (Rosen 1972). Hence, the quantum energies of microwaves and radiowaves fall short by several orders of magnitude with regard to the breakage of chemical bonds. However, it is not impossible that the energy of microwaves generally influences the rotational motion of hydrogen bonds which, as noted above, are about 10 times weaker than the chemical bonds in water. Although microwave energy is sufficient to partly rotate the molecule of water, such a process is not easily achievable for water that is bound to proteins in biosystems.

If the water molecules are bound so that they are unable to rotate in an electric field at frequencies higher than those corresponding to the protein relaxation region, then the dielectric constant at microwave frequencies will be ascribable to "free water" in the solution, apart from small contributions from atomic and electronic polarization. This water is referred to as irrotationally bound (LSBU 2006).

Water undergoes radical changes when it approaches the surface of DNA. As the molecules approach the double helix the motion of individual molecules becomes slower. It seems that water molecules linger longer around some 'troughs' in the double helix that is formed by specific base pairs, and the level of hydration mirrors the base pair sequences.

The extent of damage to the RNA of *Staphylococcus aureus* cells during sub-lethal microwave injury was greater than that during conventional sub-lethal heating according to Khalil and Villota (1989). The cells were suspended in 0.10 M·dm^{-3} sodium phosphate buffer, (pH 7.20), heated for 30 min at 50 ^{o}C and then cooled to 37 ^{o}C (a glass heat exchanger was placed in the oven cavity so that the cell suspension would flow in a glass coil 0.5 cm I.D. and 1.0 m length). This glass coil was fitted within a glass cylindrical tube in which kerosene was allowed to flow in a counter-current manner, and cells were heated in a microwave oven of 700 W. Kerosene doesn't heat in a microwave field and it is used in order to remove the heat from the sample as an attempt to isolate the microwave effect. The temperature was monitored by inserting 2 copper-constantan thermocouple leads at the inlet and outlet ports of the circulating sample line, just outside the cavity. When cells were allowed to recover, the conventionally heated ones regained normal profiles of the 16S and the 23S RNA after 180 min., whilst the microwave-heated ones restored the 16S after 180 min, but the 23S after 270 min. These results are explicable by assumptions that there is overheating taking place in certain cell components attributable to variations in the dielectric properties of cell constituents. Another factor responsible for the localized heating may be water molecules bound to cellular macromolecules. Of course, water shells possess physical properties which markedly differ from those of bulk water and therefore behave differently in a microwave environment.

Manoilov and others (1974) have investigated the effects of mm-wavelength on certain aspects of the protein metabolism of anaerobic and aerobic bacteria and fungi, in particular *Cl. sporogenes, Cl. histoluticum (anaerobes), Act. norsie* and *Penicillium nigricans*. The microbes were irradiated at wavelengths of 7.2 and 7.6 mm (in free space) at an average power flux density of 4-5 mW/cm^2 by a backward-wave-tube and the authors focused on two groups of amino acids: those with acidic properties (glutamic and aspartic acids), and those with alkaline properties (histidine, lysine, and arginine). Whilst the number of "acidic" amino acids in the nutrient medium increased after growth of the microbes irradiated at 7.2 mm, no differences in their contents in the medium were detected after irradiation at 7.6 mm.

In the case of the "alkaline" amino acids, the amounts found in the culture medium were smaller during growth of bacteria irradiated at 7.2 mm, and at a frequency larger in the case of 7.6 mm. Changes in the contents of "acidic" and "alkaline" amino acids were also observed after irradiation of aerobes, anaerobes, and fungi at 7.2 mm; the metabolism of other amino acids was subject to substantial variations, both qualitative and quantitative. The authors argued that electromagnetic radiation in the millimeter band has a significant influence on protein metabolism by bacteria, which is manifested either in the form of activation or inactivation of proteolytic enzymes or by a modification in the activity of enzymes participating in the metabolism of the individual amino acids.

Kiselev and Zalyubovskaya (1974) examined the structural elements of cells, viruses, and micro-organisms after they were irradiated with microwaves. Their studies showed that the mm-irradiation of isolated cells caused damage to the cell membrane, degeneration of the cytoplasm, and an increase in cell size when irradiated at 46.1 GHz.

The total nucleic acid and albumin contents of cells irradiated at 46.1 GHz showed increases. Whilst the control group had RNA and DNA contents of 74.9 ± 5.1 µg and 96.8 ± 9.4 µg, respectively, and albumin 109.8 ± 6.7 µg, the values after irradiation were 97.3 ± 3.6 µg for RNA, DNA 137.7 ± 6.2 µg for DNA and 130 ± 8.6

mg for albumin. Possibly, microwaves had influenced their synthetic processes via alterations in metabolism. A decrease in the number of viable cells was observed after irradiation at various wavelengths: in the range 5.9-7.5 mm, the 6.5 mm wavelength showed more conspicuous biological activity. What the authors meant with the last statement was a sharp increase in pH and fibroblasts and cell survival.

Porcelli and others (1997) exposed 2 thermophilic and thermostable enzymes, *S*-adenosylhomocysteine hydrolase (AdoHcy) and 5'-methylthioadenosine phosphorylase (MTA phosphorylase) to 10.4 GHz microwaves in order to discriminate between their thermal and non-thermal effects. The authors concluded that the exposure caused a non-thermal, irreversible, and time-dependent inactivation of both enzymes. The exposures were carried out in a waveguide system where accurate microwave dosimetry and thermal control were provided. Various SAR (specific absorption rates) were used in the range of 1.5 – 3.1 W/g, and the temperature varied from 70–90 ^{o}C. Results showed that at 90 ^{o}C AdoHcy hydrolase retained only 18% activity after 40 min irradiation compared to a control sample incubated at the same temperature without irradiation. Under the same conditions, MTA phosphorylase still retained 78% activity after 40 min, a greater inactivation (58%) occurring only after 90 min. Such enzymatic inactivation observed was most likely ascribable to a non-thermal microwave effect since AdoHcy hydrolase appeared fully active after 90 min of incubation at 70 ^{o}C and after 30 min at 90 ^{o}C. In a previous investigation, Cacciapuoti and others (1994) found that MTA phosphorylase remained completely stable for up to 2 h of incubation at 100 ^{o}C. Comparison of the experimental results showed that the effect exerted by microwaves depends on the structure of the specific protein. In fact, at 90 ^{o}C, when the power absorbed (SAR) by the 2 enzymes was similar, the decrease in their activity values differed significantly. The effect of the electromagnetic field does not depend on the enzyme concentration of the sample, since experiments carried out at different protein concentrations did not reveal any modification in the inactivation kinetics.

 Davis and others (1986) showed that long-chain DNA in saline buffer does not absorb microwaves significantly more than its solvent, but that specific short-length

molecules can absorb microwaves resonantly. This suggests that microwave absorption increases with time as the endonuclease cleaves the long chain of DNA into shorter lengths. According to the observations of this research group, microwave absorption is chain length-dependent. The absorption found for short DNA molecules may be important, and that is because long-chain DNA is wrapped around with proteins and short resonant lengths can result between binding sites which represent a discontinuity on the molecule from an acoustic impedance standpoint. Therefore, if excitation of the DNA results, the relaxation of the mode should be sufficient so that it results only in local heating. For microwave-irradiation levels below currently accepted levels of significant bulk-heating (about 1 mW/g), even for DNA molecules with absorption cross sections of 2 orders of magnitude above the surrounding liquid, there is no significant rise in temperature because of thermal conduction of the rapid heat removal from the vicinity of DNA. This, however, does not eliminate the possibility of thermal effect; on the contrary, Davis and others (1986) argued that the possibility of effects resulting from the microwave frequency excitation of an acoustic mode of the double helix does not make it necessary that this acoustic mode is promoting structural or conformational changes. It may be that conversion to another mode, particularly one with a long relaxation time that accomplishes this; ordered motion of the double helix probably reduces the ability of site recognition for some other active molecule.

Belyaev and others (1993) used the method of anomalous viscosity time dependence to study the influence of mm electromagnetic radiation (EMR) on the genome conformation state of *Escherichia coli* K12 cells. They used the 42.28 – 41.37 GHz frequency range and the results indicated that the frequencies of the resonance interaction of *E. coli* cells with low-intensity mm waves are determined by the genome structure. Their research showed that the frequency-dependence of the effects in 2 of the ranges investigated had a pronounced resonance character, with resonance frequencies of 41.32 GHz and 51.76 GHz. There was a substantial difference between the effects of millimetre waves at these resonance frequencies. Only right-handed circular polarization proved effective when intact cells were exposed to EMR at frequencies of the first resonance. Left-handed circularly

polarized microwaves did not affect the cells. Conversely, only left-handed polarization was effective when cells were exposed to EMR at frequencies of the second resonance. The results suggested the existence of selection rules on helicity at resonance absorption of EMR quanta and they provided experimental evidence for the quantum character of interactions between mm waves and cells.

Signs of effective polarization of both resonances were inverted when EMR was applied to the cells previously exposed to X-rays at 20 Gy, and this led to the conclusion that the target of the resonance interaction between differently polarised EMRs and cells was the same, whilst X-rays modified the target's conformation. Apart from DNA, no other molecules are currently known to be able to change their conformation at such small doses of microwave radiation. Therefore, the results acquired here represent a major DNA target of resonance interaction between mm waves and cells.

Bohr and Bohr (2000) reported that microwave irradiation can affect the kinetics of the folding processes of some globular proteins, especially β-lactoglobulin. In such a case, the application of microwaves holds promise for a wide range of biotechnological applications, such as protein synthesis and protein aggregation, applications which may additionally have implications for biological systems. It still has not been examined how external radiation can influence the conformation of proteins and the authors suggested that microwaves can cause such effects through a stimulation of the coherent intrinsic dynamics in biomolecular macromolecules, such as DNA, RNA, and proteins. This is in agreement with the theories that claim that protein folding arises from a competition between torsional and bending forces, and is not only driven by entropy (Bohr and Bohr 2000).

Bohr and Bohr (2000) monitored the refolding of the protein β-lactoglobulin by the optical rotation dispersion (ORD) technique, which measures the polarization of light. The re-folding experiment for β-lactoglobulin consisted of transforming the sample from the 'cold-denatured' state to the folded state by raising the temperature from 5 to 44 $^{\circ}$C, the latter temperature being utilized to allow to equilibrate completely over about 3 h. Subsequent to performing this re-folding

experiment, the cooling-heating cycle was monitored as a kinetic loop, and the results showed a kinetic hysteresis loop which is the result of the slow reaction kinetics and the measurement of the loop allowed the study of abrupt changes in reaction kinetics.

In order to radiate the solution of this globular protein, the authors used the standard magnetron of a microwave oven operating at 2.45 GHz the oven was redesigned in order to accommodate a polarimeter. The power of exposure was 800 W, causing a temperature increase of the protein sample of about 0.3 $^{\circ}$C; the power absorbed from the 3.0-mL sample was 0.75 W. After the microwave irradiation the sample holder was placed back to the polarimeter to measure the polarization again. The experimental procedure employed involved the equilibration of denatured β-lactoglobulin in solution at 4 $^{\circ}$C. Primarily, the temperature was increased to 48 $^{\circ}$C without the application of microwaves and then it was diminished to 4 $^{\circ}$C and during the decrease microwaves were applied at a temperature of 20 $^{\circ}$C. After re-equilibration at 4 $^{\circ}$C the temperature was raised to 48 $^{\circ}$C again, and at 8 $^{\circ}$C during the re-folding increase microwaves were also applied. The authors discovered that by application of microwaves at 8 $^{\circ}$C during the heating cycle, the polarization made a large 'jump' towards the folded state, and that temperature effects were more separable from microwave effects during the cooling cycle. During this cycle, a large 'jump' toward the denatured state was observed. The results acquired demonstrate that without microwave irradiation, this unfolding/re-folding takes a few hours to reach equilibrium, whilst with microwaves the equilibrium at that temperature is reached in the order of seconds and faster than 1 min.

Experiments supporting the thermal effect

Shazman and others (2007) built a system that allowed the output of high microwave energy (satisfactory temperature control), while in parallel accurately performing a similar heating procedure, of the same time-temperature profile, in a conventional non-microwave heating apparatus. The microwave oven was operated

at 2.45 GHz, and the specific absorption rate was 1000 W/kg with continuous radiation up to 48 h. Using this apparatus the authors studied 5 phenomena, including the Maillard reaction, protein denaturation, mutagenesis of bacteria, glucose mutarotation, and saturation solubility of sodium chloride; no athermal effect was detected in any of these experiments.

For the *Maillard reaction,* the results showed that there was an insignificant difference between the absorbance readings of solutions heated in the microwave oven and the bath, hence it was concluded that the athermal effect exerted no influence on this complex reaction system.

The same was true for protein denaturation. The differences observed between microwave and conventional heating were small, and therefore were attributed to the inconsistency in protein aggregation or even adherence of aggregates to the spectrophotometer cell (cuvette) during heating. Thus, the authors suggested that the slight differences in the development of turbidity during microwave heating, when compared to bath heating, may well be within the experimental error, and hence there was no evidence for athermal effects.

With regard to the mutagenesis *of bacteria*, the authors had to remove the hot spots in the domestic microwave cavity by stirring the test solution, otherwise rapid mutagenesis might be induced simply by the overheating of specific loci. The authors could not detect any difference between the *mutarotation* performances in microwave and water bath heating processes. Some of the hypotheses behind athermal effects of microwave-heating suggest that microwave-radiation may modify the solvent properties of water. That was tested by using the method of saturation solubility of salt and the experimental results revealed no change between the refractive index of the salt solution in the microwave oven and that obtained on bath-heating.

Several different types of organic reactions were carried out both in sealed Teflon vessels in a microwave oven and under traditional reflux conditions. Gedye and others (1988) described the use of microwave ovens for synthesizing esters from carboxylic acids, carboxylic acids from alkyl benzenes and amides, and ethers from

alkyl halides. In fact, these organic reactions occurred up to 1,240 times more rapidly in microwaved sealed Teflon containers than by classical reflux methods. The factors that affect these syntheses were further examined. The first experiment involved heating 50 mL of several organic compounds in open vessels in a microwave oven for 1 min at 560 W at a frequency of 2.45 GHz, to determine the types of molecules that absorb microwave energy. It was found that all polar compounds absorbed significant amounts of microwave energy, while little or no microwave energy was absorbed by non-polar solvents. Conclusively, the rate at which a molecule absorbs microwave energy depends on the polarity of the molecule and, as a consequence, on its dielectric constant. Hence, microwave-heating will only cause significant rate enhancements in organic syntheses in polar solvents. Furthermore, the homogeneity of the reaction has little effect on the rate enhancement and the microwave technique can be used to increase the rates of both homogeneous and non-homogeneous reactions.

The rate of reaction varied inversely with the volume of the container and it increased when the pressure in the Teflon bottle increased. The greater rate of reaction in the microwave oven also occurred when the high pressure in the sealed Teflon vessels allowed the microwaves to superheat the reaction mixture. The point at which the maximum amount of microwave energy was retained by the solvent (the maximum heating rate) was observed at different volumes for different solvents, and this showed that microwaves only heat the molecules but do not activate them in any different manner.

In a different series of experiments, Gedye (1997) re-examined 3 different reactions that were reported to be substantially accelerated by microwave irradiation at atmospheric pressure to determine if there was such a non-thermal effect.

Srikrishna and Nagaraju (1992) reported that microwave irradiation accelerated the ortho-ester Claisen re-arrangement of allylic alcohols in DMF in open vessels. In a microwave oven, the reaction appeared to occur 250 times faster. Gedye (1997) performed the same experiments (synthesis of chalcones by crossed-aldol condensations in a microwave oven) only to discover that the yield of 4 of them

(52%) in the microwave reaction was not significantly higher than that (47%) obtained by conventional heating. The reaction times reported were reduced from hours to minutes using microwave-heating, the results confirming that the evaporation of ethanol occurred in the microwave-heated reactions so the microwave-heated reactions would have been expected to give higher yields in the same time period in view of a more concentrated solution and a higher reaction temperature. There was a rate enhancement in this reaction after using solid NaOH but that was only 1.5 times greater, so this could be attributed to superheating of the solvent or to 'hot-spots' in the reaction mixture by the microwave exposure rather than to a non-thermal effect.

Finally, Adamek and Hajek (1992) have reported that the addition of CCl_4 and CCl_3CO_2Et to styrene in the presence of a homogeneous Cu(I)-amine catalyst in CH_3CN occurs more rapidly under microwave-heating than conventional heating at the same temperature. The investigation of Gedye (1997) showed an increase of only 1.5x with the addition of CCl_3CO_2Et, and no rate increase with the addition of CCl_4. Higher rate enhancements were observed when the reactions were conducted in the presence of a small amount of solid CuCl, under heterogeneous conditions. The higher rate enhancements observed under heterogeneous conditions can be accounted for by the increased temperature of the solid CuCl in the microwave reaction; but careful reconsideration of the experimental apparatus indicates that the small rate enhancements of reactions by microwaves observed may be attributable to localized 'hot-spots' or to superheating of the solvent.

Experiments supporting the non-thermal effect

The main challenge wishing to distinguish between thermal and non-thermal (or athermal) effects is the difficulty in keeping the temperature constant during microwave irradiation processes. In order to overcome this, Sato and others (1996) developed a system to maintain constant temperature. Using this system, the death rates of *E. coli* cells exposed to microwave irradiation were examined and compared with those obtained by a conventional 'heat-kill' method. They employed a

magnetron generator and a wave guide-type applicator and used 2 microwave power sources: (1) continuous wave (CW) at 2,45 GHz which was operated at 35, 40, and 46 W and (2) pulsed wave (PW) at 3 GHz with a maximum power of 50 kW and a mean power of 35 W and 0.7 µs pulse duration and 1 ms repetition period.

Results arising from CW and PW irradiations at 45 ^{o}C showed that only 20% of the cells were killed as a consequence of heating for a period of 40 min, whereas 50% and almost 90% of the cells exposed to CW and PW irradiations, respectively, were killed. These experiments were repeated at a temperature of 50 ^{o}C and similar results were obtained. According to Sato and others (1996), these data suggest that microwave treatment has its own non-thermal effect and, in particular, the PW has a more pronounced killing effect than the CW. Several other attempts have been made to assign the non-thermal effect of microwaves to the interactions of the electric field with the cells. In particular, Barnes and Hu (1977) argued that the non-thermal effects of microwaves observed are attributable to a reorientation of long-chain molecules and to ion shifts across membranes and it is this ion transport that is responsible for an increase in potential difference and electrical current across cell membranes. Indeed, microwave irradiation has been found to exert a significant effect on the secondary and tertiary structures of proteins and nucleic acids (Straub and Carver 1975). Although the precise mechanism of the non-thermal effect is unknown, violent motion of dipoles in molecules induced by microwave fields appears to enhance the reactivity of polyatomic molecules, such as proteins and phospholipids, at high temperatures. Microwaves either cause ions to accelerate and collide with other molecules or cause dipoles to try to rotate and line-up with rapidly alternating electrical fields (the pearl chain effect).

Conclusions

Pulsed microwave exposure investigations coupled with further experiments, using higher frequencies towards millimetre wavelengths, have found a pronounced killing

effect towards microorganisms at lower power levels. The biological activity of cells is greatly influenced by microwave-irradiation and, as a result, structural modifications to DNA and RNA occur. Possible explanations offered revolve around the lethal thermal stress levels exerted under microwave exposure which induce loss of membrane integrity with particular frequencies inhibiting cell growth, whereas some appear to increase it. However, it is widely accepted that the thermotolerance of microorganisms strongly depends on factors such as their lipid, salt, and protein contents and those of the surrounding carrier environment. The argument that selective absorption of microwave energy by cells is ascribable to the difference in the dielectric loss tangent from the one of the surrounding media, has not, however, been put forward convincingly. Lack of microwave field control during experiments conducted in conventional ovens (as opposed to tuned cavities and waveguide geometric configurations), in addition to *in situ* thermal gradient measurements at microscale, raise important questions that still await answers. A future research area worth pursuing is to expose cells in waveguides, using modulated microwaves; and further experiments performed in this area may provide valuable information regarding the non-thermal microbiocidal properties of microwaves and the molecular basis thereof.

PART 4: THERMAL CONVERSION OF LDHs INTO OXIDES USING MICROWAVES AND CONVENTIONAL HEATING

4.1 Calcination of Layered Double Hydroxides (LDHs)

So far, calcinations of LDHs occur in furnaces. This is time consuming and expensive and the heat transfer mechanism involved is conduction. This results in thermal gradients, which results in uneven heating. Microwaves can be used in the future for calcinations in order to determine if the products and their properties are different.

4.2 Dielectric Heating

Typical frequencies for microwave processing of materials are: 915 MHz, 2.45, 5.8 and 24.124 GHz. The successful use of microwaves requires the processor to have a good understanding of the strengths and limitations of the microwaves. Among their strengths are:

• penetration

•controllable electric field distributions

•rapid, volumetric and selective heating

•self limiting reactions

While an empirical understanding of microwave processing is important in moving developmental processes into production, a more fundamental approach is required for development of optimised process cycles, equipment and controls. The microwave heating effect uses the ability of some liquids and solids to transform electromagnetic energy into heat and thereby drive chemical reactions (Mingos 1991). This *in situ* mode of energy conversion has magnitude that depends on the properties of the molecules. This allows some control of the material's properties

and may lead to reaction selectivity. A material can be heated by applying energy into it in the form of high frequency electromagnetic waves. The origin of the heating effect by the high frequency electromagnetic waves arises from the ability of the electric field to polarize the charges in the material and the inability of this polarization to follow the extremely rapid reversals of the electric field (there is an accompanied relaxation time). In a given frequency band, the polarization vector, **P** lags the applied electric field ensuring that the resulting current, $\frac{\partial P}{\partial t}$, has a component in phase with the applied electric field, which results in the dissipation of power within the insulating material. Coupled with these polarization effects, a dielectric can be heated through direct conduction effects due to, for example, redistribution of charged particles under the influence of the externally applied electric field forming conducting paths, particularly in mixtures of heterogeneous materials (Metaxas 1988). The interaction of an electric field with a dielectric has its origin in the response of charged particles to the applied field. The displacement of these particles from their equilibrium positions gives rise to induced dipoles which respond to the applied field. Such induced polarization arises mainly from the displacement of electrons around the nuclei (electronic polarization) or due to the relative displacement of atomic nuclei because of the unequal distribution of charge in molecule formation (atomic polarization). Apart from these mechanisms, there are also the polar dielectrics, which contain permanent dipoles due to the asymmetric charge distribution of unlike charge partners in a molecule (like water dipole) which tend to re-orientate under the influence of a changing electric field, thus giving rise to orientation polarization. Finally another source of polarization arises from charge build-up in interface between components in heterogeneous systems, termed interfacial, space charge or Maxwell-Wagner polarization. These two mechanisms together with dc conductivity form the basis of high frequency heating.

4.3 LDH Description and Preparation

The term of Lamellar Double Hydroxides (LDHs) is used to designate synthetic or natural lamellar hydroxides with two kinds of metallic cations in the main layers and interlayer domains containing anionic species plus water. This family of compounds is also referred to as *anionic* clays, by comparison with the more usual *cationic* clays whose interlamellar domains contain cationic species. Mg(II) was replaced by metals that have similar radius (in this case: Cu(II), Fe(II) and Co(II)). Cr(III) replaced 10% of Al, but the effort to replace 100% of aluminium with chromium failed(APPENDIX 6). The structure of LDHs can be seen in F*ig. 4.1* and *4.2*. In F*ig.4.1* the octahedral units share edges to form the brucite $Mg(OH)_2$ type layers which contain divalent and trivalent cations with a net positive charge. Between these layers anions and water intercalated to balance the excess positive charge. In *Fig.4.2* spacing between the (0 0 1) planes (d_{001}) can be seen, which can be determined from the lowest angle reflections in the powder XRD patterns. This distance is 7.6-7.8 Å (Rives 2001). Before calcinations, the thickness of one layer of Mg/Al is 4.8 Å and the thickness of the interlayer distance is approximately 3 Å (Rives 2001).

Fig.4.1: from: http://www.tececo.com.au/technical.nanocomposites.php
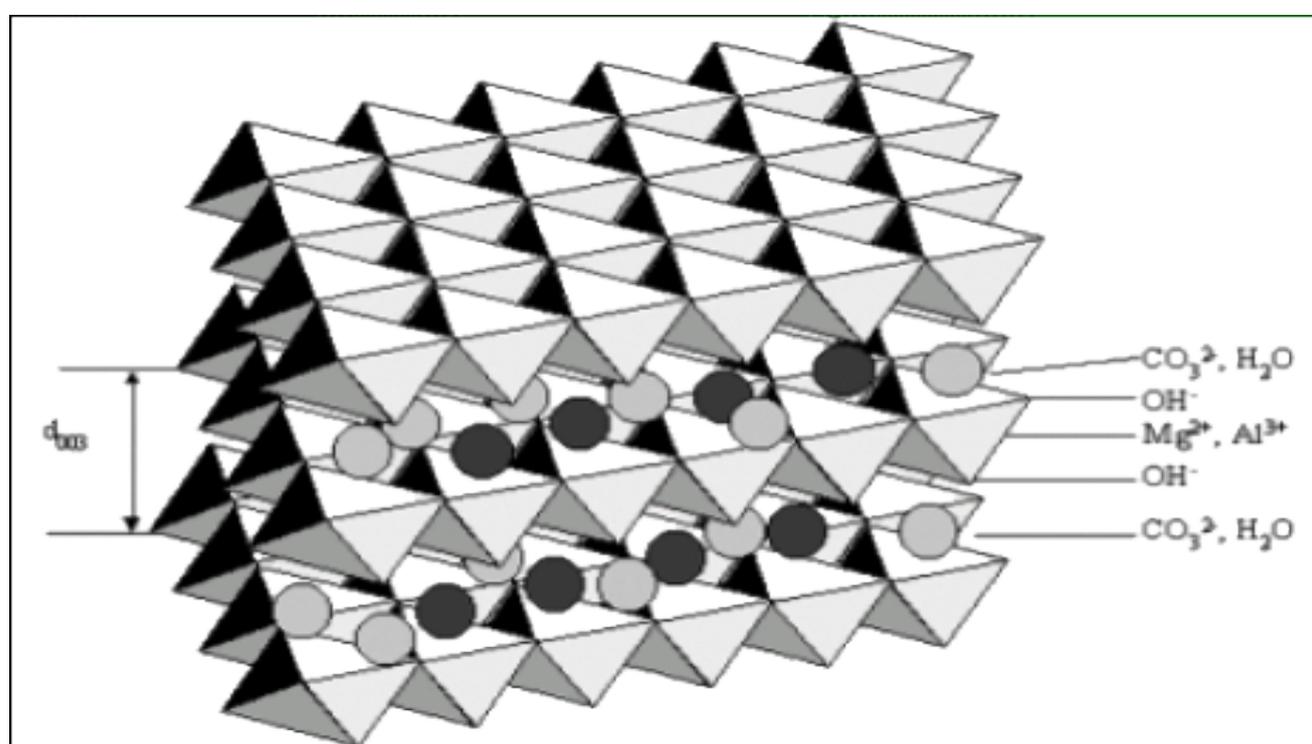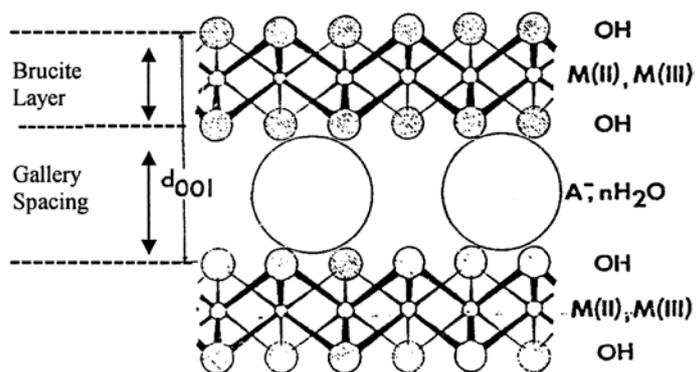
Fig. 4.2: from: www.crops.org

Preparation of Mg-Al-CO$_3$

The LDHs were prepared according to the instructions of Hudson (1995) paper. Mg-Al LDHs (molar ratio Mg:Al = 3:1), were prepared and in some cases 10% of Mg molar mass was replaced by other metals, namely Fe(II), Cu(II) and Co(II) and in two of the cases the total or 10% of Al(III) was replaced by Cr(III). LDHs where the Cu content increased were also produced.

An aqueous solution of Mg(NO$_3$)$_2$·6H$_2$O (85.47 g, 0.33 mol) and Al$_3$(NO$_3$)$_3$·9H$_2$O (62.52 g, 0.33 mol) in doubly deionized water (233 cm^3) and either Co(NO$_3$)$_2$,?H$_2$O, Fe ditto or Cu ditto at the appropriate concentrations to give the target compositions of Al:Mg:M(transition metal) 1:1.5:1.5 was added dropwise to an aqueous solution of NaOH (380 cm3; 23.35 g, 0.58 mol) and anhydrous Na2CO3 (0.33 g; 0.32 mol). This addition was carried out with fast stirring (ca 300 rpm).

Found Mg 16.28; Al 8.85; C, 2.49; H, 3.66; N, 0.69% which were the values calculated for Mg6Al3.4(OH)18.82(CO3)1.51(NO¬3)0.36•4.5H2O.

There was aging step as well, the suspension of the LDH precipitate was held at 60 ^{o}C for 2 hours to increase crystallinity. The filtered precipitate was washed very thoroughly in part to remove any traces of entrained sodium salts which can affect the catalytic properties rather a lot. Then it was dried in the oven at 100 ^{o}C or less

4.4 Experimental Results for Mg-Al LDHs

4.4a TG and DSC

Layered Double Hydroxides constitute the counterpart for the long time known cationic clays; they are formed by positively charged layers, with balancing anions and water molecules in interlayers. The most widely known LDHs contain M^{+2} and M^{+3} cations in the layers, but other systems contain M^{+}/M^{+3} or even M^{+2}/M^{+4} and $M^{+2}/M^{+3}/M^{+4}$ are also known (Rives 2001). As with cationic clays, the interlayer anions can be exchanged, although exchange of carbonate is rather difficult, so anionic exchange representing an alternative way for synthesis of new hydrotalcites. Also as cationic clays, hydrotalcites can be pillared with polynuclear anions, so anionic exchange representing an alternative way for synthesis of new hydrotalcites. Also as cationic clays, hydrotalcites can be pillared with polynuclear anions, including metal-containing oxometalates or coordination compounds (Rives 2001).

LDHs are less stable than cationic clays and when they are heated they undergo collapsing, even at moderate temperatures leading to crystalline three dimensional phases which precise nature depends on several factors. Moreover the mildly calcined product shows an ability to recover the original layered structure after its exposure to moist air (*Fig. 4.7b*) or when immersed in aqueous solution containing anions, this method has been used again as an alternative route to prepare LDHs. The memory effect of LDHs was observed in my experiments as well.

One of the most interesting application of LDHs is their role as precursors for heterogeneous catalysts, the catalytic performance of which strongly depends on the method followed during thermal decomposition from the original LDH to the final mixture of metallic oxides. Differential Scanning Calorimetry and Thermogravimetric analyses both show the reactions that occur when LDHs are heated and the heat involved in each of the processes.

 The DSC curves for LDHs have three endothermic peaks. The samples were heated in flowing air atmosphere and the heating rate was 5 ^{o}C/min. The results for Mg-Al LDHs show the first peak at approximately 70 ^{o}C corresponds to the loss of loosely bound water in the interlayers (Rives 2001). The second, at 244 ^{o}C is the loss of water that is formed by the loss of structural OH^{-} and the third peak at ~ 424 ^{o}C corresponds to the decarbonation of the interlayer, i.e. loss of CO_2 (*Fig. 4.3*).
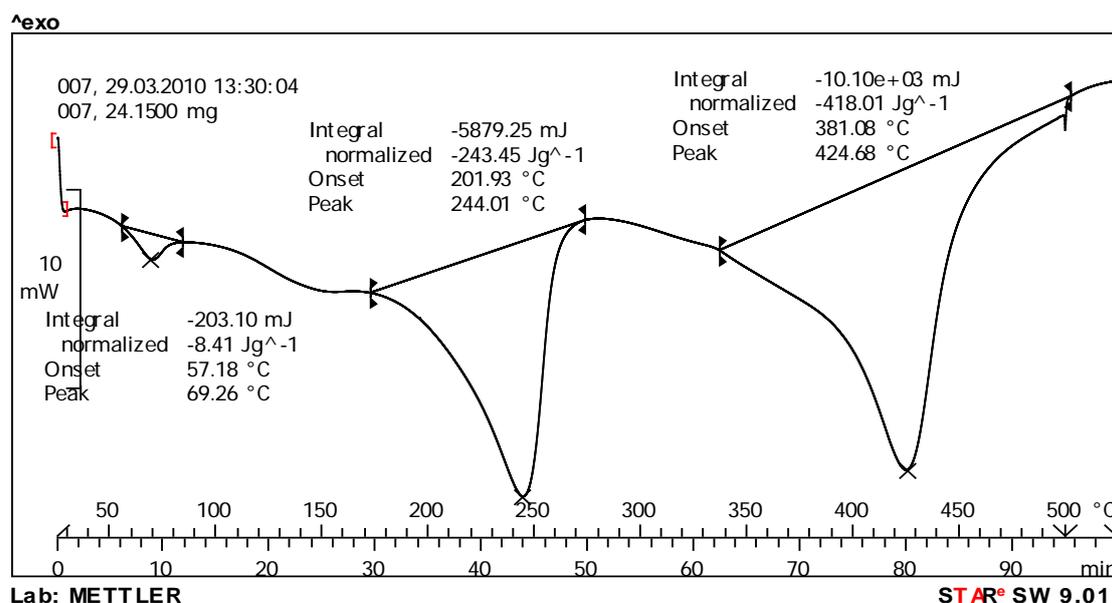
Fig. 4.3: *DSC results for 007 LDH, three endothermic processes are observed.*

TG curves can be used to determine the amount of water in the interlayer space of LDHs (Rives 2001). In the case of Mg,Al-CO_3 LDH, the final product after high temperature calcinations (1000 ^{o}C) is a mixture of MgO and Al_2O_3 or MgO and $MgAl_2O_4$ (spinel), in both the cases the calculations for weight loss are the same. Decarbonation and dehydroxylation account together for the weight losses up to ~450 to 500 ^{o}C. No peak appears in my experiments at 305 to 320 ^{o}C even though it should according to Rives and according to the same source this peak is because of dehydroxylation of OH$^-$ bound to aluminium. There is a peak at 375 to 400 ^{o}C and this one has been attributed to dehydroxylation due to OH$^-$ bound to Mg and the main CO_2 evolution.

4.5 Powder X Ray Diffraction

4.5a X-Rays

X-rays were discovered in 1895 by Wilhelm Conrad Roentgen who was awarded the 1901 Nobel Prize in Physics for his discovery. X-rays are a type of radiation that have short wavelengths and are very high in energy. The wavelengths of X-rays are typically between 0.1 and 100 Angstroms. This is of the same order as typical

molecular bond distances which lie in the range of 0.8 to 3 A and this enables the X-rays to interact with the contents of a crystal allowing a crystallographic experiment to be performed (Ooi 2010).

X-rays are generated when an electron in an excited state relaxes back to its ground state. The total amount of energy emitted is the equivalent of the energy difference between the excited state and the ground state; and also corresponds to the specific wavelength of the emitted radiation, where $E = hv$ (E is the energy emitted, h is Planck's constant and v is the frequency of the wavelength). When an electron relaxes to its ground state from an excited one, the types of radiation that are emitted depend on which atomic shells are involved in the transition. The atomic shells, K, L and M are represented in *Fig. 4.4*. The figure also shows the types of radiation that are emitted when the electron moves between these shells. When an electron moves from L to K, it gives Kα wavelength. The Kα wavelength is known as the 'characteristic X-ray' of a given substance and it changes from element to element since each has different energy levels. Copper and molybdenum are the most common sources used for X-ray diffraction experiments.
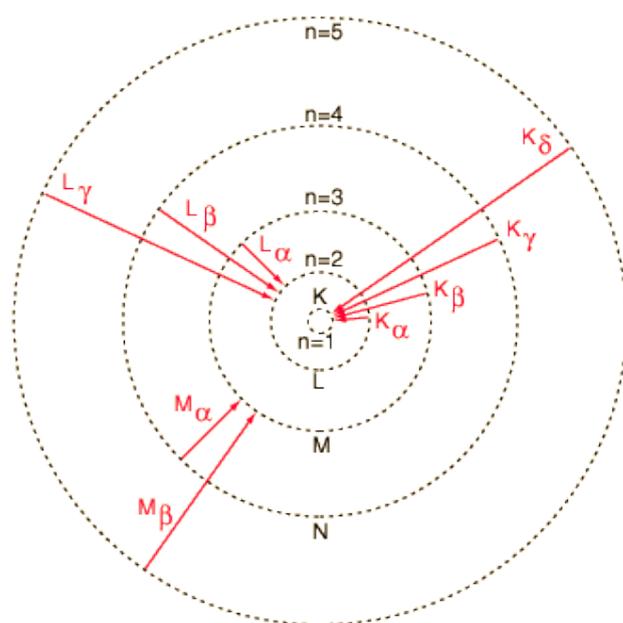
Fig. 4.4: *Cu Kα radiation*

4.5b Diffraction by crystals

During an X-ray diffraction experiment, a crystal is irradiated with X-rays. The interaction between the oscillating electrons within each atom in the incoming X-ray beam causes the X-rays to diffract in all directions. The diffracted X-ray beams from all the Miller sets gives rise to diffraction spots. The diffraction of X-rays by a crystal lattice can be explained by Bragg's law.

4.5c Bragg's law

A qualitatively simple method for obtaining the conditions for diffraction was derived in 1912 by W L Bragg who considered the diffraction as the consequence of contemporaneous reflections of the X-ray beam by various lattice planes belonging to the same family, physically, from the atoms lying on these planes (Miller sets as aforementioned). Let θ be the angle between the primary beam and the family of lattice planes with indices h, k, l (having no integer common factor other than 1). The difference in path between the waves scattered in D and B is equal to AB + BC = 2dsinθ (*Fig. 4.5a*). If this is a multiple of λ then the two waves combine themselves with maximum positive interference:

$2d_H\sin\theta = n\lambda$ (1)
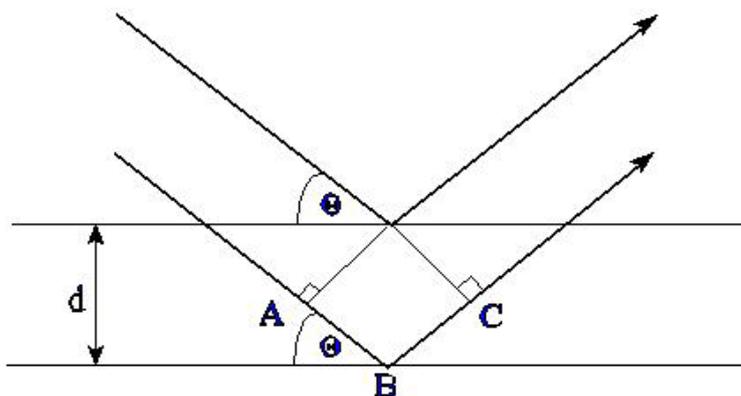
Fig. 4.5a: *Bragg's law*

Since the X-rays penetrate deeply in the crystal a large number of lattice planes will reflect the primary beam: the reflected waves will interfere destructively if equation (1) is not verified (Giacovazzo and others 2002). Equation (1) is Bragg's equation and the angle for which it is verified is Bragg's angle: for n = 1, 2, 3, ... we obtain reflections (or diffraction effects) of first order, second order, etc., relative to the same family of lattice planes H.

   The point of view can be further simplified by observing that the family of fictitious lattice planes with indices $h' = nh$, $k' = nk$, $l' = nl$ has interplanar spacing $d_{H'} = d_H/n$. Now equation (1) can be written as:

$$2(\,d_H/n)sin\theta = 2d_{H'}sin\theta = \lambda \qquad (2)$$

Where h', k', l' are no longer obliged to have only the unitary factor in common (Giacovazzo and others 2002). In practice, an effect of diffraction of nth order due to a reflection from lattice planes H can be interpreted as reflection of first order from the family of fictitious lattice planes H' = nH. If the scatterer object is periodic (crystal) we observe a non-zero amplitude only when $\mathbf{r}^* = \mathbf{r_H}^*$

where $\mathbf{r}^* = 1/d_H$ and $\mathbf{r_H}^* = h\boldsymbol{a}^* + k\mathbf{b}^* + l\boldsymbol{c}^*$ ($\mathbf{r_H}^*$: generic lattice vector of the reciprocal lattice). So

$$\mathbf{r}^* = 1/d_H = 2sin\theta/\lambda. \qquad (3)$$
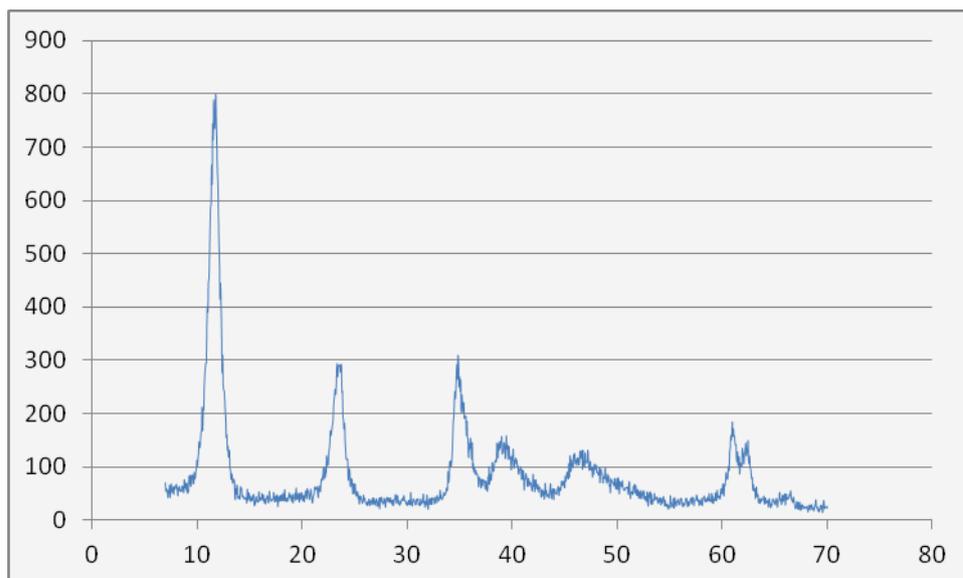
Fig. 4.5b: *Mg-Al LDH before calcinations. The broad XRD peaks show that the material has poor crystallinity.*

4.6 conventional calcinations

The untreated and treated LDHs were examined by X rays using Cu K α radiation of wavelength 1.5418 Angstroms, the diffractometer was Burker AXS – D8 Advance. Samples were placed in an inert material holder and scanned from $2\theta = 7^o$ to 70° at 0.05^o counting for 2 seconds at each angle. All diffraction patterns were measured at room temperature.

The LDHs were heated from 300 up to 900 ^{o}C using two different methods: furnace (conventional calcinations) and microwave waveguide. In the case of conventional calcinations, the sample is heated due to the effects of conduction, i.e. there is a creation of thermal gradient which results in a hotter surface.

Anionic clays are thermally unstable and upon heating their structure collapses, even at low temperatures. Dehydroxylation starts at 100 ^{o}C already (Hudson, 1995). LDHs also exhibit memory effect, when mildly calcined at a maximum of 600 ^{o}C and then exposed to the atmosphere for 2-10 days (*Fig. 4.6a, b* and *Fig.4.7 b*). In this case they absorb moisture and regain, at least up to an extent their previous layered structure.
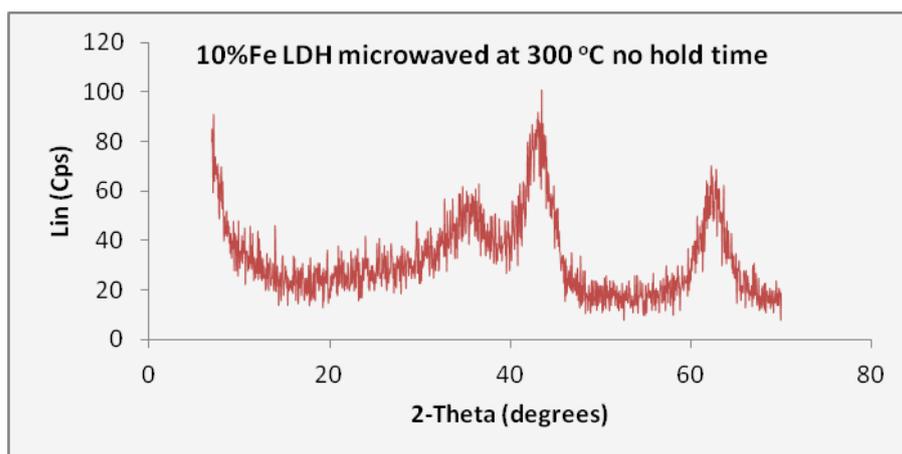
Fig. 4.6a
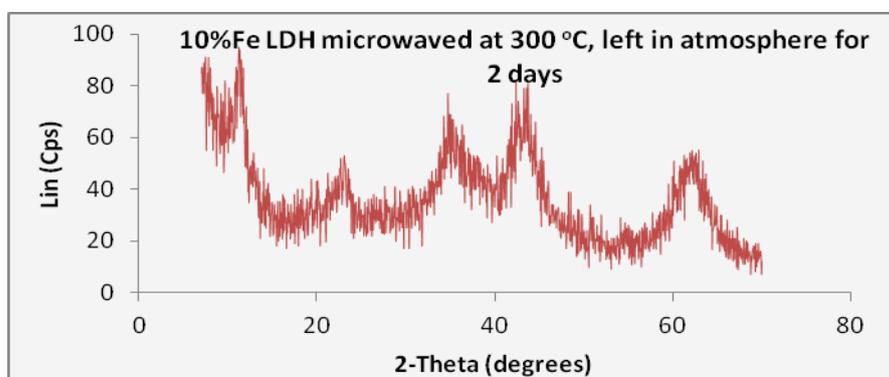
Fig. 4.6b
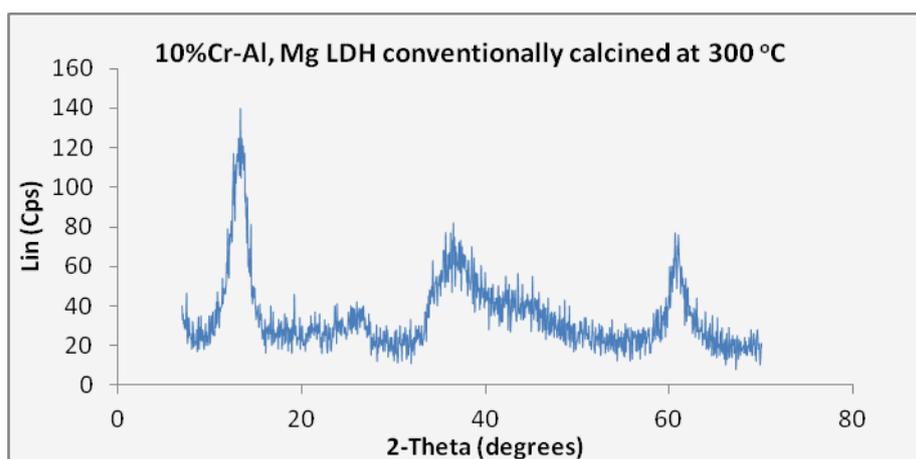
Fig. 4.7a
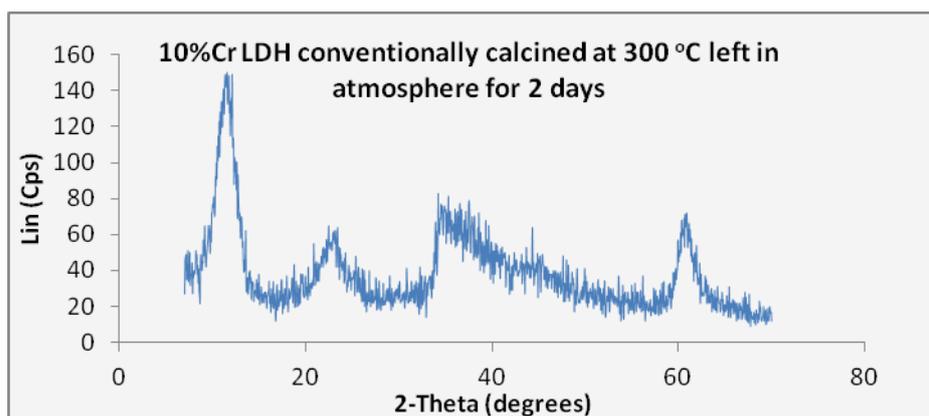
Fig. 4.7b: *X ray diffraction patterns from LDHs subject to a series of conventional calcinations is presented here and then compared to the literature.*
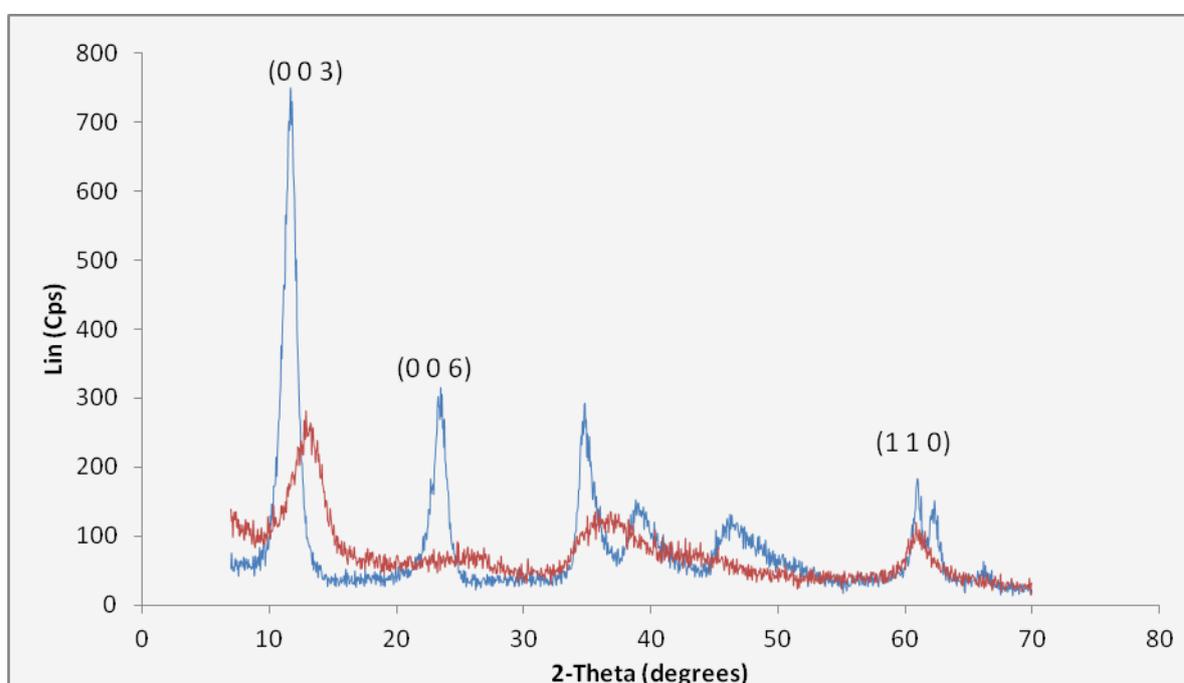
Fig. 4.8a: *Mg-Al LDH before (blue line) and after conventional calcinations at 300 °C (red line).*

The diffraction pattern of the untreated LDH is shown in *Fig. 4.5a*. According to Rives 2001 and Hudson 1995,

(0 0 1) diffraction peak (the first peak, occurring at low angles ~12°), which corresponds to the sheet-sheet distance perpendicular to the sheet plane (basal spacing) starts decreasing at 200 °C. In *Fig. 4.8a*, at 300 °C the resultant XRD pattern shows that the material is largely amorphous and that a big part of the intensity of

the first peak is lost. This is due to the loss of interlayer water and carbonate (Hudson 1995). At the same temperature, the previously sharp 006 reflection which gives d_{006}, the distance between the metal hydroxide layer and the interlayer carbonate anions, becomes a broad series of reflections something that indicates substantial loss of carbonate series (Hudson 1995).

When the temperature is further increased, amorphous materials are formed, like in *Fig. 4.8b* at 400 ^{o}C and at 500 ^{o}C highly disordered MgO is observed.
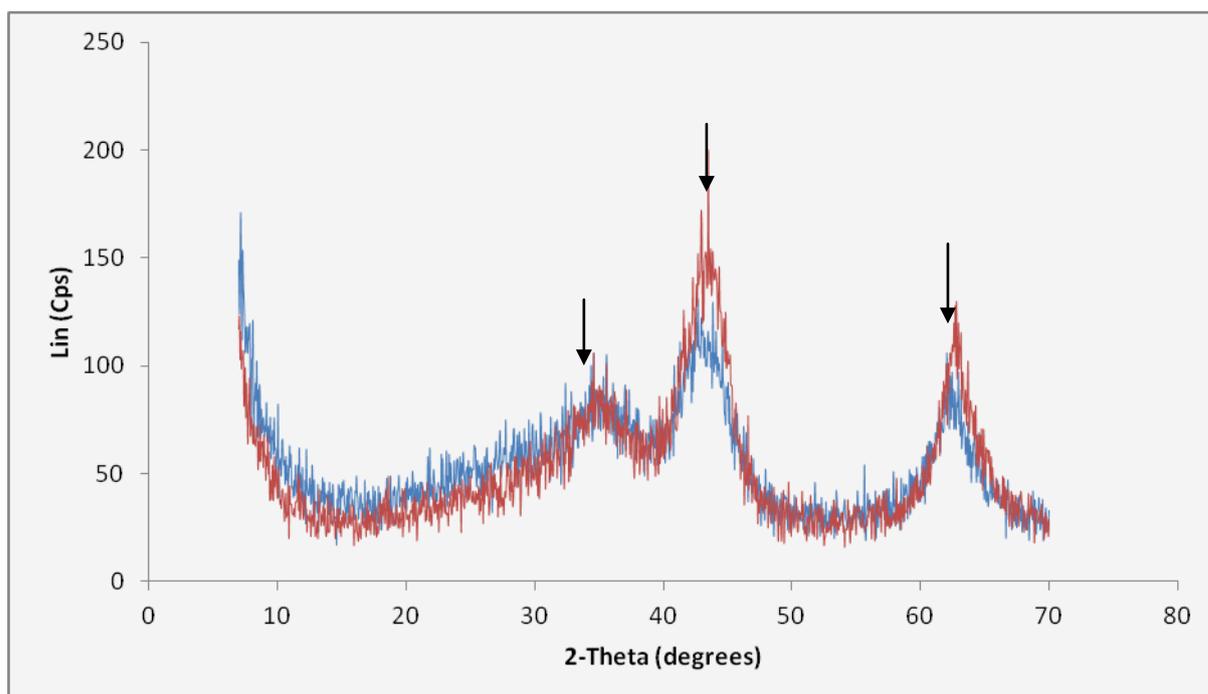
Fig. 4.8b: *red line* 500 ^{o}C, *blue line* 400 ^{o}C. *The material is amorphous even though MgO can already be seen. The arrows show MgO.*

In particular, at 300 ^{o}C there is amorphous material with peak broadening and the XRD patterns show that crystallinity increases (narrower diffraction lines indicate larger crystal) at 700 ^{o}C and finally MgO and spinel become very clear at 900 ^{o}C (*Fig.4.8d*). At the temperature of 600 ^{o}C (*Fig. 4.8c*) starts the migration of aluminium to MgO which results in the formation of spinel.
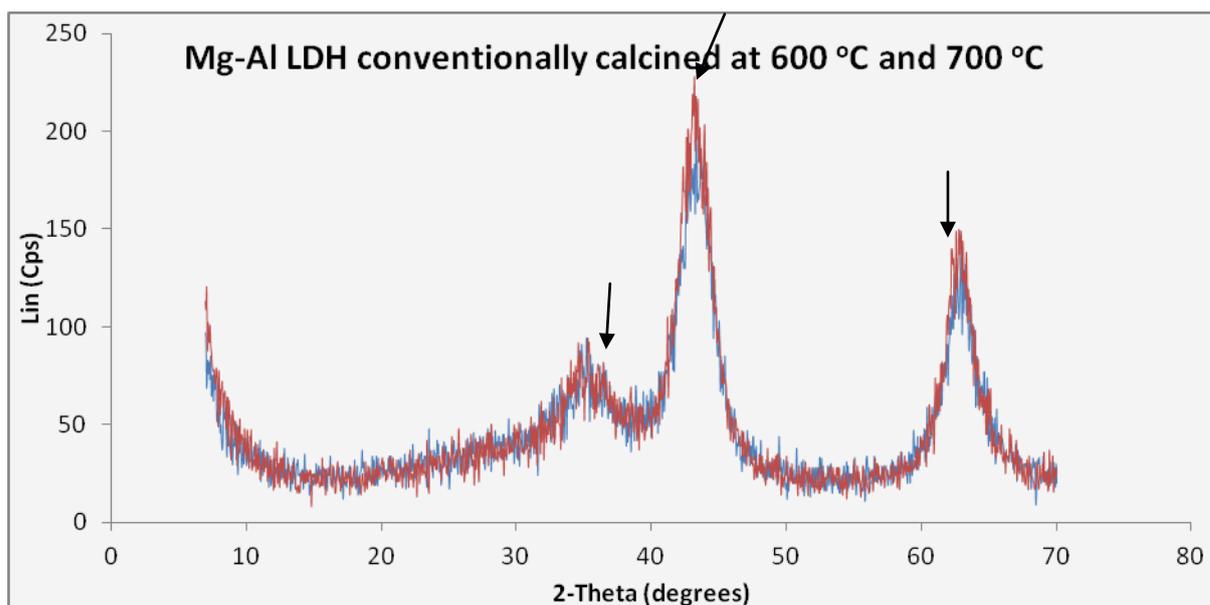
Fig. 4.8c: LDH conventionally calcined at 600 ^{o}C (blue lines) and 700 ^{o}C (red lines), *the better crystallinity is apparent from the sharper peaks, again MgO is detected. The black arrows show MgO*
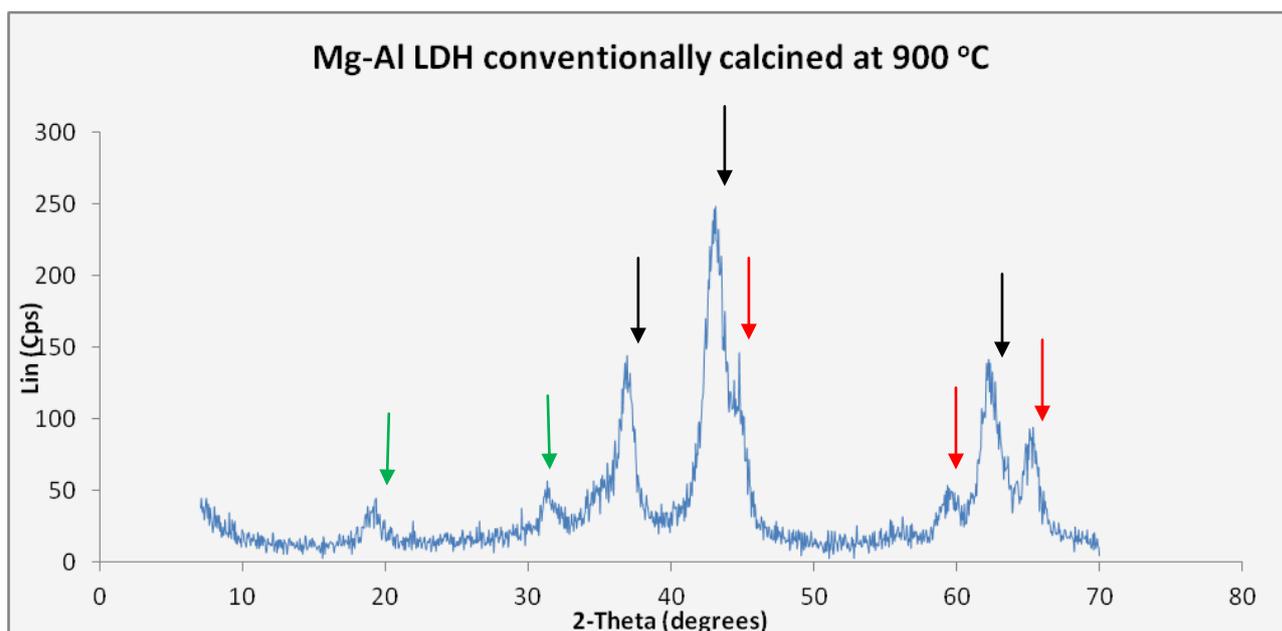
Fig.4.8d: *Mg-Al LDH conventionally calcined at 900 ^{o}C. The sharper diffraction peaks show better crystallinity. Black solid arrow is MgO.* Red *arrow is* spinel. Green *is for unknown peaks At 900 ^{o}C the oxide solid solution is decomposed to MgO and* $MgAl_2O_4$.

At 900 ^{o}C the crystallinity is increased (Rives 2001). One question that remains is what happens with CO_2 assuming that NO_3^- remnants are washed away by water during the production of LDHs. Decarbonation of Mg-Al-CO_3 was thought to occur between 400 and 500 ^{o}C. Hibino and others (1995) demonstrated that when the proportion of Mg/Al is 2:1 instead of 3:1 and the specific surface area is larger, then there is bigger release of CO_2 up to 350 ^{o}C, indicating that some of the CO_2 should be absorbed on the external surface of the crystallites and is thereof released at low temperatures (~150-250 ^{o}C). The minimum Mg:Al ratio that is required is 2:1 in order to avoid edge sharing Al(OH)$_6$ octahedra. Hibino has shown that in samples with large Al content CO_2 evolution is observed even at 900 ^{o}C; these authors claim that during collapsing of the structure some carbonate remains trapped inside the decomposed material, thus hindering complete decarbonation, which takes place only when Al^{+3} migrates to MgO to form $MgAl_2O_4$ spinel. For lower Al such a process should not be observed, such a case is this series of experiments.

Conclusions

What remains to be seen is what happens when LDHs are microwaved in a rectangular waveguide, instead of being conventionally calcined. The XRD patterns will show if the same reactions occur, the only difference might be the temperature. Do microwaves induce the same reactions but at lower temperatures probably due to localized heating? When does crystallinity start improving? The process of oxide production probably speeds up in the case of microwaves. After the water from the interlayer is evaporated, microwaves interact with other permanent dipoles in the material to continue heating it up. Another possibility of heat generation is that microwaves induce dipoles at the interfaces of the material (Maxwell-Wagner polarization and a mechanism of microwave interaction) heated and as a consequence they react with them and the heating continues. In the second stage of mass removal from the collapsing LDHs requires that OH$^-$ is removed and the third CO_2. OH$^-$ is attached to octahedral in brucite layers. Microwaves probably speed up

the creation of oxides but the mechanism is not clear. The central part of a sample is usually the hottest spot so in this case there is localized heating that probably speeds up the reactions especially when the sample size is small in particular less than 2 cm.

An important aspect is that the microwave calcinations should occur at the same experimental conditions as the furnace ones. This applies to the temperature ramp, hold time and mass of the sample. Also, an inherent problem with microwaves is repeatability. It is a common problem with microwaves that many times when experiments are performed under the same conditions the results can vary. Therefore the experiments in the waveguide must be performed under identical conditions as well.

The experiments that are recommended to be performed in the waveguide performed will bring results that are probably not due only to heating. The so called microwave effect has never been fully understood. The exact mechanism of interaction between microwaves and matter is not known. In these kinds of experiments microwaves probably contribute to the total energy of the electric dipoles, something that makes them overcome energy barriers and chemical reactions start.

4.7 Cu enriched LDHs

Mg was partially replaced by another divalent metal, copper. Initially 10% was replaced and then 20, 30, 40 and finally 50%. Magnesium and copper have similar radius and the mixture of final oxides will also include CuO.

PXRD

4.7a Conventional calcinations

Again, the broad diffraction peaks show amorphous material but the crystallinity increases at 900 $^{\circ}$C when diffraction peaks become sharp. MgO and CuO appear at

600 °C and at 700 °C but apart from these two oxides spinel also makes its appearance. Finally at 900 °C there still remains pure hydrotalcite in the domains of CuO, MgO and spinel.
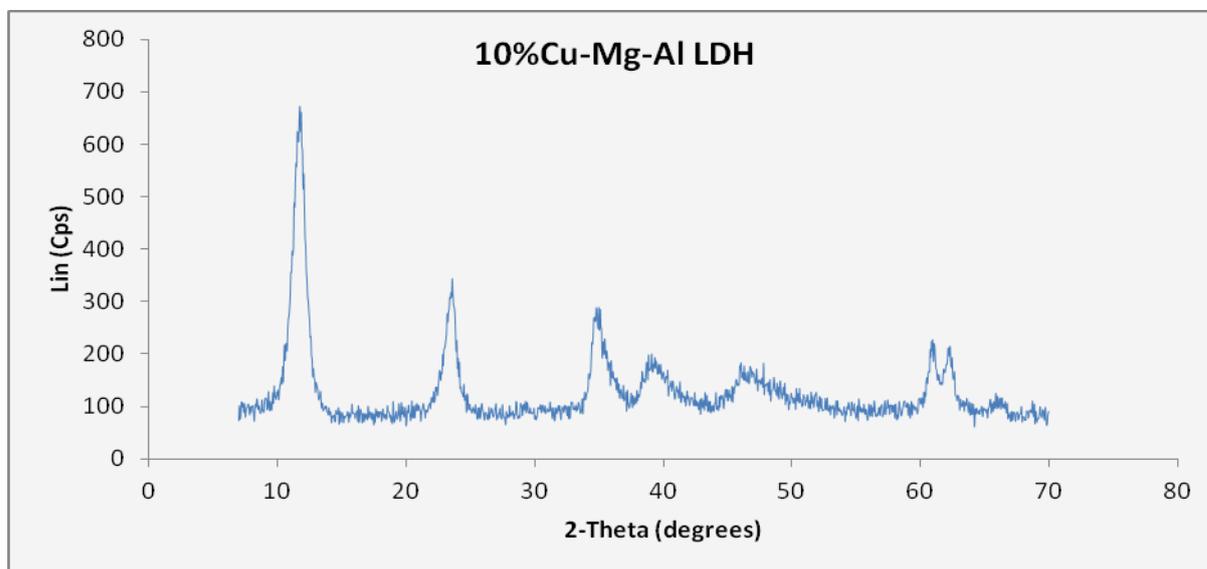

Fig. 4.9a: *untreated 10%Cu LDH*
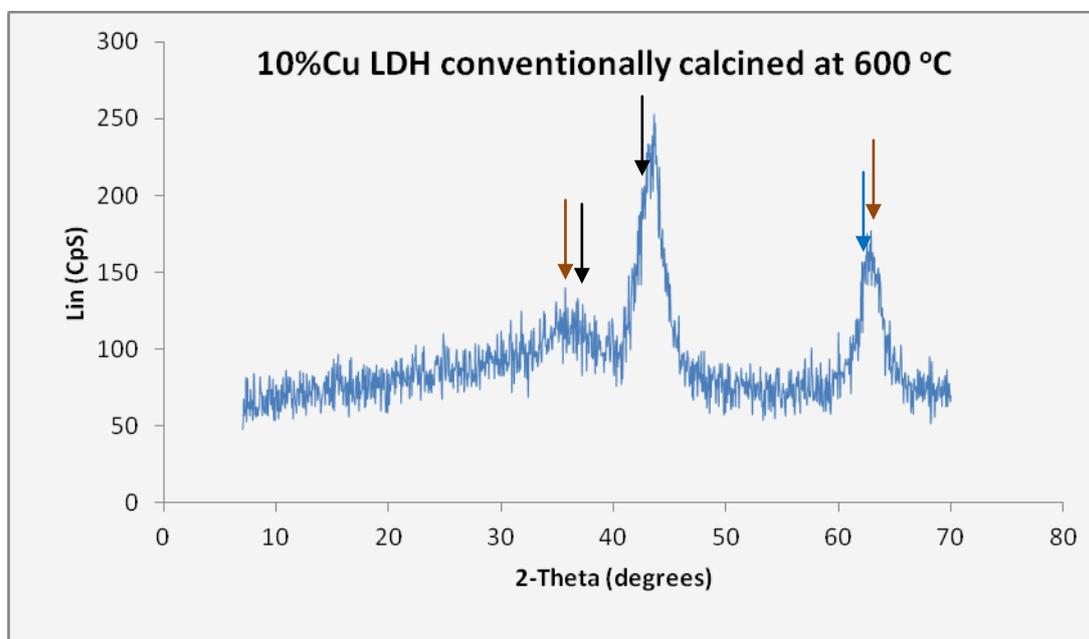
Fig. 4.9b: *10%Cu conventionally calcined at 600 °C. Orange arrows are CuO, black are MgO and blue is MgO plus pure hydrotalcite*
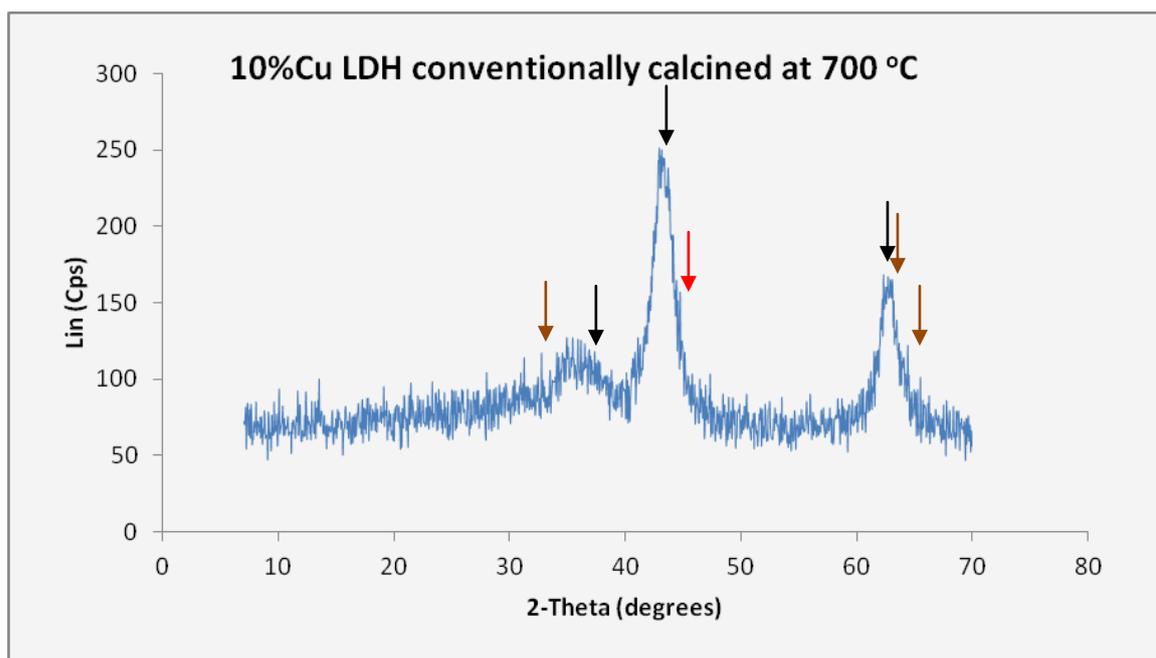
**Fig. 4.9c:** *10%Cu LDH conventionally calcined at 700 °C. Orange arrows are CuO, black are MgO and red is CuO plus pure hydrotalcite*
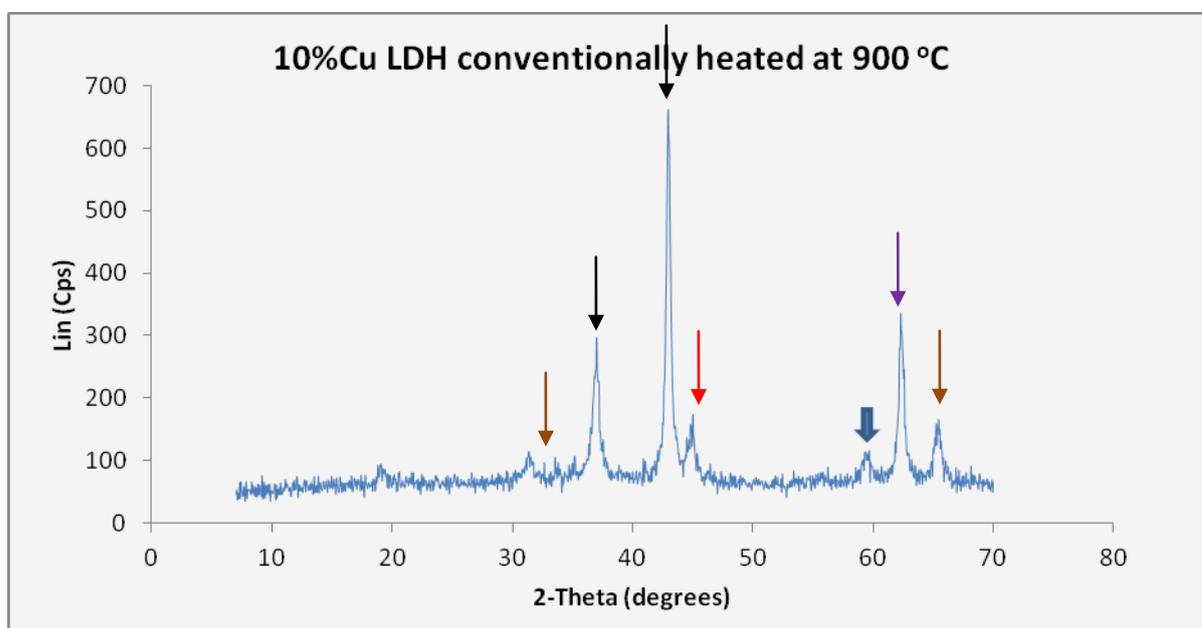
Fig. 4.9d: *Conventionally heated 10%Cu LDH at 900 °C. Orange arrows are CuO, black MgO, red is CuO plus pure hydrotalcite, block arrow is spinel plus pure hydrotalcite and purple is CuO, MgO and pure hydrotalcite*

As the temperature increases, more quantity of CuO is formed or simply CuO is formed in more different areas of the heated sample, there is also increasing quantity of MgO. Concerning CuO, it is formed in the domains of pure hydrotalcite at $2\theta = 45^{o}$ and again there is formation of MgO in pure hydrotalcite domains at $2\theta = 62^{o}$.

20%Cu content (conventional and microwave calcinations)
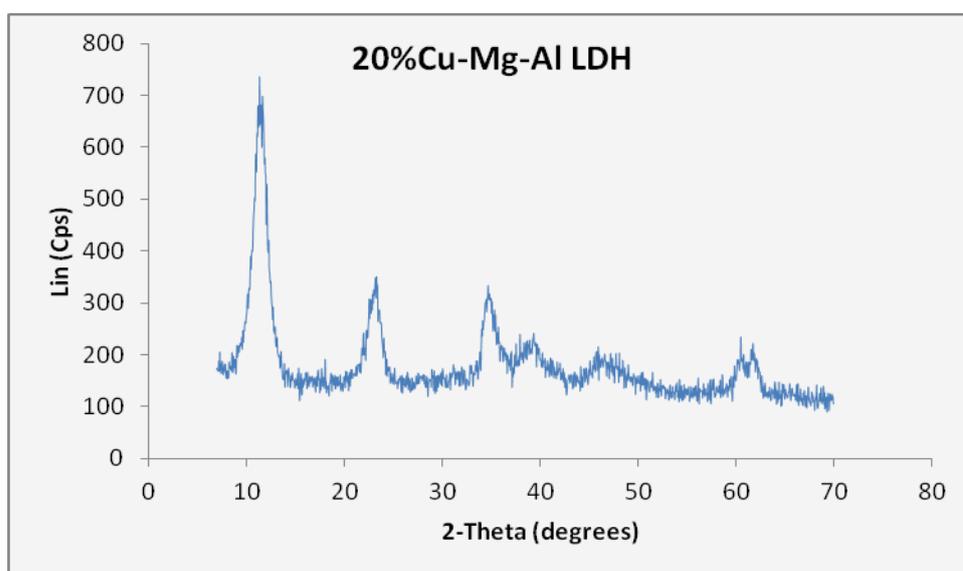
Fig. 4.10a: *untreated 20%Cu-Mg-Al LDH*
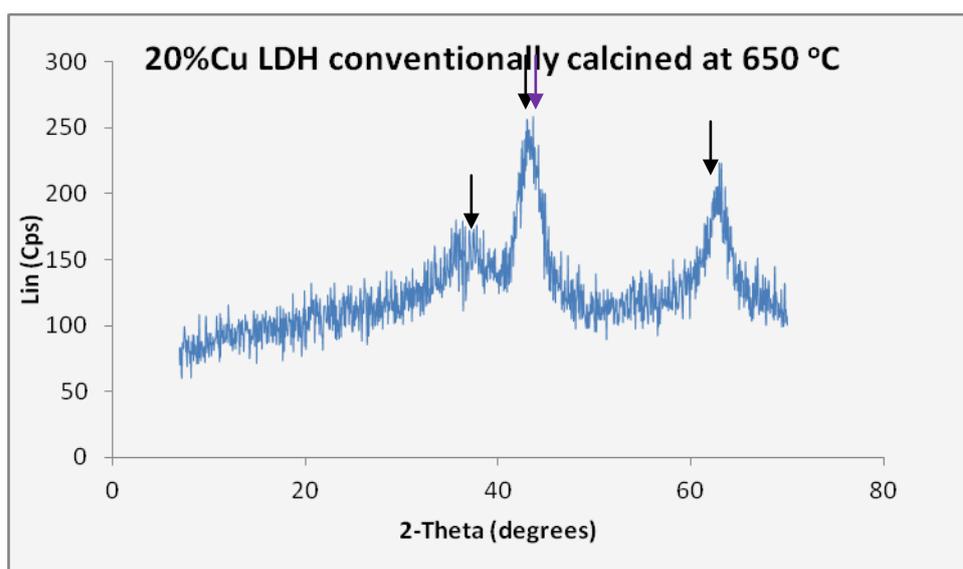
Fig. 4.10b: 20%Cu LDH conventionally calcined at 650 °C. Black arrows are MgO, and the *purple* one is a mixture of CuO plus hydrotalcite
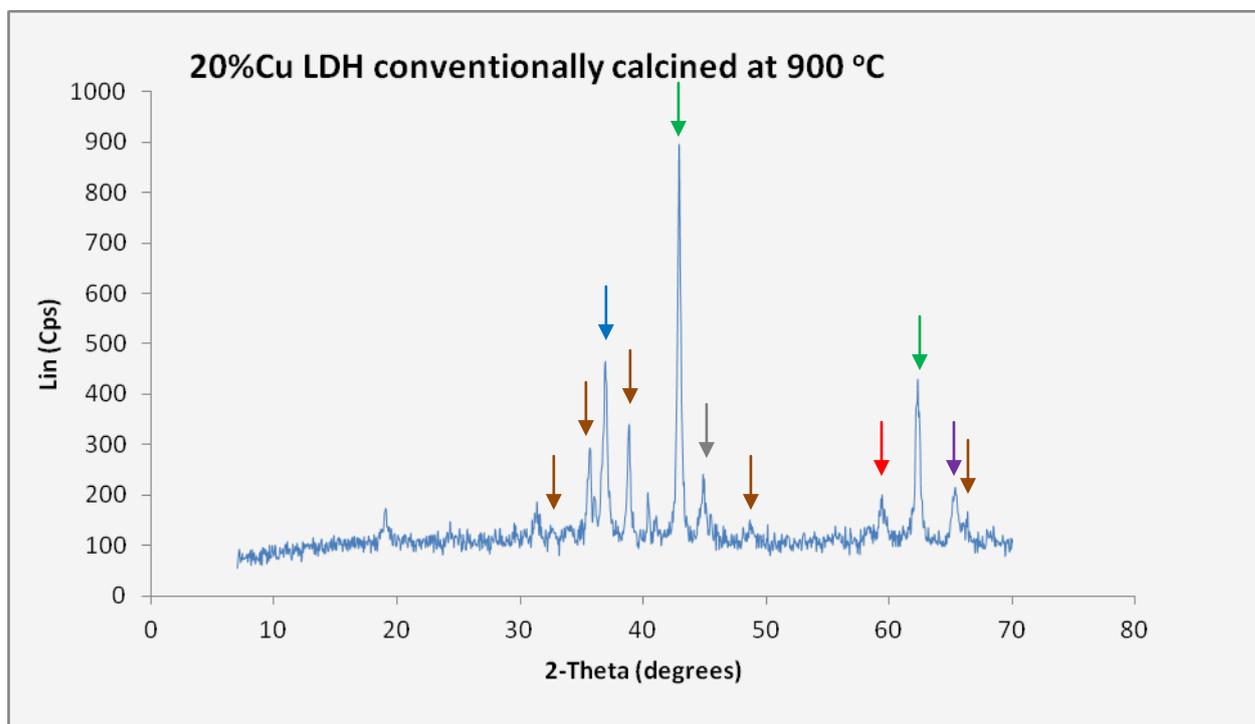
Fig. 4.10c: 20%Cu LDH conventionally treated at 900 °C. *Orange arrows* are CuO, *blue* is MgO plus pure hydrotalcite, *green* are a mixture of MgO plus CuO, *grey* is pure hydrotalcite plus CuO *red* is spinel and *purple* is spinel plus CuO. There is an unknown peak below 20 °C

A first comparison between 10% and 20%Cu content shows that at 900 °C, there is more CuO when the content of copper is higher, something that is expected. At low angles, in both the cases there are unknown peaks which could be spinel or CuO. In the case of 20%Cu these peaks are more crystalline. CuO exists as a mixture with MgO or in the domains mixed with spinel or pure hydrotalcite. In the case of 20%Cu, when it was microwaved at 500 °C the resultant XRD pattern showed that CuO comes in a mixture of spinel while when 10%Cu was microwaved at the same temperature the material was still amorphous but pure CuO was formed. Increasing Cu-content could give increasing quantity of CuO.

30%Cu-Mg-Al LDHs
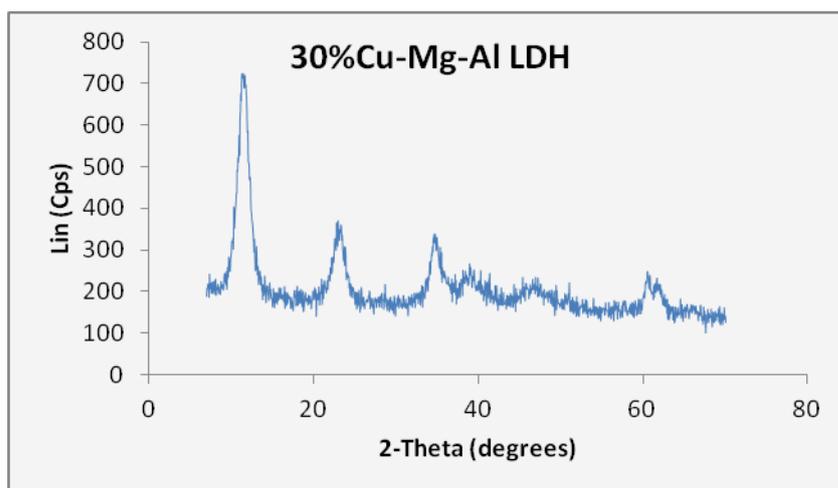

Fig. 4.11a: _30%Cu-Mg-Al LDH_
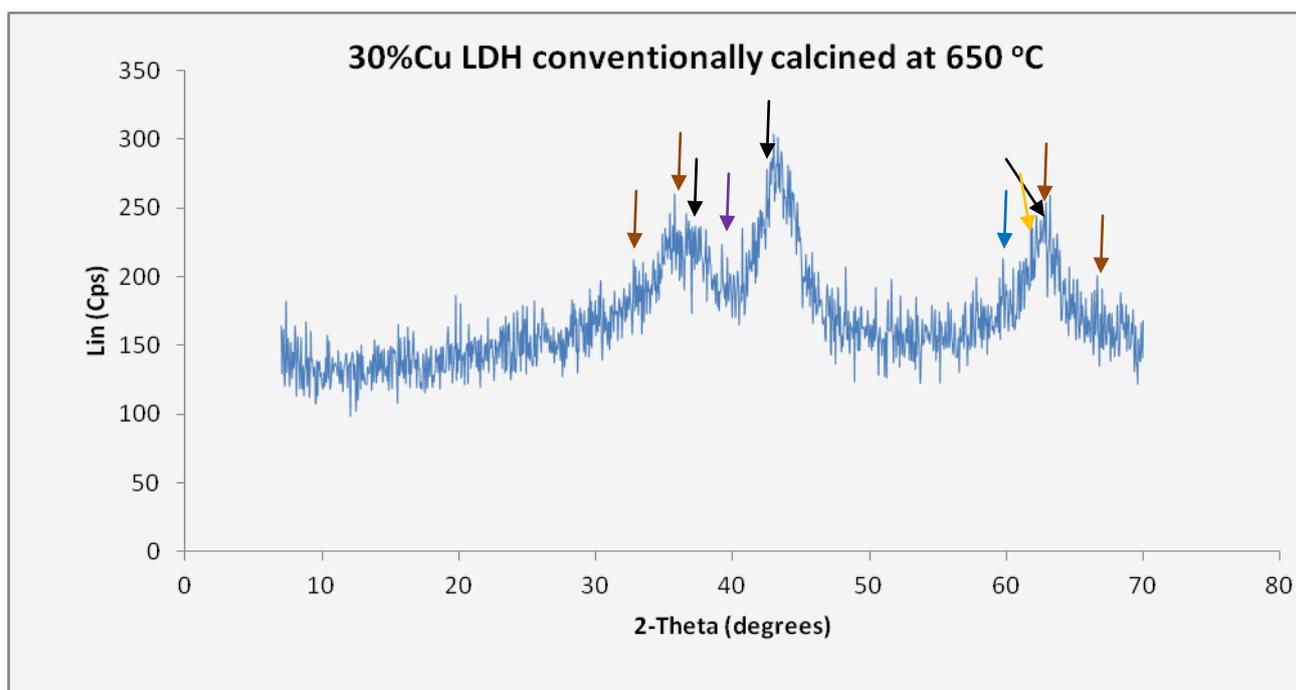
Fig. 4.11b: _30%Cu conventionally calcined at 650 ^{o}C. Orange arrows are CuO, black are MgO, purple is CuO plus pure hydrotalcite, blue is spinel plus pure hydrotalcite, yellow is pure hydrotalcite_
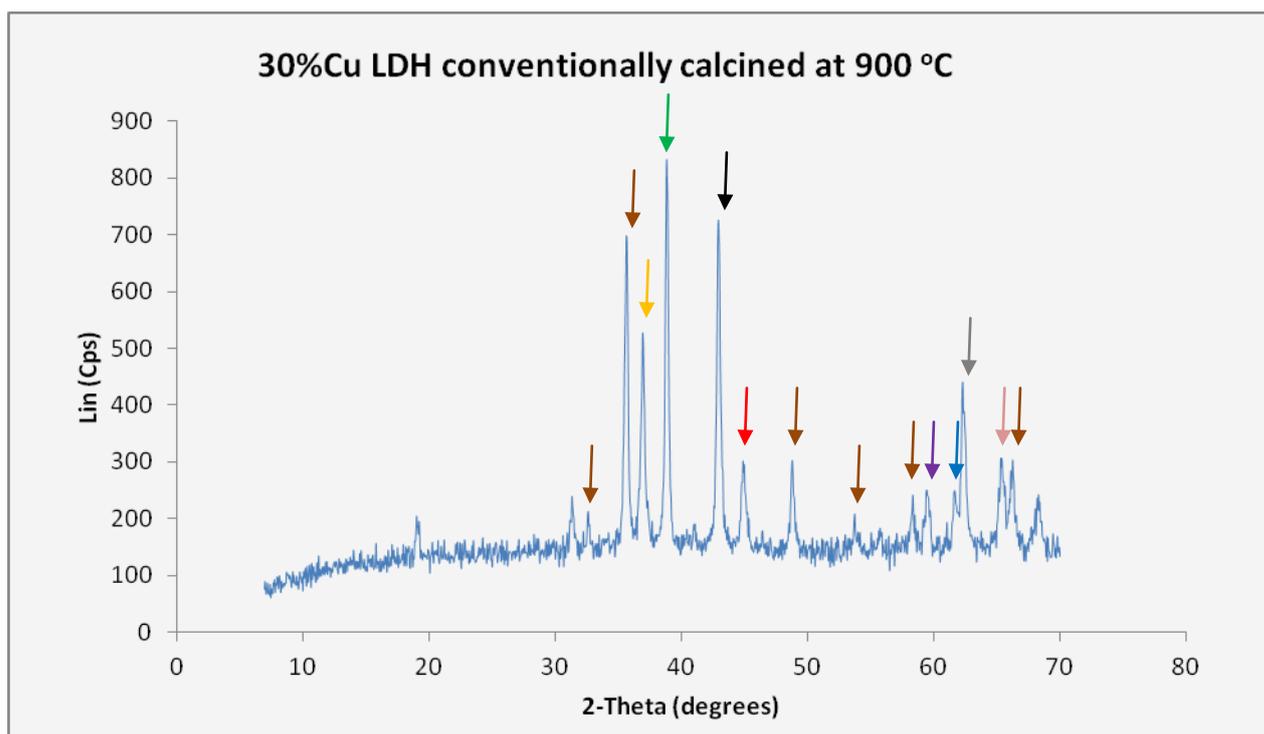
Fig.4.11c: *30%Cu conventionally calcined at 900 °C. Orange arrows are CuO, black is MgO, yellow is pure hydrotalcite plus MgO and CuO, green is pure hydrotalcite plus CuO, red is spinel plus pure hydrotalcite plus CuO, purple is spinel plus pure hydrotalcite, blue is pure hydrotalcite, grey is MgO plus CuO and pink is spinel plus CuO.*

When the Cu content reaches 30% CuO is much more evident, either on its own or as a mixture of oxides or in the domains of spinel and pure hydrotalcite.
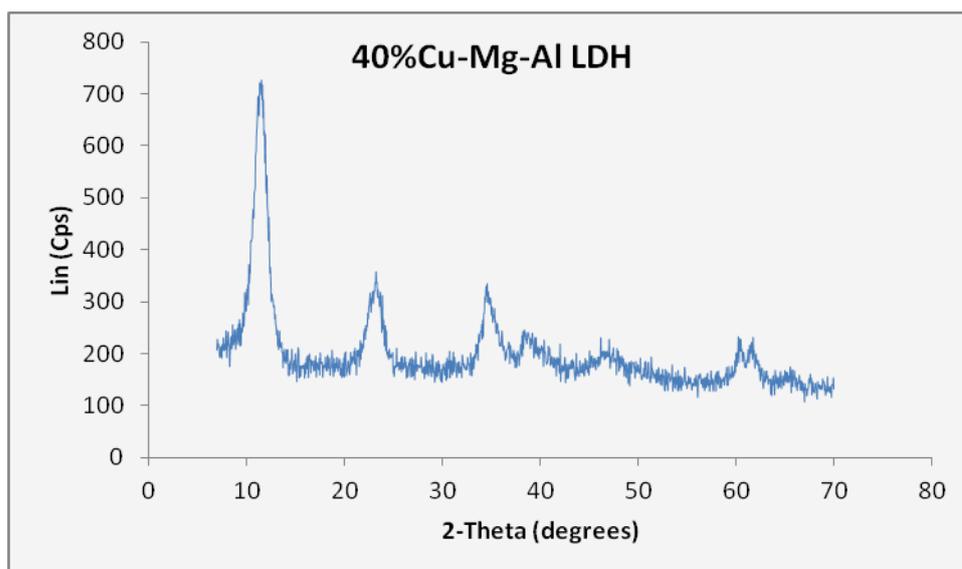
**Fig. 4.12a:** *untreated 40%Cu-Mg-Al LDH*
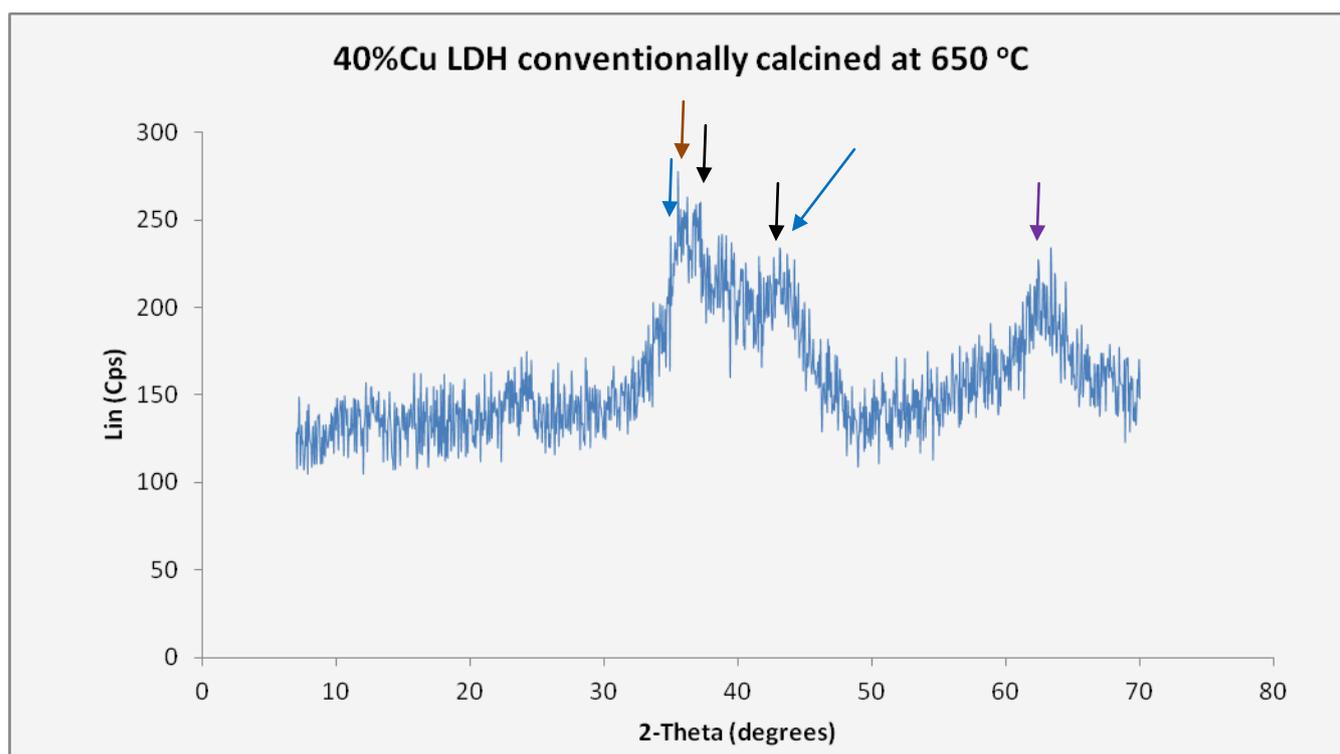
Fig. 4.12b: *Orange arrows is CuO, black is MgO, blue are pure hydrotalcite and purple is a mixture of pure hydrotalcite, MgO and CuO*
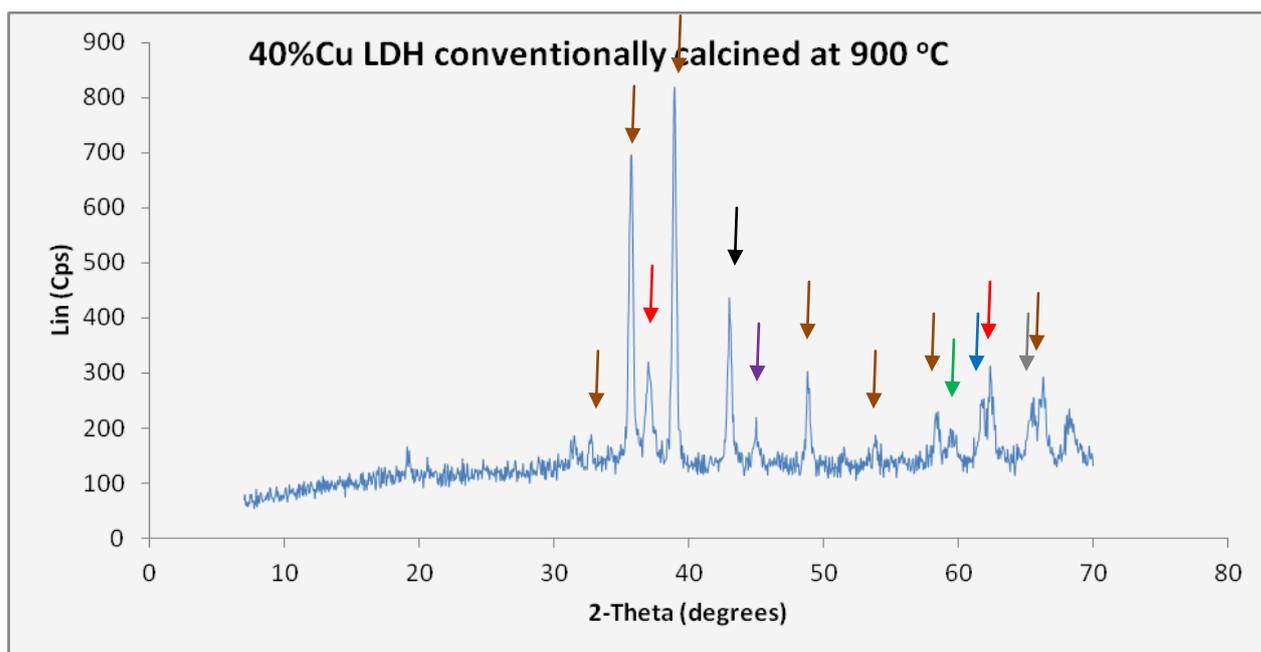
Fig. 4.12c: *Orange arrows are CuO, black is MgO, red are mixture of MgO and CuO plus pure hydrotalcite, purple is spinel plus pure hydrotalcite plus CuO, green is spinel plus pure hydrotalcite, blue is pure hydrotalcite and grey is spinel plus CuO.*

<u>50% Cu</u>
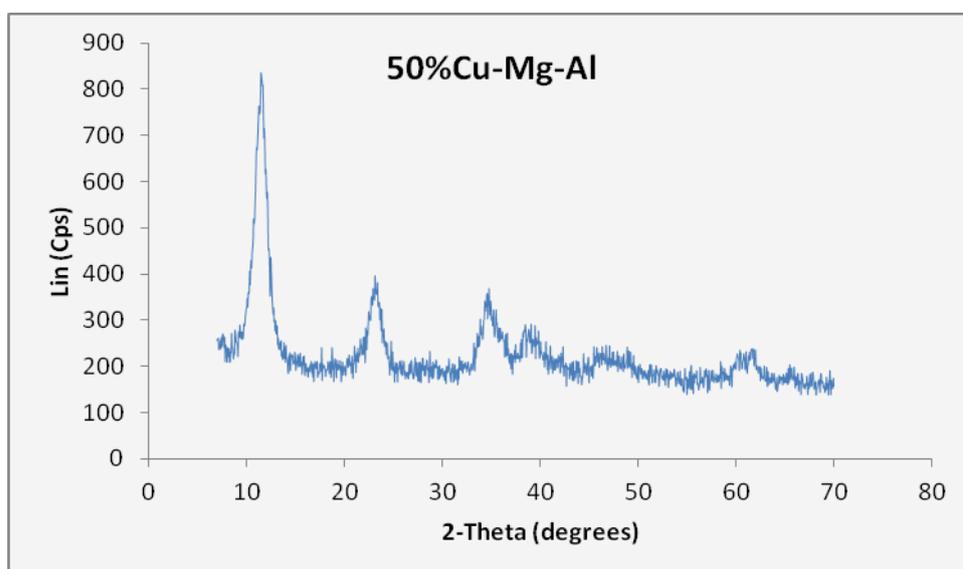
Fig. 4.13a: *untreated 50%Cu-Mg-Al LDH*
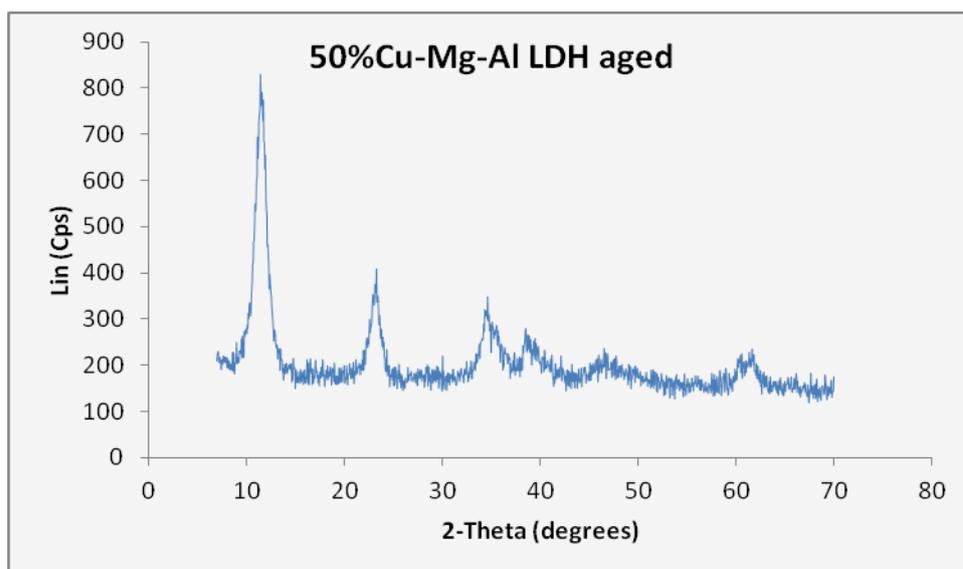
**Fig. 4.13b:** untreated 50%Cu-Mg-Al LDH , aged for 2 hours at 65 ^{o}C.
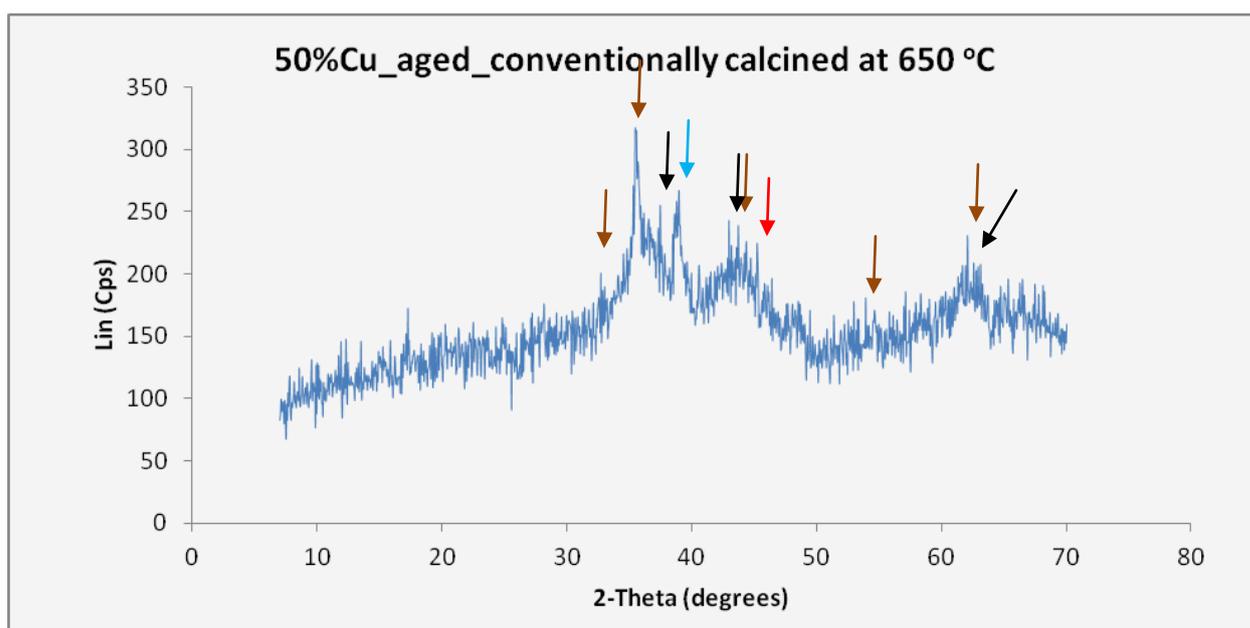
**Fig. 4.13c:** *Orange arrows* are CuO, black are MgO, *blue* is pure hydrotalcite plus CuO and *red* is spinel
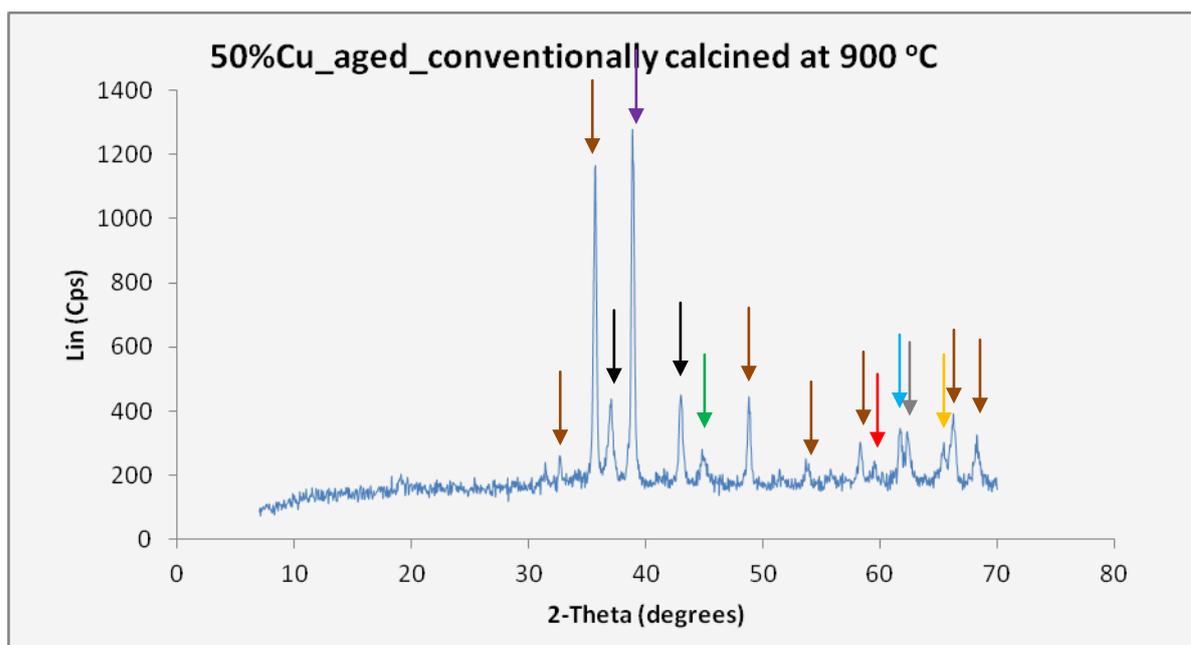
Fig. 4.13d: *Orange arrows CuO, black are MgO, purple is pure hydrotalcite plus CuO, green is spinel plus pure hydrotalcite plus CuO, red is spinel, blue is pure hydrotalcite, grey is pure hydrotalcite plus MgO plus CuO and yellow is spinel plus CuO.*

When comparing the results between Mg-Al LDHs and Cu-Mg, Al LDHs at 900 ^{o}C, conventional calcinations, one can see that the diffractions peaks when copper is added at any quantity are sharper. This is likely related to the paramagnetism of copper Cu^{+2}. There is increasing interaction between microwaves and the sample when copper is added. Pure hydrotalcite domains are present even at high temperatures when copper is present.

4.8 Explanation of a and c parameters

The parameter *a* is the distance between metals. The layer of LDHs is consisted of:

$[Me^{II}_{1-x}Me^{III}_{x}(OH)_2]^{+x}$. The distance between the metals is the same as between the OH groups on the same side of the layer. When part of Mg is replaced by copper, there is a slight increase in the *a* parameter, since the radius of Mg is 0.66 Å and Cu is

0.72 Å. The increase of a parameter is in agreement with that. Even though copper is more electronegative than Mg, the *c* parameter increases when copper is added.

A common trait between these two parameters is that they reach a maximum when more Cu is added and then they decrease. Parameter *a* reaches maximum when copper content is 40% (*Fig. 4.14a*)and parameter *c* when Cu is 30% (*Fig. 4.14b*). The maximum of *a* parameter is probably an indication of phase segregation when copper reaches 50%.
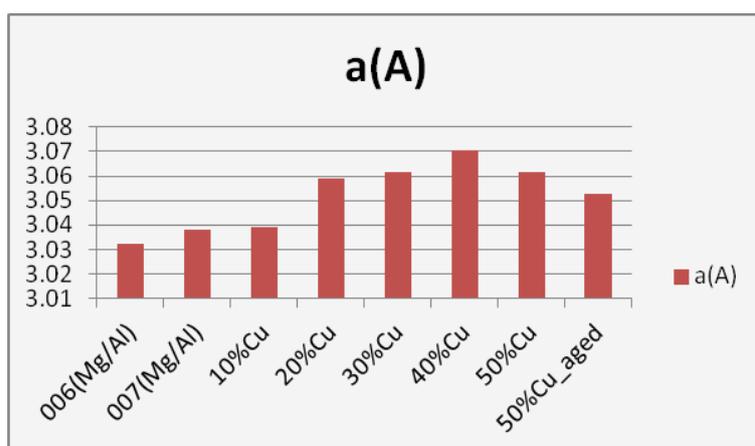

Fig. 4.14a
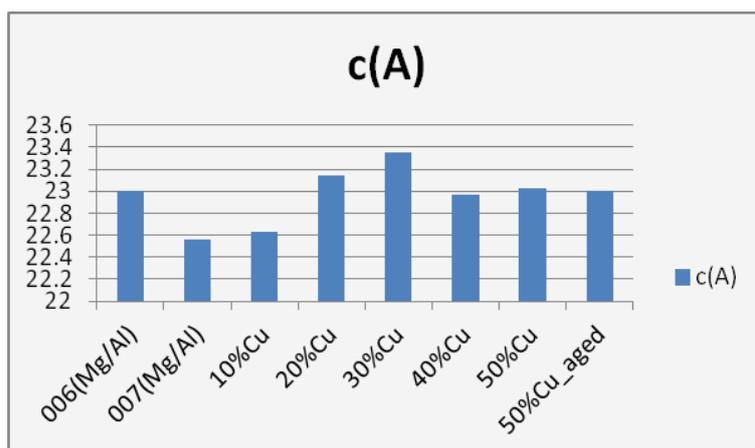
Fig. 4.14b

Table 1	c(A)	a(A)

006(Mg/Al)	22.99784	3.0322
007(Mg/Al)	22.56146	3.03798
10%Cu	22.63169	3.03904
20%Cu	23.14734	3.05882
30%Cu	23.35688	3.06162
40%Cu	22.96643	3.07032
50%Cu	23.02943	3.06142
50%Cu_aged	22.99959	3.05258

The mass loss that accompanies both the calcination methods is arbitrary, in the case of copper. Concerning the conventional method, this can be seen in *fig 4.14c*.
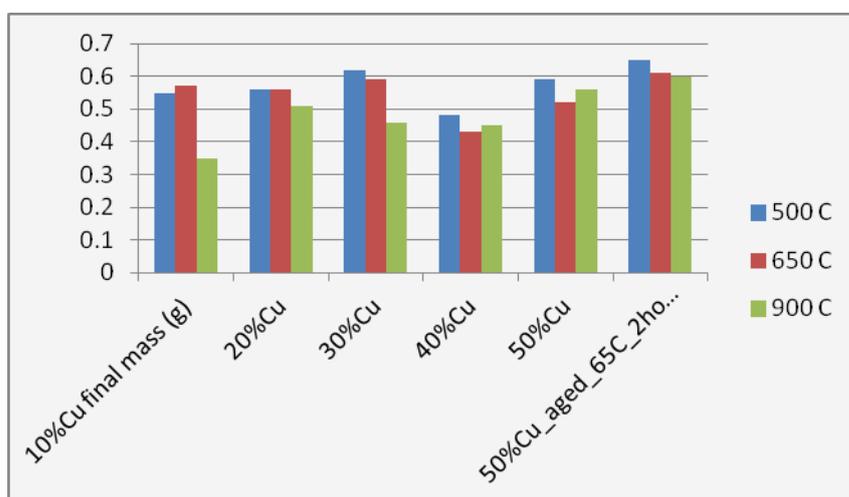
Fig. 4.14c

Table 2

	500 °C	650 °C	900 °C
10%Cu final mass (g)	0.55	0.57	0.35
20%Cu	0.56	0.56	0.51
30%Cu	0.62	0.59	0.46
40%Cu	0.48	0.43	0.45
50%Cu	0.59	0.52	0.56
50%Cu_aged_65C_2hours	0.65	0.61	0.6

4.9 BET-N$_2$ adsorption

It has long been known that a porous solid can take up relatively large volumes of condensable gas. In 1777 Fontana had noted that "air" expelled from charcoal on heating is reabsorbed on cooling. It soon became realized that the volume taken up varies from one charcoal to another and from one gas to another; and in suggesting that the adsorptive power of a solid depended on the area of exposed surface, de Saussure in 1814 anticipated our present day views on the subject. Mitscherlich in 1843, on the other hand, emphasised the role of the pores in charcoal, and estimated their average diameter to be 1/2400 in; he considered that carbon dioxide became condensed in layers 0.005 mm thick and in a form nearly as dense as liquid dioxide. These two factors, surface area and porosity (or pore volume), are now recognised to play complementary parts in adsorption phenomena not only in charcoal but in a vast range of other solids. It thus comes about that measurements of adsorption of gases or vapours can be made to yield information as to the surface area and the pore structure of a solid, Gregg and Sing (1967).

The term *adsorption* appears to have been introduced by Kayser in 1881 to connote the condensation of gases on free surfaces, in contra-distinction to gaseous *absorption* where the molecules of gas penetrate into the mass of the absorbing solid. The wider term "sorption" proposed in 1909 by McCain embraces both types of phenomena, adsorption and absorption Gregg and Sing (1967). In my experiment the material was in the form of a fine powder, in such a case the particles stick together and they form aggregates, or secondary particles. In this simplest case the particles aggregate together by mere adhesion at room temperature under the influence of surface forces. The surface is largely internal in nature and it's extend will be less than that of the original particles of powder by an amount equal to the area lost by formation of particle-to-particle junctions. These aggregated solids will also possess a pore volume, made up of gaps between the particles within a grain, a volume often amounting to a considerable fraction of the "lump volume". Many of the pores are thus comparable in size and related in shape to the primary particles

themselves. The pores present in a grain formed by aggregation of spheres, for example, would have walls composed of parts of the surfaces of spheres (*Fig. 4.15*).
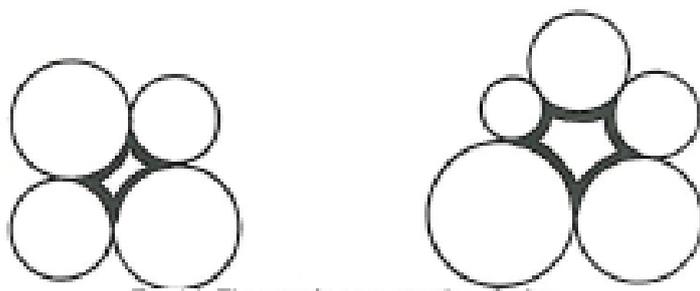

Fig. 4.15: *Different pores in solids, Gregg and Sing (1967)*

In my experiments thermal treatment of substances, calcinations, is also involved and this leads to thermal decomposition, i.e. the formation of active solids. In particular, I start with LDHs to get a mixture of oxides: Solid A $\rightarrow$ Solid B (active) + gas (*Fig. 4.16*). This is a somewhat complex process, it seems that when the new phase B is formed, several crystallites of B are produced from each one of A, so that the crystallite size is reduced and the area correspondingly increased, even though there is only a slight increase of surface area in my calcinations products. The shrinkage brought about by the fact that the density of the product in general is greater than that of the parent solid, will tend to favour the formation of cracks between each new crystallite of B and its neighbours; the surface of the crystallites will thus be accessible to molecules of an investigating fluid Gregg and Sing (1967).

Many crystalline bodies contain "natural" cracks. These probably originate from imperfections in the crystal-especially dislocations-which arise from impurities or even from very slight fluctuations in conditions during growth. So long as the cracks are wide enough to admit molecules of an adsorbed gas, or ions, or molecules from solution, they will result in internal surface. The line of demarcation between the external and the internal surface is drawn in an arbitrary way. The external surface is taken to include all the prominences and all the cracks that are wider than they are deep; the internal surface is comprises the walls of all cracks, pores and cavities which are deeper that they are wide.
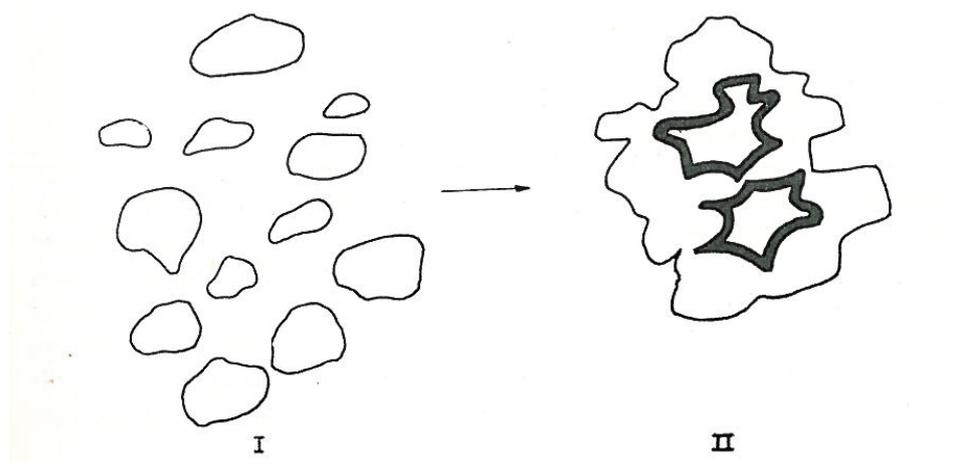
Fig. 4.16: *Formation of pores in solids, Gregg and Sing (1967)*

4.10 Classification of pore sizes: micro, macro and mesoporous

Pores vary in size and shape. Pores of width below 20 Å are described a microspores, pores of width above 200 Å are described as macrospores and those with widths between 20 – 200 Å are described as mesoporous, the materials examined in my experiments are mesoporous.

4.11 The adsorption isotherm

When a highly dispersed solid is exposed in a closed space to a gas or vapour at some definite pressure, the solid begins to adsorb the gas. This is made manifest by a gradual reduction in the pressure of the gas and by an increase in the weight of the solid. After a time the pressure becomes constant at the value p and correspondingly the weight ceases the increase any further. The amount of gas thus absorbed can be calculated from the fall in pressure by application of the gas laws if the volumes of the vessel and of the solid are known; or it can be determined directly as the increase in weight of the solid in the case where the spring balance is used.

The adsorption is a consequence of the field force at the surface of the solid (the *adsorbent*) which attracts the molecules of the gas or vapour (the *adsorbate*). The forces of attraction emanating from a solid may be of two main kinds, physical (the

so called van der Waals like in my experiments) or chemical which results in the formation of a chemical bond. The amount adsorbed per gram (*x*) of solid depends on the equilibrium pressure *p*, the temperature *T* and also on the nature of the gas of the solid. For a given gas adsorbed on a given solid, maintained at a fixed temperature:

$x = f(p/p_o)_{T,gas,solid}$

where p_o is the saturation vapour pressure of the adsorbate.

The majority of isotherms that result from physical adsorption may be grouped into five classes, proposed by Brunauer, Emmett and Teller (BET), *Fig. 4.17*. The type IV isotherm, which is the one exhibited in my experiments, possesses a *hysteresis loop,* the power branch of which represents measurements obtained by progressive addition of vapour to the system and the upper branch by progressive withdrawal.
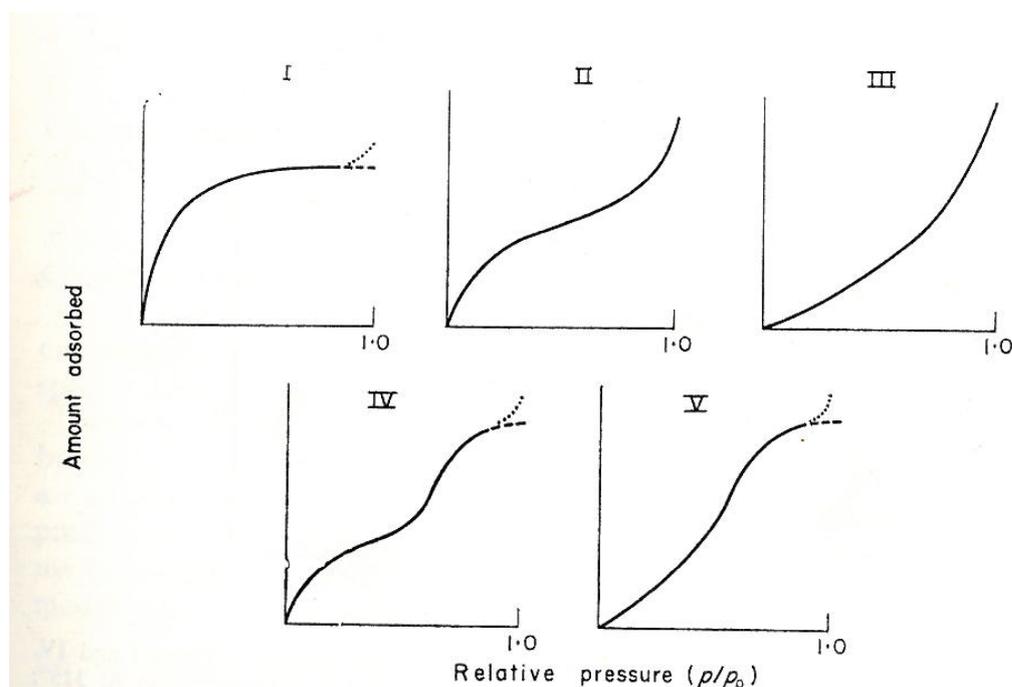

Fig. 4.17: Five different types of isotherms (Gregg and Sing 1967)

4.12 Dispersion forces

Dispersion forces derive their name from the close connection between their origin and the cause of optical dispersion. These forces, first characterized by London,

originate through the rapidly changing electron density in one atom, which induces a corresponding electrical moment in a near neighbour and so leads to attraction between the two atoms.

The total potential energy U(r) of two atoms separated by distance *r* is given by:

$$U(r) = \frac{b}{r^{12}} - \frac{C}{r^{6}} \qquad (4)$$

(Gregg and Sing, 1967) where b is an empirical constant and C is related to the polarizabilities of the atoms. The first term of equation (4) is the repulsion one and the second is the attractive one, however from that equation it can also be seen that the potential decreases rapidly with distance so not all the interactions between atom A and each atom B need to be considered. The quantity *r* is the distance from a definite point, say P, on the surface of the adsorbent to the centre of the atom of the adsorbate (say X), the line PX being normal to the plane of the surface. To calculate the force *F* at any point along the normal PX, it is necessary to take the first derivative of U with respect to *r*:

$$F = \frac{dU(r)}{dr} \qquad (5)$$

This force is zero at r_o which corresponds to the equilibrium position of the adsorbed molecule with respect to the surface; this distance is equal to the diameter of a single molecule and the value of U at this minimum ($-U_0$) represents approximately the energy of adsorption, Gregg and Sing (1967). Alternatively, stated ($+U_0$) is the energy of desorption, i.e. the energy that must be supplied to the adsorbate atom from the solid surface (adsorbent) and return it to the gas phase. The general shape of the potential curve remains the same, however its detailed course depends on the position of P relative to the atoms of the adsorbent. Conclusively, the dispersion forces are always present and unless the adsorbate molecule possesses a strong dipole moment, will represent the major contribution to the total energy of adsorption. Their dependence on distance is such that the first layer of adsorbed molecules will be strongly held, and higher layers more weakly so with an energy not much in excess of the latent heat of sublimation or of vaporization. Electrostatic

forces will become significant only if the adsorbent molecule has large dipole moment, particularly if there is possibility of hydrogen bond formation. Finally the dispersion forces are considerably stronger in micropores than above a plane surface and will be weakest in prominences.

4.13 Physical adsorption of gases by non-porous solids

The BET equation

Brunauer, Emmett and Teller approach the problem of adsorption kinetically. In particular they extended the model of Langmuir, laid down in 1916 by adding second and higher molecular layers. Experimental evidence in the meanwhile proved that multilayer adsorption was the case most of the times. Within each layer dynamic equilibrium is assumed to prevail; *(Fig.4.18)* in layer *i* for example, the number of molecules evaporating per second is equated to the number condensing per second on layer immediately below, the (i-1)th layer.
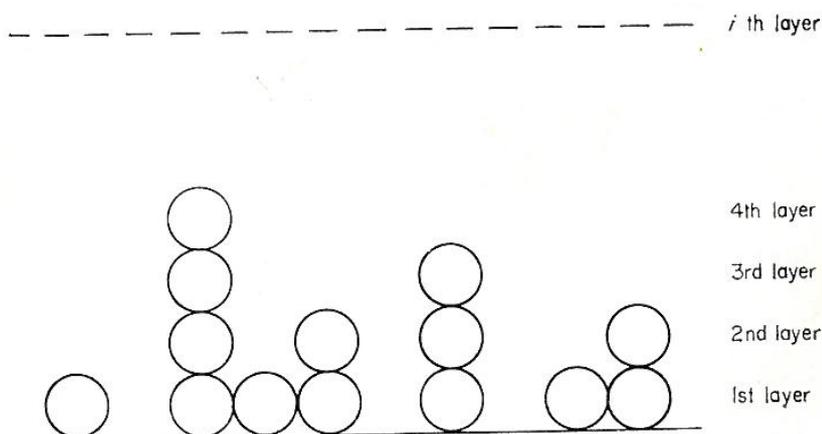

Fig. 4.18: Gas molecules which accumulate at the surface of the solid are continuously oscillating (Gregg and Sing, 1967)

The equation was derived by summing to infinity the adsorption of successive incomplete layers of adsorbed molecules, each of which was considered to be in equilibrium with the layer below it. For the first layer:

rate of adsorption = rate of desorption

$$k_a P S_o = ka S_1 \qquad (5)$$

k_a rate constant for adsorption

ka rate constant for desorption

P pressure for adsorbate gas

S_o sites have no adsorbed molecules

S_1 sites have 1 adsorbed molecule

S_i sites have i adsorbed molecules

For the *i*th layer,

$$k_{ai} P S_o = kai S_i \qquad (6)$$

The rate constant for the desorption step kai is related to the energy of activation for desorption by the expression:

$$kai \; a \; \exp(-E_i/RT) \qquad (7)$$

For the first layer E_1 is considered to be the same as the differential enthalpy of desorption but for all subsequent layers, E_i is assumed constant and identical to the enthalpy of evaporation L and *a* is a constant which probably represents the oscillation frequencies of the molecules.

The adsorption/desorption rate constants are considered identical for all layers above the first

i.e. $k_{a2} / ka_2 = k_{a1} / ka_1 = $ constant $\qquad (8)$

After assuming for i = 0 to i = infinity, the final form of the BET equation is;

$$\frac{V}{V_m} = \frac{c\left(P/P_o\right)}{\left(1 - P/P_o\right)\left(1 + [C - 1]P/P_o\right)} \quad (9)$$

C is a constant, given by the expression:

$$C = \frac{\frac{k_{a1}ka_2}{k_{a2}ka_2}exp(E_1 - L)}{RT} \quad (10)$$

The equation is usually rearranged so that the plot of $P/V(P_o - P)$ against P/P_o gives a straight line, i.e.

$$\frac{P}{V(P_o - P)} = \frac{1}{V_mC} + \frac{(C - 1)P}{V_mCP_o} \quad (11)$$

$$\text{slope} = \frac{C - 1}{V_mC} \qquad\qquad \text{intercept} = \frac{1}{V_mC}$$

$$V_m = \frac{1}{slope + intercept} \quad (12)$$

Since the monolayer volume is known, the surface are of the solid can be calculated from the equation:

$$S = \frac{V_mAN}{V_{mol}} \quad (13)$$

Where N is Avogadro's number, A is the cross sectional area of the adsorbate gas, V_m is the volume of gas in monolayer and V_{mol} is the molar volume of gas at STP. The limitations of the BET method are due to the assumptions made in deriving it from the Langmuir theory, and the enthalpy of desorption approximation for the different layers. The theory does not allow for preferential adsorption on active sites. This will cause the amount adsorbed at low pressures to be more than that predicted by the BET equation. In summing layers to infinity, it ignores the possibility that at saturation on some solids, the number of layers is less than infinite. The assumed absence of lateral interactions is at variance with the assumption that all the layers except the first have the same enthalpy of desorption which is identical to the enthalpy of evaporation. The multilayer can't be liquid-like if only vertical

interactions are considered, since in a liquid, a molecule has on average, 12 nearest neighbours.

Despite these limitations, the BET method has been widely used as it represents a mathematical means of determining the monolayer volume and does not rely on skill at judging the precise position of point B on the adsorption isotherm. The sharpness of the knee at point B depends on the magnitude of C. The higher its value, arising from a high net enthalpy of desorption (E_1-L) the sharper the knee. Nitrogen has been extensively used as an adsorbate because on most non-porous solids, it gives a type II isotherm with a well defined knee. In these cases, comparison of the surface areas obtained by the BET and point B method shows good agreement. The monolayer adsorption is complete when point B is reached, Gregg and Sing (1967).

 The adsorption isotherm for my experiments is type IV. This is the type of isotherms shown by mesoporous solids and it has some similarities to type II isotherms, the only difference is the hysteresis loop. This hysteresis loop indicates (*Fig. 4.21)* the amount *x* adsorbed is greater at any given relative pressure along the desorption branch HLF than along the adsorption branch FGH. The loop is reproducible provided that during the adsorption increasing run some point intermediate between H and K or K' was reached; if desorption commences from some intermediate point on the loop such as X, then the loop will be scanned and the isotherm will follow some such path as XY.
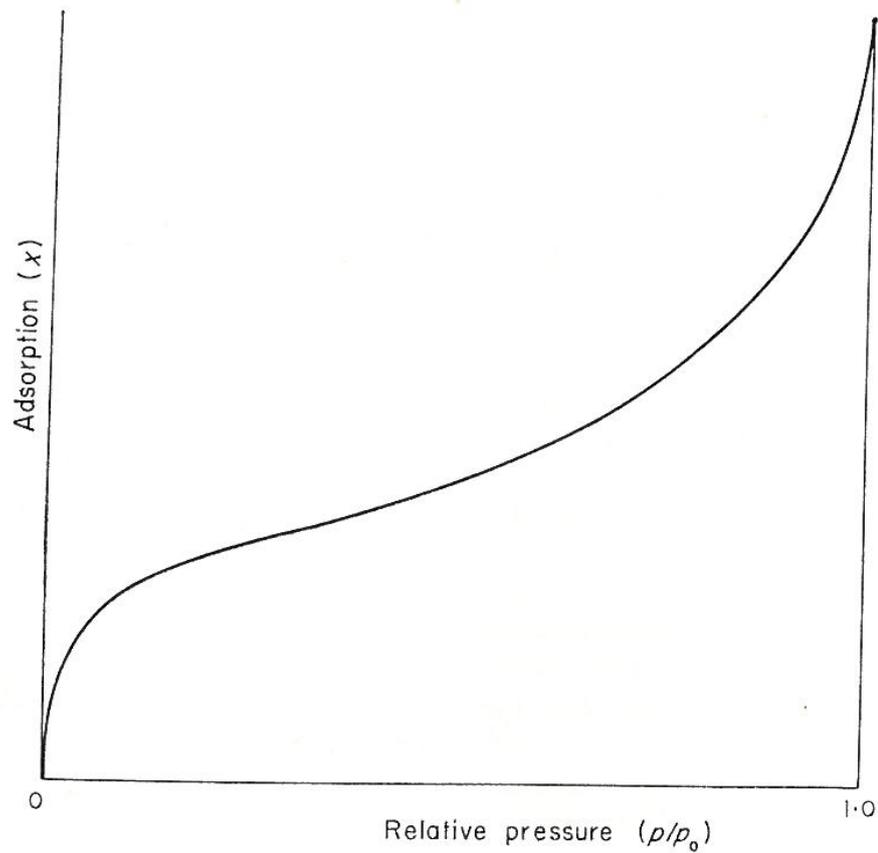
FIG. 3.1. A Type II isotherm.
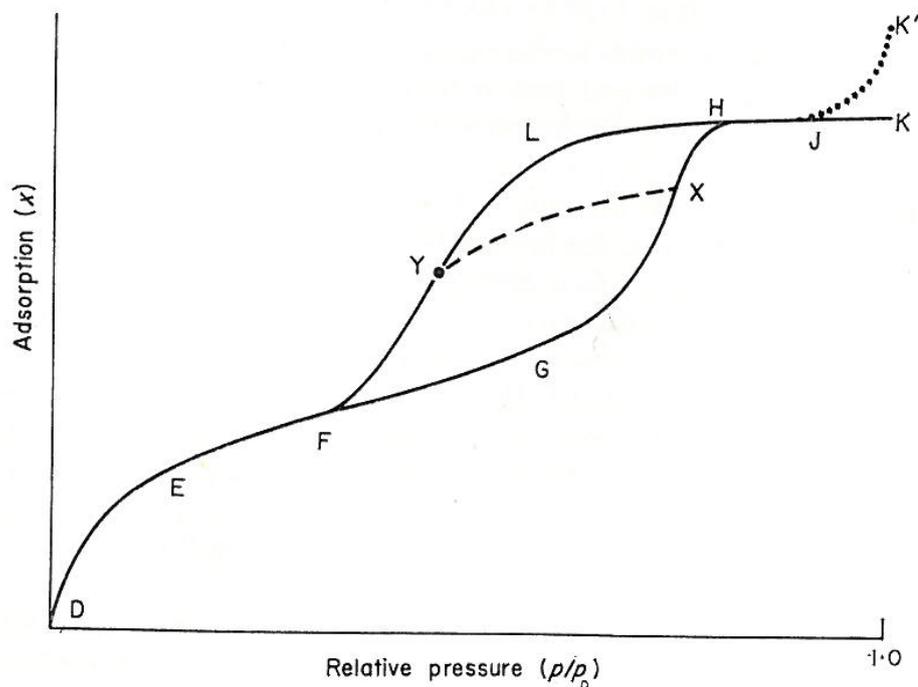

Fig. 4.19: *Type II and type IV isotherms (Gregg and Sing 1967)*

In mesopores, capillary condensation of the adsorbate to a liquid is believed to occur, and to give rise to the branch HLF of the isotherm; branch JK', when present is

ascribed to capillary condensation in relatively coarse pores (macropores) or in the interstices between the grains of the solid.

Along the low pressure branch, DEF, monolayer adsorption is taking place on the walls of the pores, in exactly the manner visualised for non-porous solids (isotherm type II), the process is reversible and there is no hysteresis. At a point somewhere between E and F, or in some case actually at point F where the loop opens, the monolayer is completed. Along the branch FGH a multilayer is gradually built up, again just as in porous solids. The multilayer growths in thickness as pressure increases along the branch FGH till at H the pores are completely filled with adsorbate in a liquid-like condition. Thereafter adsorption being confined to the outside of the grains, must increase very slowly and the flat branch HJ results. When adsorbate is withdrawn from the system after reaching point H, the desorption branch HLF is traversed: the liquid within any pore begins to evaporate from a meniscus which stretches across the pore, as soon as the equilibrium pressure in the system has fallen to a critical value p given by insertion of the value of r(pore radius) in the Kelvin equation

$$\ln p/p_o = -\frac{2\gamma V}{rRT}\cos\phi \quad (14)$$

Here p_o is the saturated vapour pressure at the temperature, T(K) of the system, γ and V are the surface tension and the molar volume of the adsorbate in liquid form, R is the gas constant per mole and ϕ is the angle of contact between the liquid and the wall of the pore. This equation also plays an important role in calculations of pore size distribution Gregg and Sing (1967).

The catalytic activity of LDHs changes when they are calcined. In the following experiments the temperature at which they were performed was -196 ^{o}C and the adsorbate gas was nitrogen. My experimental results show that surface area for Mg-Al LDHs (*Fig. 4.20b*) starts increasing at 300 ^{o}C and it is maximum at ~400 ^{o}C in the case of Mg-Al LDHs while the same is true when 10% of Mg is replaced with copper. In the case when 10% of Mg is replaced with cobalt, the max surface area shifts at 500 ^{o}C. When chromium is used, it replaces aluminium there is an increase at surface

area that starts at ~300 °C which reaches a local maximum at 400 °C, however the absolute maximum occurs at ~600 °C. In all the cases, at 900 °C there is a very sudden drop in surface area. Microwaved Mg-Al don't give conclusive results due to the lack of data.
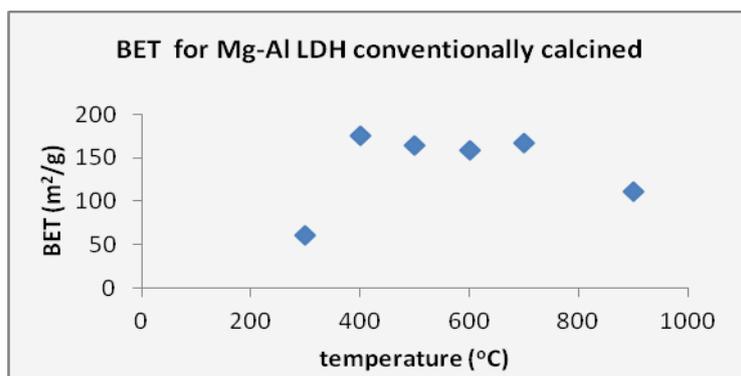
Fig. 4.22a
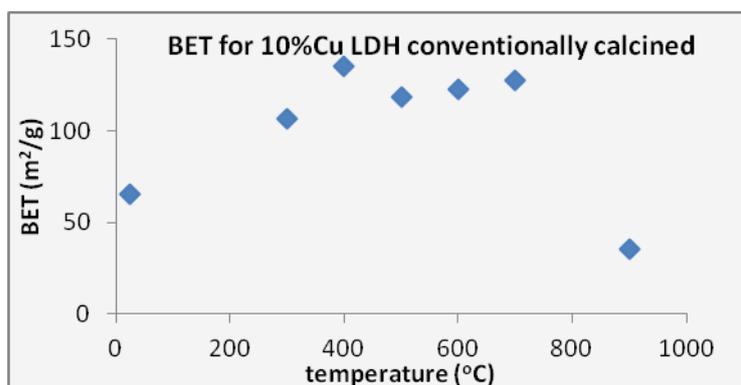
Fig. 4.22b
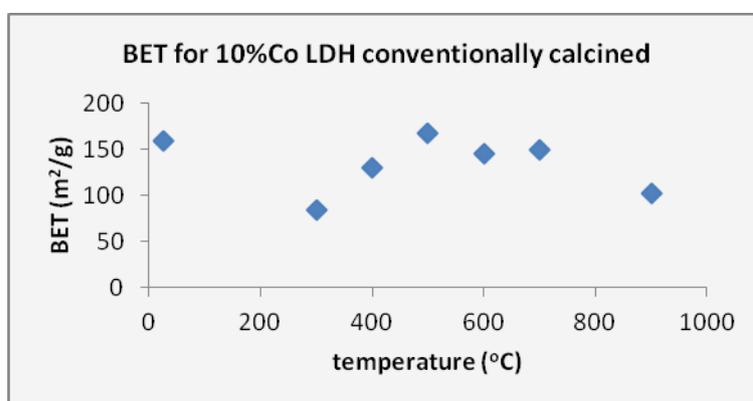
Fig. 4.22c
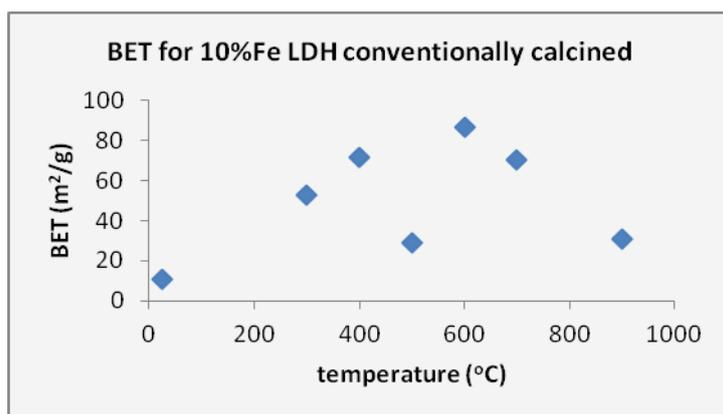
Fig. 4.22d
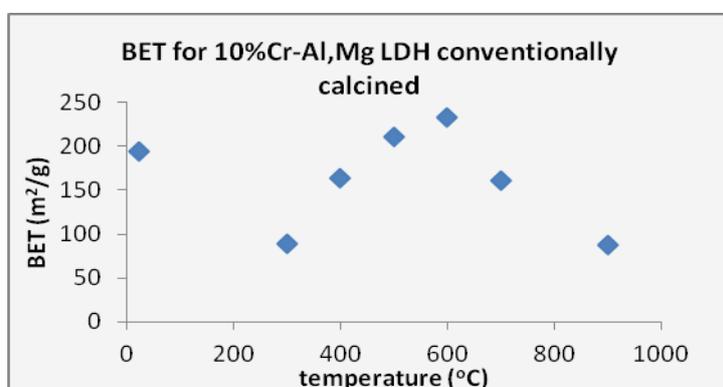
Fig. 4.22e

Dehydroxylation and decarbonation of LDHs are reversible processes, as long as the temperature doesn't exceed 600 °C Reichle and others (1986). In the experiments performed up to 500 °C Reichle and others (1986) observed that delamination can't be the mechanism for hydrotalcite decomposition. The exiting steam and carbon dioxide escaped through holes in the crystal surface which then appear as small, fairly regularly spaced craters. This escape mechanism explains the relatively small increase in the surface area on heating. It appears that the interlaminar forces in hydrotalcite are sufficiently strong, even during heating, so that interstitial venting is not possible. In my experiments the surface area for Mg-Al LDHs was slightly increased up to 600 °C calcinations and this kind of increase continued smoothly up to 900 °C, indicating that the same mechanism of venting of steam and carbon

dioxide continues. This is in agreement with Reichle and others (1986) who proved a modest increase in surface area, a retention of the crystal morphology, the appearance of pockmarks on the crystal surface and numerous fine pores which are in the range 20 – 40 Å.

Concerning the LDHs where 10% of magnesium was replaced by other metals, the trend is exactly the same, excluding chromium, which replaces 10% of aluminium. The graph and the trend there is less conclusive.

In order for the surface area surface graphs to make any sense more data points are needed at this stage this work is inconclusive.

4.14 Explanation/Comparison

DSC-TG

Reichle and others (1986) reported that decarbonation starts already at 300 ^{o}C, where water vapour and CO_2 escape through fine pores generated at the brucite like layers which results in the increase in specific surface area.

The DSC peak that is below 100 ^{o}C was reported by Miyata (1980). According to this explanation it arises when samples are equilibrated at room temperature (like in my case where the samples were kept in a furnace at 70 ^{o}C overnight) and its value depends on the specific samples tested, while the other two peaks remain unchanged. Similar results have been reported by other authors for Mg-Al-CO_3 LDHs. The value of this peak was ranging from 8.41 Jg^{-1} to 13.59 Jg^{-1} (*fig. 32*) , according to literature it should had been H = 43 ± 7 $KJmol^{-1}$, this value is higher than what is normally expected during evaporation (ca. 40 $KJmol^{-1}$) therefore the water is condensed and not simply physisorbed. There is agreement between the temperature peaks obtained at DSC and TG (weight loss) processes in my series of experiments with Mg-Al (3:1 molar ratio) LDHs. It is worth observing that this peak is

missing when the LDHs are dry, like in the case of 008 dried (*fig. 4.21*) and can arise when they are exposed to moist air even during handling. This process is reversible.

^exo

```
008,dry, 22.04.2010 17:04:25
008,dry, 14.7400 mg

? Integral        -7193.64 mJ
  normalized      -488.04 Jg^-1
Onset             28.53 °C
Peak              217.59 °C

5
mW
```

Lab: METTLER   ST A R^e SW 9.01
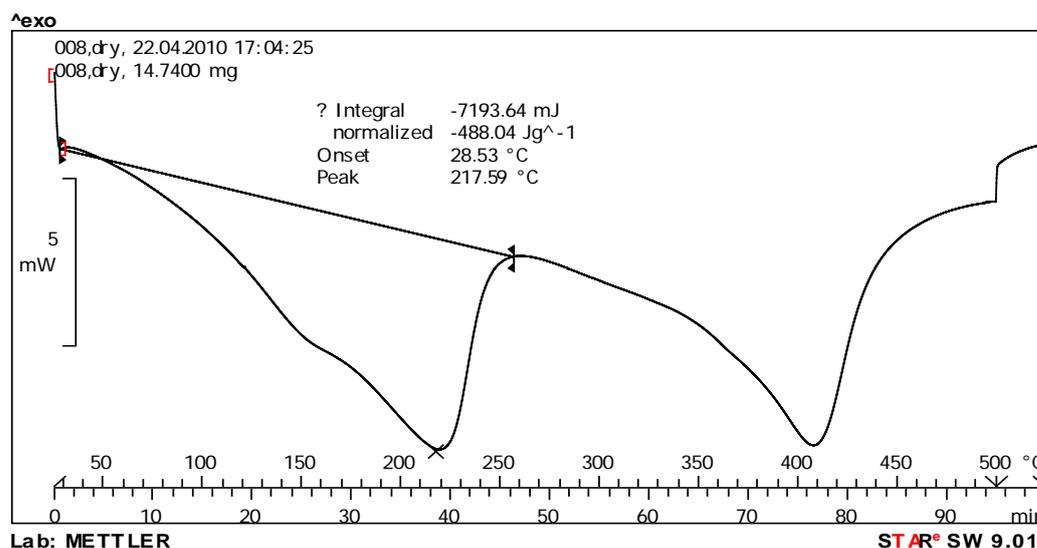
Fig.4.21: *The peak at 70 ^{o}C which corresponds to loss of loosely bound water is missing.*

The second stage of removal of water corresponds to the interlayer one. This removal can be separated into two stages (Stanimirova 1999): 1) 140 – 180 ^{o}C and 2) 240 – 260 ^{o}C. In the first stage the interlayer is dehydrated but this has no effect at the interlayer distance, d(0 0 3), which is ~7.8 Å. This is because the carbonate ions, which have the same radius with water (3.0 Å) act as chemically-unbonded pillars. Full dehydration is achieved at the second stage of water removal. The dehydration enthalpy change is according to L. Pesic (1992): H = 55±2 KJmol^{-1} and this value is close to what is expected for physisorbed water (Could I measure the enthalpy for the two separate stages in my results for 007?). In this stage there is decrease of interlayer spacing from 7.7 A to 6.6 Å, something that has a pronounced effect on the structure of LDHs, simply because the radius of carbonate ions is 3.0 Å and they can't be accommodated in the interlayer anymore. The brucite-like sheet is 4.8 Å therefore the interlayer spacing is 1.8 Å and as a consequence the grafting of carbonate ions in the brucite layers starts. In that case, the hydroxyl groups of the parent layers are substituted by oxide groups of the carbonate ions in the corners of

some [Mg(OH)$_6$] octahedra in the layers. PXRD results show that there is broadening of the (0 0 3) peak at these temperatures, something that indicates that the structure of the LDH is still layered but it becomes partially disordered. My conventional calcination experiments start from 300 ^{o}C, however one can still see that the crystallinity is poor and additionally the (0 0 3) peak is much broader indeed.

Rives (2001) observed that after calcinations at 350 ^{o}C the PXRD pattern shows only broad peaks roughly coincident with those of MgO, the decrease from the tabulated values is assigned to the formation of non-stoichiometric spinel containing Al^{+3} ions in the MgO lattice or alternatively to the formation of a solid solution of Al^{+3} ions in the MgO lattice. In my PXRD patterns at 900 ^{o}C after conventional calcination there is clear distinction between spinel and pure MgO.

OVERALL CONCLUSION

Microwaves interact in an unknown way with matter. That includes bacterial cells and inorganic matter. The poor control over experimental conditions doesn't allow the microwave effect to be isolated. Apart from the poor control of the experimental equipment, the lack of measurement of the two most important parameters of the experiments in both the series of experiments, i.e. measurement of the electric field (V/m) and specific absorption rate (mW/mm^2) make the interpretation of results unreliable.

No safe conclusions can be drawn about how microwaves interact with matter and why this interaction is different when compared with other heating methods.

REFERENCES

Adamek F and Hajek M. 1992.

Microwave-assisted catalytic addition of halocompounds to alkenes.

Tetrahedron Letters 33(15):2039-2042.

Alcamo Edward I. 1994

Fundamentals of Microbiology

Fourth Edition

The Benjamin/Cummings Publishing Company, Inc.

Aleixo J A G, Swaminathan B, Jamesen K S, Pratt D E. 1985.

Destruction of pathogenic bacteria in turkeys roasted in microwave ovens.

Journal of Food Science 50:873-880.

Anaya I, Aguirrezabal A, Ventura M, Comellas L, Agut M. 2008

Survivability of *Salmonella* cells in popcorn after microwave oven and conventional cooking.

Microbiological Research 163(1):73-79.

Asami K, T Hanai and N Koizumi. 1980.

Dielectric Approach to Suspensions of Ellipsoidal Particles covered with a Shell in Particular Reference to Biological Cells

Japanese Journal of Applied Physics: 19(2) 359-365.

Bai X-M, A F Voter, R G Hoagland, M Nastazi and B Uberuaga. 2010.

Efficient annealing of radiation damage near grain boundaries via interstitial emission

Science, 327: 1631-1634

Baldwin R E, Cloninger M, Fields M. 1968.

Growth and destruction of Salmonella Typhimurium in egg white foam products cooked by microwaves

Applied Microbiology 16:1929-1934.

Baldwin R E, Fields M, Poon W, Korschen B. 1971.

Destruction of Salmonella by microwave heating of fish with implications for fish products

J Milk Food Technol 34:467-470.

Barnes F S, Hu C-LJ, 1977.

Model for some non-thermal effects of radio and microwave fields on biological membranes

IEEE Transactions on Microwave Theory and Techniques 25:742-746.

Barnes F. S. and Chia-Lun Hu. 1977

'Model for some non-thermal effects of radio and microwave fields on biological membranes

IEEE Transactions on Microwave Theory and Techniques 25(9) 742-746.

Bazanova E B, A K Bryukhova, R L Vilenskaya, E A Gel'vich, M B Golant, N S Landau, V M Mel'inkova, N P Mikaelyan, G M Okhokhonina, L A Sevast'yanova, A Z Smolyanskaya and N A Sycheva. 1974.

'Certain methodological problems and results of experimental investigation of the effects of microwaves on microorganisms and animals

 Sov Phys-Usp 16 (4) 569-570.

Belyaev I Y, Alipov Y, Polunin V, Shcheglov V. 1993.

Evidence for dependence of resonant frequency of millimetre wave interaction with *Escherichia coli* K12 cells on haploid genome length.

Electro- and Magnetobiology 12:39-49.

Berek H E and K A Wickersheim, 1988

Measuring Temperatures in Microwaveable Packages

Journal of Packing Technology 2:164-168.

Boch P, Lequex N. 1997.

Do microwaves increase the sinterability of ceramics?

Solid State Ionics 101-103, 1229-1233

Bohr H, Bohr J. 2000.

Microwave-enhanced folding and denaturation of globular proteins.

Physical Review E 61:4310-4314.

Bohr H, Bohr J. 1999.

Microwave-enhanced folding and denaturation of globular proteins.

Physical Review E 61:4310-4314.

Buffler C R. 1993.

Microwave cooking and processing: Engineering fundamentals for the food scientist.

Van Nostrand Reinhold. New York.

Cacciapuoti G, Porcelli M, Bertoldo C, De Rosa M, Zappia V. 1994.

Purification and characterization of extremely thermophilic and thermostable 5'-methylthioadenosine phosphorylase from the archaeon Sulfolobus solfataricus. Purine nucleoside phosphorylase activity and evidence for intersubunit disulfide bonds.

J Biol Chem 269(40):24762-24769.

Celandroni F, Longo I, Tosoratti N, Giannessi F, Gheraldi E, Salvetti S, Baggiani A, Senesi S. 2004.

Effect of microwave radiation on *Bacillus subtilis* spores.

Journal of Applied Microbiology 97:1220-1227.

Chen D. S. D., 'Finite Element Analysis of Temperature Distribution in Microwaved Particulate foods'. Paper presented at the International Winter Meeting Sponsored by 'The AMERICAN SOCIETY OF AGRICULTURAL ENGINEERS' Hyatt Regency in Illinois Center, Chicago, Illinois, 18 – 21 December 1990.

Cheng D, 1989.

Field and Wave Electromagnetics

Second Edition

World Student Series Edition

Chipley J R. 1980.

Effects of microwave irradiation on microorganisms.

Advances in Applied Microbiology 26:129–145.

Craven S E, Lillard H S. 1974.

Effect of microwave heating precooked chicken on Clostridium perfringens.

Journal of Food Science 39:211-212.

Cunningham F E. 1978.

The effect of brief microwave treatment on numbers of bacteria in fresh chicken patties.

Poultry Science 57:297-297.

Dahl C A, Matthews M E, Marth E H. 1980.

Fate of Staphylococcus aureus in beef loaf, potatoes and frozen and canned green beans after microwave-heating in a simulated cook/chill hospital foodservice system.

Journal of Food Protection 43:916-923.

Dardanoni I, Toregrossa M V. 1985.

Milllimeter-wave effects on *Candida albicans* cells.

Journal of Bioelectricity 4(1):171-176.

Datta A K 1991

Mathematical Modelling of Biochemical Changes during Processing of Liquid Foods and Solutions

 Biotechnol Prog 7:397-402.

Datta A K 2000.

Fundamentals of heat and moisture transport for microwaveable food product and process development. In:

Datta A K, R C Anatheswaran (RC, editors). Handbook of microwave

technology for food applications.

Marcel Dekker, Inc. New York.

Davis C C, Edwards G S, Swicord M L, Sagripanti J, Saffer J. 1986.

Direct excitation of internal modes of DNA by microwaves.

Bioelectrochemistry and Bioenergetics 16:63-76.

Decareau R. 1985

 Microwave in the Food Processing Industry, Academic Press, Inc.

Deng Y, R K Singh and J H Lee

Estimation of Temperature Profiles in Microwaved Particulates Using Enzyme and Vision System

Lebensm. – Wiss.-Technol. 36:331-338

Devyatkov, N D. 1974.

Influence of millimetre-band electromagnetic radiation on biological objects

 Sov. Phys.-Usp. 16(4) 568-569.

El Malki K, A De Roy and J P Besse. 1989.

New Cu-Cr layered double hydroxide compound: discussion of pillaring with intercalated tetrahedral anions

Eur J Solid State Inorg Chem, 339

Fermi E, Pasta J and Ulam S. 1955.

Studies of nonlinear problems.

Los Alamos Scientific Laboratory Report of the University of California.

Fung D Y C and F E Cunningham. 1980.

Effect of Microwaves on Microorganisms in Foods

Journal of Food protection 43(8) 41-650.

FDA [U.S. Food and Drug Administration]. 2000.

Irradiation in the production, processing and handling of food 21 CFR Part 19.

U.S. Government Printing Office, Washington D.C.

Fleischman G J. 1996.

Predicting temperature range in food slabs undergoing long-term low-power microwave heating

J Food Eng 27(4):337-351.

Froehlich H. 1968.

Long-range coherence and energy storage in biological systems"

International Journal of Quantum Chemistry 2:641-649.

Froehlich H. 1977.

Possibilities of long-range and short-range electric interactions of biological systems.

Neurosci Res Progr Bull 15:67-72.

Fruin J T, Guthertz L. 1982.

Survival of bacteria in food cooked by microwave oven, conventional oven and slow cookers.

Journal of Food Protection 45:695-698.

Fujikawa F, Ushioda H, Kudo J. 1992.

Kinetics of *Escherichia coli* destruction by microwave irradiation.

Applied and Environmental Microbiology 58:920-924.

Giacovazzo C, Monaco H L, Artioli G, Viterbo D, Ferraris G, Gilli G, Zanotti G and Catti M. 2002.

Fundamentals of Crystallography 2nd edition

Oxford Science Publications

Gedye R N. 1997.

The question for non-thermal effects in the rate enhancement of organic reactions by microwaves

Microwaves: Theory and Applications in Materials Processing 4:165-172.

Gedye R N, Smith F, Westaway K C. 1988.

The rapid synthesis of compounds in microwave ovens

Can J Chem 66: 17 – 26.

Gentry T S, Roberts J S. 2005.

Design and evaluation of a continuous flow microwave pasteurization system for apple cider

LWT-Food Science and Technology 38:227-238.

Gershenfeld N. 1999.

The Nature of Mathematical Modelling

Cambridge University Press.

Geveneke D J, Kozempel M,Scullen O J, Brunkhorst C. 2002.

Radiofrequency energy effects of microorganisms in foods

Innovative Food Science and Emerging Technologies 3:133-138.

Goldblith S A and D I C Wang. 1967.

Effect of Microwaves on *E. coli* and *B. Subtilis*

Applied Microbiology 15(6) 1375-1971.

Grant E H. 1957.

The dielectric method of estimating protein hydration

Phys Med Biol 2:17-28.

Gregg S J and Sing K S W. 1967.

Adsorption, surface area and porosity

Academic Press.

Grundler W, Keilmann F. 1978.

Non-thermal effects of millimetre microwaves on yeast growth

Z Naturforsch 33:15-22.

Gunasekaran G, Yang H W. 2007.

Optimization of pulsed microwave heating

Journal of Food Engineering 78:1457-1462.

Ha T, Ting Y, Liang J, Caldwell W B, Beniz A A, Chemla D S, Schultz P G, Weiss S. 1999.

Single molecule fluorescence spectroscopy of enzyme conformational dynamics and cleavage mechanism

Proc Natl Acad Sci USA 96:893-898.

Hanai T., K. Asami and N. Koizumi. 1979.

'Dielectric Theory of Concentrated Suspensions of Shell-Spheres in Particular Reference to the Analysis of Biological Cell Suspensions

Bull Inst Chem Rers, Kyoto Univ (4) 297-305.

Heddleson R A, Doores S. 1994.

Factors affecting microwave heating of foods and microwave-induced destruction of food pathogens-A review

Journal of Food Protection 57:1025-1035.

Heddleson R A, Doores S, Anantheswaran R C. 1994.

Parameters affecting destruction of *Salmonella* spp. by microwave heating

Journal of Food Science 59:447-451.

Heddleson R A, Doores S, Anantheswaran R C, Kuhn G D. 1996.

Viability loss of Salmonella species, Staphylococcus aureus, and Listeria monocytogenes in complex foods heated by microwave energy

Journal of Food Protection 59:813-818.

Heddleson R A, Doores S, Anantheswaran R C, Kuhn G D, Mast M. 1991.

Survival of *Salmonella* species heated by microwave energy in a liquid menstruum containing food components

Journal of Food Protection 54:637-642.

Heller J H and A A Texeira Pinto. 1952.

A New Physical Method for Creating Chromosomal Aberrations

Nature 183:904.

Huang L, Sites J. 2007.

Automatic control of a microwave heating process for in-package pasteurization of beef frankfurters

Journal of Food Engineering 80:226-233.

Hudson M S Carlino and D Apperley. 1995.

Thermal conversion of a layered (Mg/Al) double hydroxide to the oxide

J Mater Chem 5(2), 323-329.

Irimajiry A, K Hanai and A Inouye. 1979.

The Dielectric Theory of "Multi-stratified Shell" Model with its Application to a Lymphoma Cell

 J Theor Biol 78:251-169.

Jeng K H D, Kaczmareck K A, Woodworth A G and Balasky G. 1987.

Mechanism of microwave sterilization in the dry state

Applied and Environmental Microbiology 53:2133-2137.

Kakutani T, S Shibatani and M Sugai. 1993.

Electrorotation of non-spherical cells: theory for ellipsoidal cells with arbitrary number of shells

 Bioelectrochemistry and Bioenergetics 31:131-145.

Khalil HM. 1983.

Evaluation of microwave energy and its potential use in food sterilization

 PhD Thesis.

Khalil H, Villota R. 1989.

The effect of microwave sublethal heating on the ribonucleic acids of *Staphylococcus aureus*

Journal of Food Protection 52:544-548.

Kindle G, Buse A, Kampa D, Meyer Konig U, Daschner F D. 1996.

Killing activity of microwaves in milk

Journal of Hospital Infection 33:273-278.

Kiselev R I, Zalyubovskaya N P. 1974.

Effects of millimetre band electromagnetic waves on the cell and certain structural elements of the cell

Sov Phys Usp 16:575-576.

Knutson K, Marth E H, Wagner M. 1988.

Use of microwave ovens to pasteurize milk

Journal of Food Protection 51:715-719.

Kozempel M F, Annous B A, Cook R D, Scullen O J, Whiting R C. 1998.

Inactivation of micrrorganisms with microwaves at reduced tempetratures

Journal of Food Protection 61(5):582-585.

Kozembel M F Bassam A A R D Cook O J Scullen and R C Whiting. 1998.

Inactivation of Microorganisms with Microwaves at Reduced Temperatures

 Journal of Food Protection 61(5) 582-585.

Lakins D G, Alvarado C Z, Thompson L D, Brashears M T, Crooks J C, Bradshears M M. 2008.

Reduction of *Salmonella Enteriditis* in shell eggs using directional microwave technology

Poultry Science 87:985-991.

Lakins D G, Echevery A, Alvarado C Z, Brooks J C, Brashears M T, Brashears M M. 2008.

Quality of mold growth on white enriched bread for military rations following directional microwave treatment

J Food Sci 73:99-103.

Laurence J P, French R, Linder , McKenzie D. 2000.

Biological effects of electromagnetic fields-mechanisms for the effects of pulsed microwave radiation on protein conformation

J Theor Biol 206:291-298.

Lechowich R V, Beuchat L R, Fox K I, Webster F H. 1969.

Procedure for evaluating the effects of 2,450 MHz microwaves upon *Streptococcus faecalis* and *Saccharomyces cerevisiae*

Applied Microbiology 10(1):106-110

Lin W, Sawyer C. 1988.

Bacterial survival and thermal responses of beef loaf after microwave processing.

Journal of Microwave Power 23(3): 183-194.

Liu F, I Turner, and M Bialkowski. 1994.

A Finite-Difference Time-Domain Simulation of Power Density Distribution in a Dielectric Loaded Microwave Cavity

Journal of Microwave Power and Electromagnetic Energy 29(3) 138-148.

Liu F, I Turner, E Siores and P Groombridge. 1996.

A Numerical and Experimental Investigation of the Microwave Heating of Polymer Materials Inside a Ridge Waveguide

 Journal of Microwave Power and Electromagnetic Energy 31(2):71-82.

Lorenson C. 1990.

The Why's and How's of Mathematical Modelling for Microwave Heating

Microwave World 11(1):14 – 23.

LSBU (London South Bank University). 2006. http://www.lsbu.ac.uk/water

Manoilov S E, Chistyakova E N, Kondrat'eva V F, Strelkova M A. 1974.

Effects of millimetre band electromagnetic waves on certain aspects of protein

metabolism in bacteria.

Sov Phys-Usp 16:573-574.

Maxwell J C. 1954.

A treatise on electricity and magnetism 3rd Edition New York

Dover Publications Inc.

McGraw-Hill Dictionary of Scientific and Technical Terms

Sixth Edition

2002

Metaxas A C, Meredith R J. 1983.

Industrial microwave heating

Peter Pellegrinous Ltd, London, United Kingdom.

Mingos D M P, Baghurst D R. 1991.

Applications of microwave dielectric heating effects to synthetic problems in

chemistry

Chem Soc Rev 20:1-47.

Miyata S. 1980.

Physicochemical properties of synthetic hydrotalcites in relation to composition

Clays and Clay Minerals 28(1) 50-56.

Moat W A. 1961.

Chemical changes in bacteria heated in the milk as related to loss of stainability

J Dairy Sci 44:1431-1439.

Morgan H. and N. G. Green. 2003.

 AC Electrokinetics: colloids and nanoparticles

Philadelphia, Research Studies Press LTD.

Mudgett R E. 1989.

Microwave food processing

Food Technology 43(10): 117-126.

Mudgett R. 1998.

A Physical-Chemical Basis for Prediction of Dielectric Properties in Liquid and Solid Foods at Ultrahigh and microwave Frequencies

PhD Thesis, Massachusetts Institute of Technology.

Mudgett R E D I C Wang S A Goldblith. 1974.

Dielectric properties of food materials

 J Microwave Power.

Murrell W G. 1969.

In: Gould G W, Hurst A, editors.

 The bacterial spore

London and New York:Academic Press. pp. 215-273.

Murrell W G, Warth A D. 1965.

In: Campell L L, Halvorson H O, editors. Spores III

American Society for Microbiology. pp 1-24.

Nyfors E, Vainikainen P. 1989.

Industrial microwave sensors

Artech House, Norwood, U.K.

Ooi L L. 2010.

Fundamentals of X-ray crystallography

Oxford University Press.

Pesic L, Salipurovic S, Markovic V, Vucelic D, Kagunya W and Jones W. 1992.

Thermal characteristics of a synthetic hydrotalcite-like material

J Mater Chem 2(10):1069-1073.

Porcelli M, Cacciapuoti G, Fusco S, Iacominno G, Gambacorta A, De Rosa M, Zappia V. 1993.

S-Adenosylhomocysteine hydrolase from the thermophilic archaeon Sulfolobus solfataricus: purification, physico-chemical and immunological properties

Biochim Biophys Acta 1164:79-188.

Porcelli M, Cacciapuoti G, Fusco S, Massa R, D' Ambrosio G, Bertoldo C, De Rosa M, Zappia V. 1997.

Non-thermal effects of microwaves on proteins: Thermophilic enzymes as model system

FEBS Letters 402:102-106.

Prausnitz S, Susskind, C, and Vogelhut P. 1961.

Longevity and cellular studies with microwaves

 In 'Proceedings of the Tri-Service Conference on Biological Effects of Microwave Radiation, 1-135.

Reichle W T, S Y Yang and D S Everhardt. 1986.

The nature of the thermal decomposition of catalytically active anionic clay mineral

Journal of Catalysis 101:356-359.

Rives V. 2001.

Layered Double Hydroxides

Nova Science Publishers.

Rosen C G. 1972.

Effects of microwaves on food and related materials

Food Technology 36-55.

Royal Society of Canada. 1999.

An Expert Panel Report:

A review of the potential risks of radiofrequency fields

 from wireless telecommunication devices

March 1999.

Russel A D. 1982.

The destruction of bacterial spores.

(London) Academic Press Inc, London, U.K.

Ryynanen S. 2002.

Microwave heating uniformity of multicomponent prepared foods.

PhD Thesis, University of Helsinki, Helsinki, Finland.

Ryynanen S. 1995.

The electromagnetic properties of food materials: a review of the basic principles.

Journal of Food Engineering 26:409-429.

Saito M., H. P. Schwan and G. Schwarz. 1996

Response of Nonspherical Biological Particles to Alternating Electric Fields

Biophysical Journal 6:313-327.

Salvatorelli G, Marchetti M G, Betti V, Rosaspina S, Finzi G. 1996.

Comparison of the effects of microwave radiation and conventional heating on *Bacillus subtilis* spores

Microbios 87:169-174.

Sastry S K and S Palaniappan. 1991.

The Temperature Difference Between a Microorganism and a Liquid Medium during Microwave Heating

Journal of Food Processing and Preservation, 15:225-230

Schwarz G, M.Saito and H Schwan. 1965.

On the orientation of nonspherical particles in an alternating electrical field

The Journal of Chemical Physics: 43(10) 3562 – 3569.

Samarketou, Singh S P, Jha R K. 1996.

Effect of direct modulated microwave modulation frequencies exposure on physiology of the cyanobacterium *Anabaena doliolum*

Asia Pacific Microwave Conference.

Sato S, Shibata C, Yazu M. 1996.

Non-thermal killing effect of microwave irradiation.

Biotechnology Techniques 10:145-150.

Schiffmann R F. 1986.

Food product development for microwave processing.

Food Processing Magazine 40(6):94-98.

Stratton J A. 1941.

Electromagnetic Theory

Mac Graw-Hill book company, Inc. New York and London.

Setlow P. 2007.

I will survive: DNA protection in bacterial spores.

Trends in Microbiology 15:172-180.

Setlow P. 1975.

Purification and properties of some unique low-molecular-weight basic proteins degraded during germination of *Bacillus megaterium* spores.

Journal of Biological Chemistry 250:

 8168-8173.

Setlow B, Setlow P. 1979.

Localization of low-molecular-weight basic proteins in *Bacillus megaterium* spores by cross-linking with ultraviolet light

Journal of Bacteriology 139:486-494.

Setlow P, Waites W M. 1976.

Identification of several unique, low-molecular-weight basic proteins in dormant spores of *Clostridium bifermentans* and their degradation during spore germination

Journal of Bacteriology 127:1015-1017.

Shazman A, Mizrahi S, Cogan U, Shimoni E. 2007.

Examining for possible non-thermal effects during heating in a microwave oven

Food Chemistry 103(2):444-453.

Shin J K, Pyun Y R. 1997.

Inactivation of Lactobacillus plantarum by pulsed-microwave irradiation

Journal of Food Science 62:163-166.

Smith J L, Buchanan R, Palumbo S A. 1982.

Effects of food environment on Staphylococcal enterotoxin synthesis

J Food Prot 46:545-555.

Srikrishna S, Nagaraju S. 1992.

Acceleration of ortho-ester Claisen rearrangement by a commercial microwave oven

J Chem Soc Perkin Trans 1:311-312.

Stanimirova Ts, Vergilov I, Kirov G and Petrova N. 1999.

J Mat Sci 34: 4153.

Straub K D, Carver P. 1975.

Effects of electromagnetic fields on microsomal ATPase and mitochondrial oxidative phosphorylation

Ann N Y Acad Sci 247:292-300.

Takashima S. 1969.

Dielectric Properties of Proteins, I. Dielectric relaxation. In "Physical Pinciples and Tchniques of Protein Chemistry", Part A, ed. Leach S J, p. 291, Academic Press New York .

Tang Z, Mikhaylenko G, Liu F, Mah J H, Pandit R, Younce F and Tang J. 2008.

Microwave sterilization of sliced beef gravy in 7-oz trays

Journal of Food Engineering 89:375-383.

Taylor L S. 1981.

The Mechanisms of Athermal Microwave Biological Effects

 Bioelectromagnetics: 2 259-267.

Thompson J S, Thompson A. 1990.

In-home pasteurization of raw goat's milk by microwave treatment

International Journal of Food Microbiology 10:59-64.

Tong C H, Lentz R R, Lund D B. 1993.

A microwave oven with variable continuous power and a feedback temperature
controller

Biotechnol Prog 9:488-496.

Vela G R and J F Fu. 1979.

Mechanism of Lethal Action of 2450 MHz Radiation on Microorganisms

 Applied and Environmental Microbiology 37(3) 550-553.

Van Loock W. 1996.

Electromagnetic energy for pasteurization and sterilization: another viewpoint

Microwave World 17:23-27.

Vaid A, Bishop A H. 1998.

The destruction by microwave radiation of bacterial endospores and amplification of the released DNA

Journal of Applied Microbiology 85:115-122.

Vicente Rives, editor 2001.

Layered Double Hydroxides: Present and Future

Nova Science Publishers, Inc.

Villamiel M, Lopez-Fardino R, Corzo N, Martinez-Castro I. 1996.

Effects of continuous flow microwave treatment on chemical and microbiological characteristics of milk

Z Lebensm Unters Forsch 202:15-18.

Von Hippel A. 1962.

Dielectrics and Waves

New York, John Wiley and Sons, Inc

Warth A D. 1978.

Molecular structure of the bacterial spore

Advances in Microbial Physiology 17:1-45.

Webb S J, Booth A D. 1969.

Absorption of microwaves by microorganisms

Nature 222:1199-1200.

Wu T M, Austin S. 1979.

Biological Bose condensation and the time threshold for biological effects

Physics Letters A 73:266-268.

Yang H W and S Gunasekran. 2001.

Temperature Profiles in a Cylindrical Model Food During Pulsed Microwave Heating

Journal of Food Science 66: 998-1004.

Yee K. 1996.

Numerical solution of initial boundary problems involving maxwell's equations in isotropic media

 IEEE Transactions on Antennas and Propagation 14(30):302-307.

Zalyubovskaya N. 1974.

Reactions of living organisms to exposure to millimetre band electromagnetic waves Sov Phys-Usp 16(4):574-575.

Zhang H and A K Datta. 2000.

Coupled Electromagnetic and Thermal Modelling of Microwave Oven Heating of Foods

 Journal of Microwave Power and Electromagnetic Energy 35(2):72-85.

Zhang H, A K Datta, I A Taub and C Doona. 2001.

Electromagnetics, Heat Transfer and Thermokinetics

 Microwave Sterilization AIChE Journal 47(9):1957-1968.

Zhao H, I Turner and F W Liu. 1996.

Numerical Simulation of the Power Density Distribution Generated in a Multimode Cavity by Using the Method of Lines Technique to Solve Directly for the Electric Field IEEE Transactions on Microwave Theory and Techniques 44(12) 2185-2194.

Zimmermann W J, Beach P. 1982.

Efficacy of microwave cooking for devitalizing trichinae in pork roasts and chops

Journal of Food Protection 45:405-409.

http://hyperphysics.phyastr.gsu.edu/hbase/waves/magnetron.htm

APPENDIX 1: Salmonella Poona

Power(W)	exposure time (min)	Before (LFU)	After (LFU)	%ATP loss	Lead	Temp. (C
4	7	99999	99999	0		
4	10	32636	13223	59.48339257		
5	5	74275	55736	24.95994615	on	
5	40	8032	43635	-443.2644422		
5	4	99999	99999	0		
5	5	43297	29656	31.50564704		
5	5	29656	26210	11.61990828		
5	5	26210	15630	40.36627242		
5	5	99999	14694	85.30585306		
5	5	43823	34396	21.51153504		
5	5	47023	30125	35.93560598	on	
5	7	30125	57173	-89.78589212	on	
5	5	16485	29864	-81.15862906	on	
5	5	7083	15040	-112.3394042		room
5	10	3220	16458	-411.1180124		29
5	10	33669	44072	-30.89785856		30
5	10	49725	99999	-101.1040724		
5	15	48936	99999	-104.3464934		31
5	15	60394	69298	-14.74318641		
5	15	56951	99999	-75.58778599		
5	20	48167	99999	-107.6089439		33
5	20	40386	99999	-147.608082		
5	20	51151	99999	-95.49764423		
5	25	46560	99999	-114.7744845		34
5	25	25370	42778	-68.61647615		34
5	25	47309	64290	-35.89380456		
5	30	77457	99999	-29.10259886		34
5	30	50378	76180	-51.21680098		29
5	30	33485	48220	-44.00477826		
5	35	51995	99999	-92.32426195		31
5	35	41702	53525	-28.35115822		
5	35	32489	48582	-49.53368833		34
5	20	19436	99999	-414.5040132		38
5	40	34051	73236	-115.0773839		34
5	60	35255	58313	-65.40348887		37
6	7	99999	99999	0		
6	7	99999	99999	0		
6	30	72035	99999	-38.82001805		
6	30	13086	43823	-234.8846095		
6	30	25631	99999	-290.1486481	on	
6	25	29557	99999	-238.3259465	on	33
6	30	8881	420215	-4631.618061	32 (Room	
6	30	14691	42039	-186.1547886		33
6	30	13089	53417	-308.1060432		
7	40	99999	43495	56.50456505		
7	45	11319	99999	-783.4614365		
7	40	92498	72035	22.12264049		
10	15	99999	99999	0	on	61
10	5	41941	95516	-127.7389666		30
10	5	13301	48109	-261.6946094		
10	5	30793	42841	-39.12577534		
11	5	17231	23391	-35.74952121		
11	5	31124	47471	-52.52216939		34
11	5	18978	53487	-181.8368637		
12	5	19772	29089	-47.122193		
13	7	99999	99999	0		
14	5	99999	99999	0		
14	5	22228	99999	-349.8785316		38
15	5	99999	99999	0		
16	10	77270	99999	-29.41503818	on	
20	5	26445	99999	-278.1395349		39
20	5	36639	99999	-172.9304839		
20	5	99999	99999	0		

%ATP Loss - Analysis Toolpack - Descriptive Statistics			
	Mean	-50.4383	
	Standard Error	19.80084	
	Median	-39.9493	
	Mode	#N/A	
	Standard Deviation	92.87415	
	Sample Variance	8625.608	
	Kurtosis	11.18048	
	Skewness	-2.90755	
	Range	451.4843	
	Minimum	-411.118	
	Maximum	40.36627	
	Sum	-1109.64	
	Count	22	

APPENDIX 2: Staphylococcus Aureus

St. aureus Power(W)	Exposure time (min)	Before (LFU)	After (LFU)	%ATP Loss	Temp (C)
2	36	99999	99999	0	
4	5	99999	99999	0	
4	7	99999	99999	0	
4	60	11684	37926	-224.5977405	
4	90	37926	52890	-39.45578231	
5	7	9038	28651	-217.0059748	
6	7	99999	99999	0	
6	60	99999	99999	0	31
6	60	88540	99999	-12.94217303	33 Room 2
7	7	99999	99999	0	
7	10	99999	99999	0	
7	20	99999	72184	27.81527815	
7	20	99999	99999	0	39 Room 2
7	20	99999	99999	0	
8	20	99999	99999	0	
8	40	99999	29975	70.02470025	
8	40	99999	99999	0	30
8	40	99999	999999	-900.0090001	30
10	5	44838	99999	-123.0228824	32
10	5	46373	46031	0.737498113	
10	5	82540	99999	-21.15216865	
11	3.5	59210	99999	-68.88870123	
12	5	99999	99999	0	
12	5	99999	99999	0	
13	7	99999	99999	0	
14	5	99999	99999	0	
20	2	75922	68659	9.566397092	
20	5	99999	99999	0	39
20		99999	99999	0	
20	5	99999	99999	0	39
30	5	99999	58024	41.97541975	44
30	5	99999	47195	52.80452805	41
30	5	99999	40912	59.08759088	
30	10	43194	45538	-5.426679631	44.2
40	4	99999	91823	8.176081761	
50	10	99999	99999	0	
50	0.17	99999	68598	31.40131401	
50	0.5	68598	12817	81.3157818	
50	0.75	12817	3517	72.55988141	
50	5	75843	66511	12.3043656	46
50	5	59419	45616	23.22994328	46
50	5	99999	45673	54.32654327	56
56	2	68659	53798	21.64464965	
60	5	99999	46199	53.80053801	58.3
60	5	67837	80596	-18.80831994	54
60	5	65846	58103	11.75925645	56

| %ATP Loss-Analysis Toolpack-Descriptive Statistics		
	Mean	-21.7126012
	Standard Erro	21.33452839
	Median	0
	Mode	0
	Standard Devi	144.6978116
	Sample Varia	20937.45668
	Kurtosis	31.47370019
	Skewness	-5.28286105
	Range	981.3247819
	Minimum	-900.0090001
	Maximum	81.3157818
	Sum	-998.779655
	Count	46

APPENDIX 3: E. Coli

| E.Coli Power(W)	Exposure time(min)	%ATP Loss	Lead	Temp.	before(LFU)	after(LFU)
1	20	-459.345076			16918	94630
4	7	43.95227998			42917	24054
4	30	16.34092626			93991	78632
4	3	-77.0520032	on	cool	8711	15423
4	10	82.96447997	on	cool	45411	7736
4	4	-36.1448772	on	cool	4031	5488
4	15	-93.4777982		29	51685	99999
4	10	-171.70688			36804	99999
4	10	0		28	99999	99999
4	10	0			99999	99999
4	15	53.95253358		29	55534	25572
4	15	-176.068562			13827	38172
4	15	0			99999	99999
4	7	-61.9642564		29	30495	49391
4	7	-32.8028126			26452	35129
5	5	-3.96366183			54268	56419
5	5	-47.8765084			6381	9436
5	5	-120.266451			7431	16368
6	7	-180.082229			15323	42917
7	60	-5.67367642			94630	99999
10	5	-192.220087		30	21337	62351
10	5	-19.7777543		34	47245	56589
10	5	-137.228667			42153	99999
11	5	4.063849325			51183	49103
11	5	-80.3108108			14800	26686
11	20	87.68287683			99999	12317
11	5	-80.518793	on	28	7556	13640
11	20	-109.032379		40	47839	99999
11	20	0			99999	99999
14	7	-33.4407385			11483	15323
15	7	-44.9873737			7920	11483
15	45	0			99999	99999
16	5	-537.168142			1243	7920
20	5	-239.002644		44	29498	99999
20	5	-86.6371147		33	48051	89681
20	5	3.936942715			48337	46434
30	5	-296.297043		42	19849	78661
30	5	-0.70256529		45	43270	43574
30	5	-140.787383			41530	99999
40	7	0			99999	99999
41	10	-855.647936	on	53	10464	99999
44	5	-102.77192		44	49316	99999
46	5	0			99999	99999
48	5	-548.375802	on	52	15423	99999
48	5	0	on	41	99999	99999
50	0.17	62.34663611			29668	11171
50	0.5	47.42637186			11171	5873
50	0.75	74.23803848			5873	1513
50	5	-34.1389037		57.1	52468	70380
50	5	-49.494148		55	45369	67824
50	5	-55.733863		52	44804	69775
57	3	-556.429619	on	55	13640	89537
60	5	-89.6826287		63.2	44585	84570
60	5	-98.8296285		60.7	38193	75939
60	5	-18.7295197			42724	50726

APPENDIX 4: 10%Fe LDH conventionally calcined

10%Fe LDH conventionally calcined at 500 °C

10%Fe LDH

10%Fe LDH conventionally calcined at 600 °C

10%Fe LDH conventionally calcined at 700 °C

10%Fe LDH conventionally calcined at 900 °C
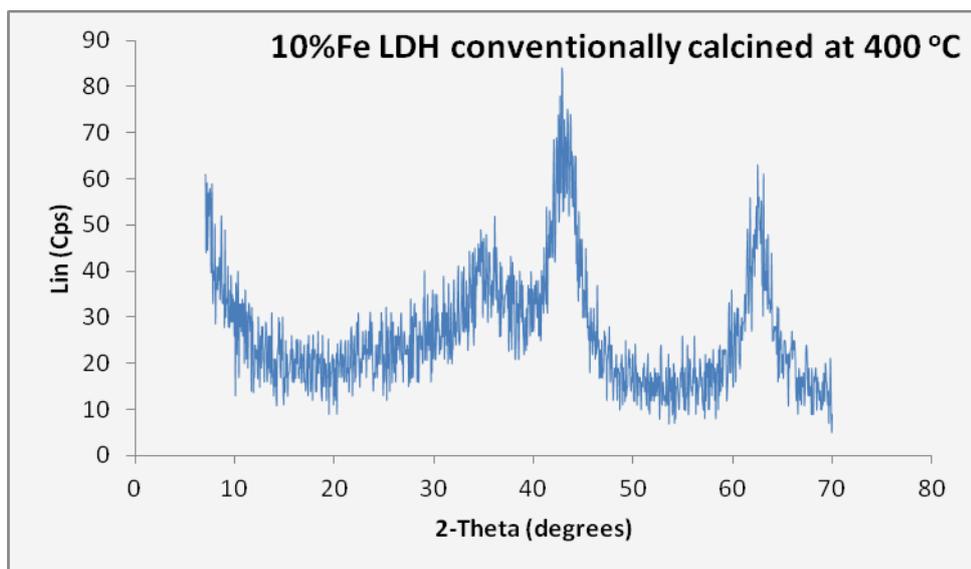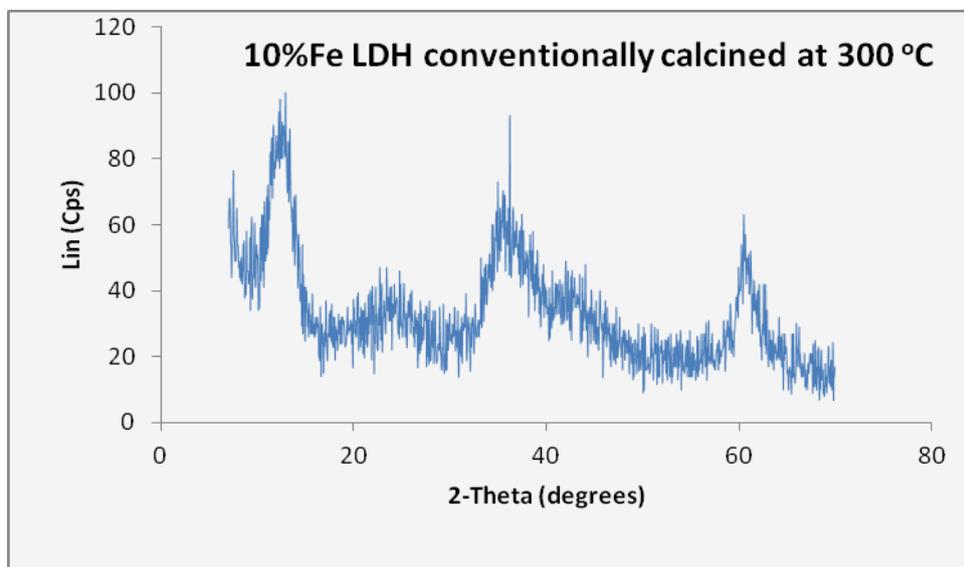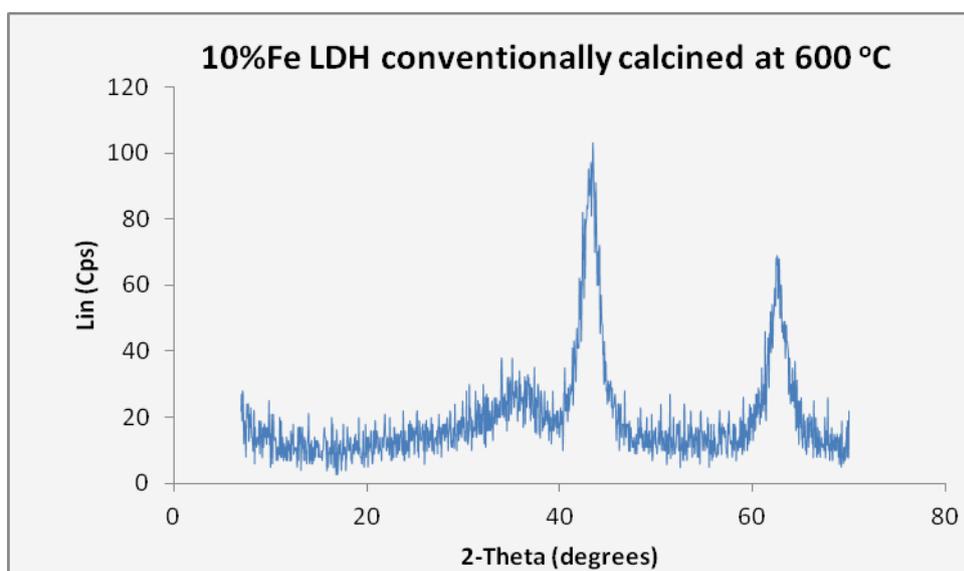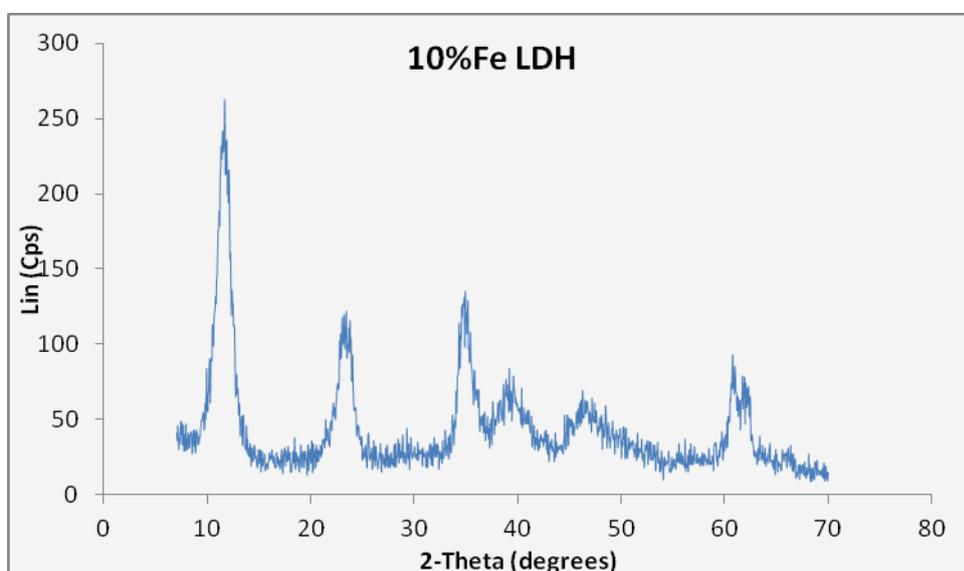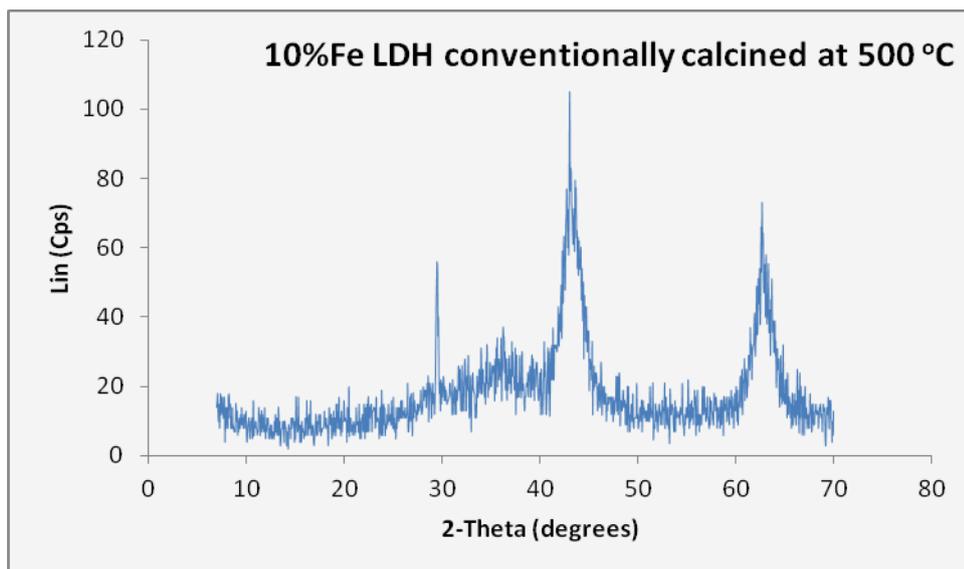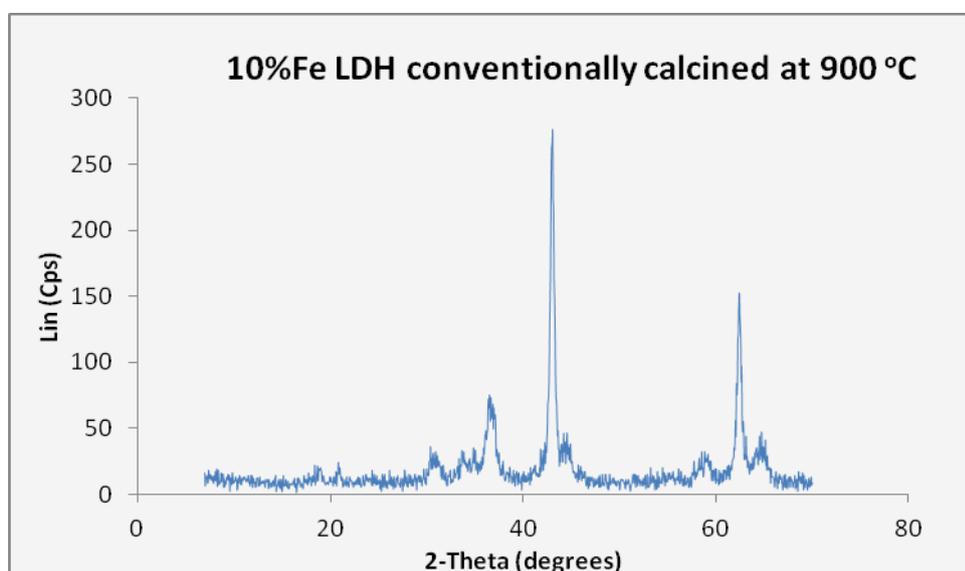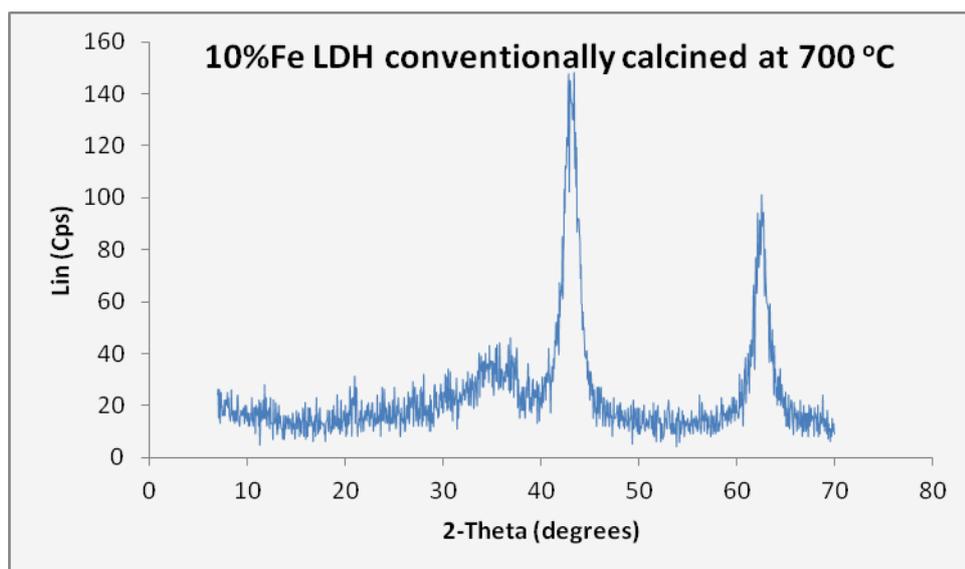
APPENDIX 5: 10%Co LDH conventionally calcined

10%Co LDH c onventionally calcined at 300 °C

10%Co conventionally calcined at 400 °C

10%Co conventionally calcined at 500 °C

10%Co LDH conventionally calcined at 600 °C

10%Co LDH conventionally calcined at 700 °C

10%Co LDH conventionally calcined at 900 °C
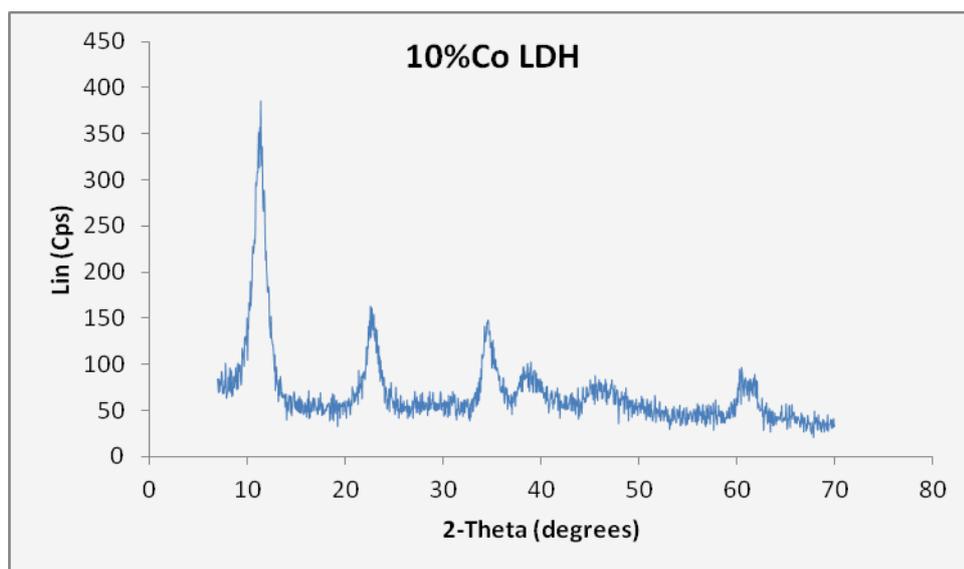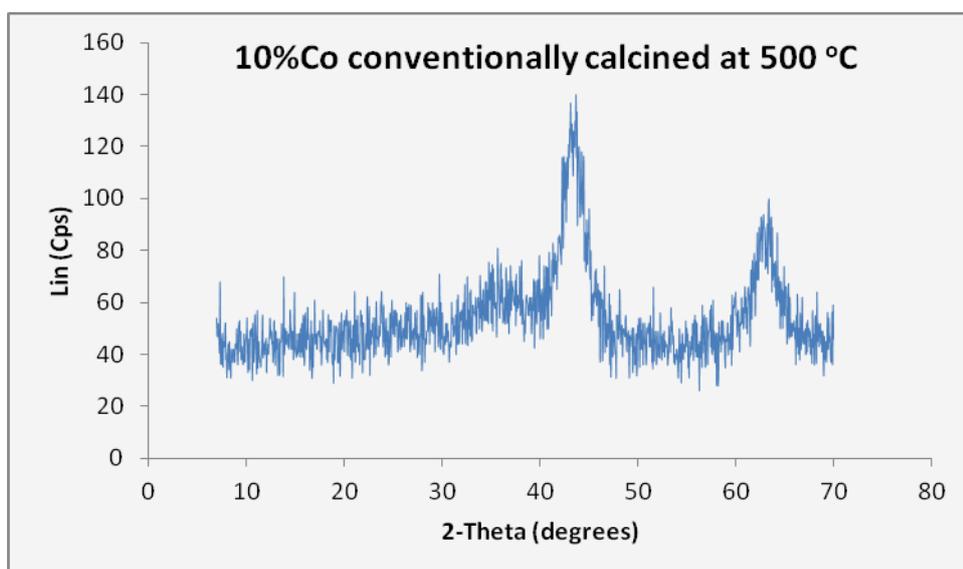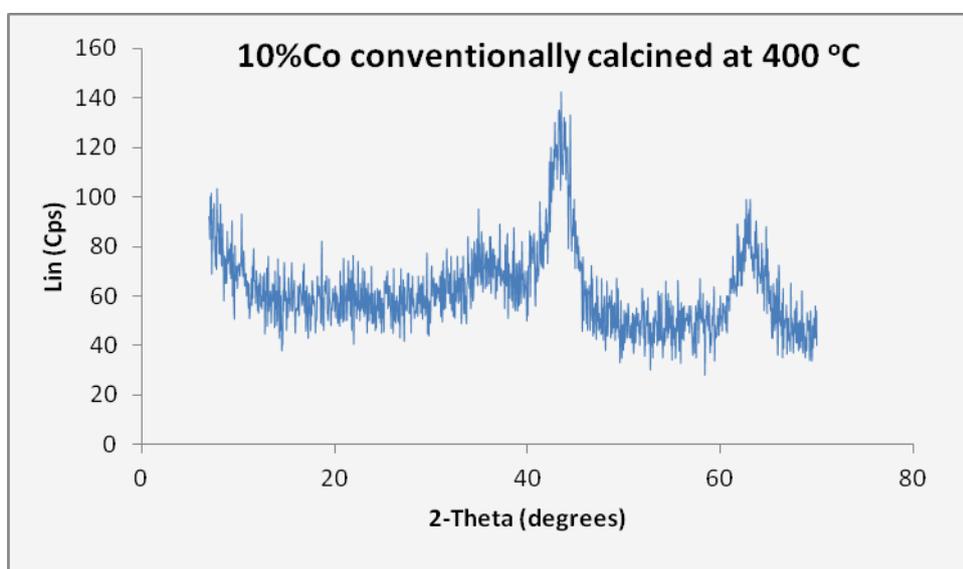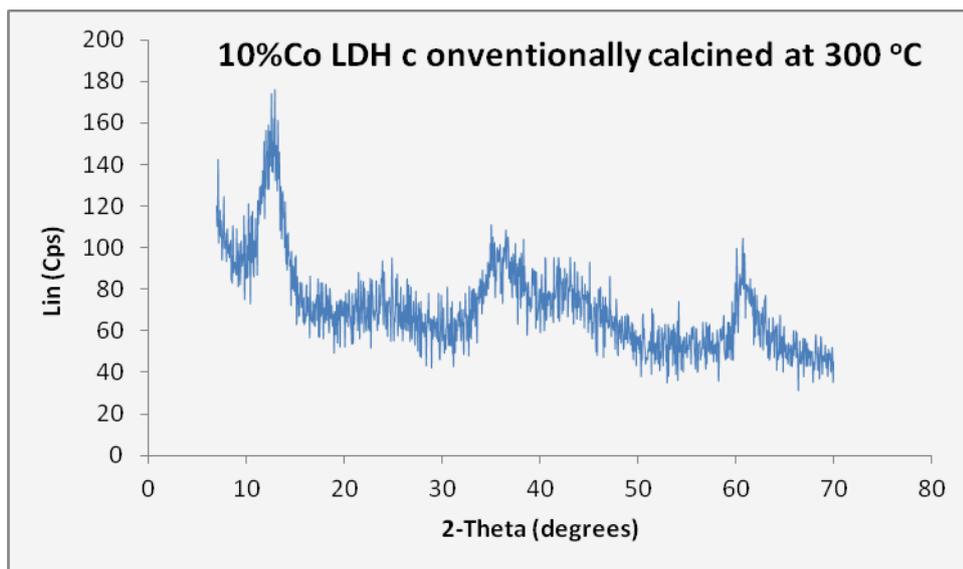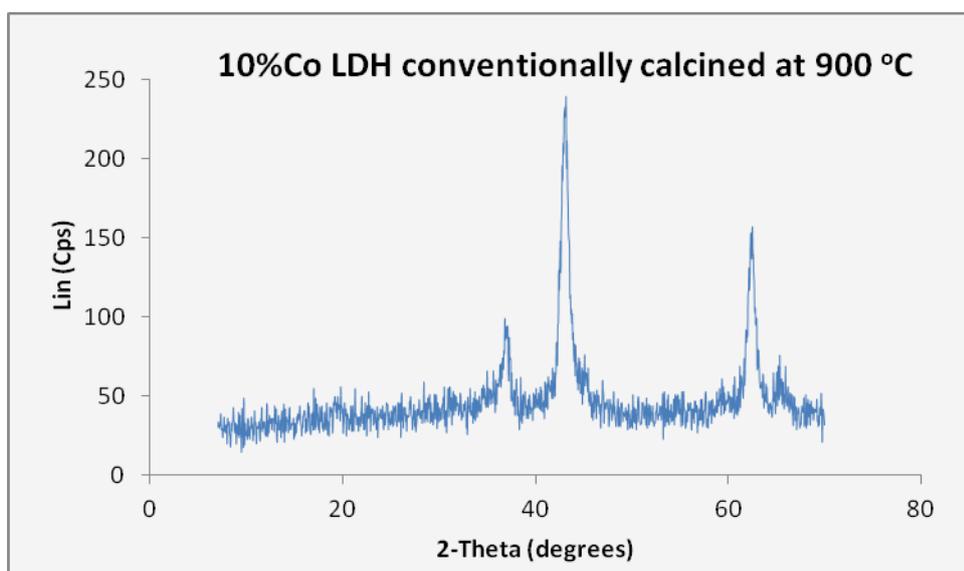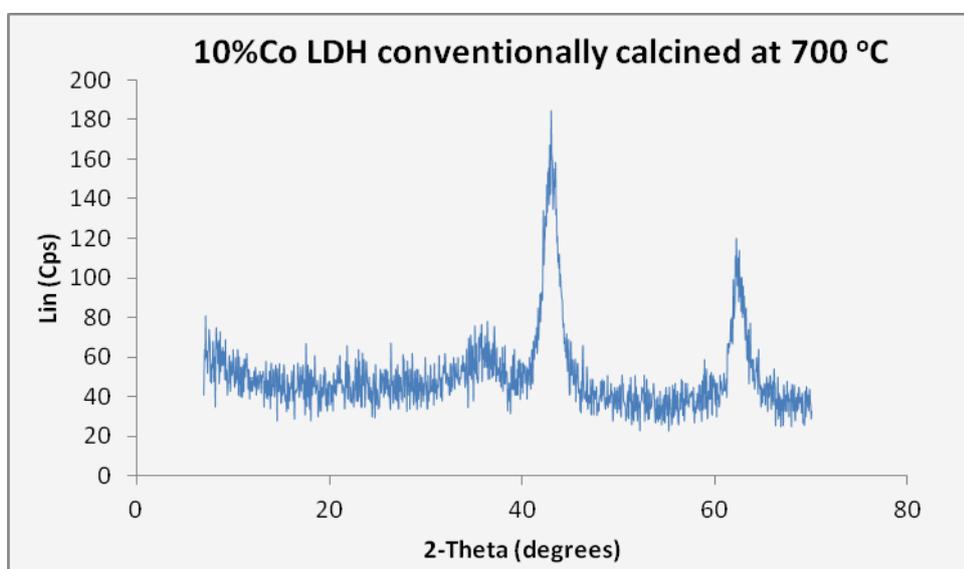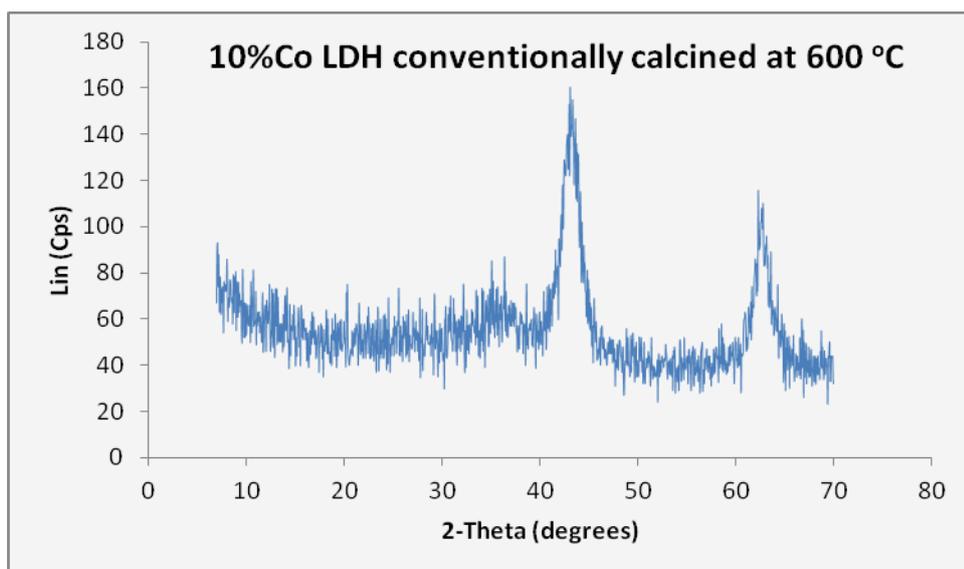
Appendix 6: LDH with Cr conventionally calcined
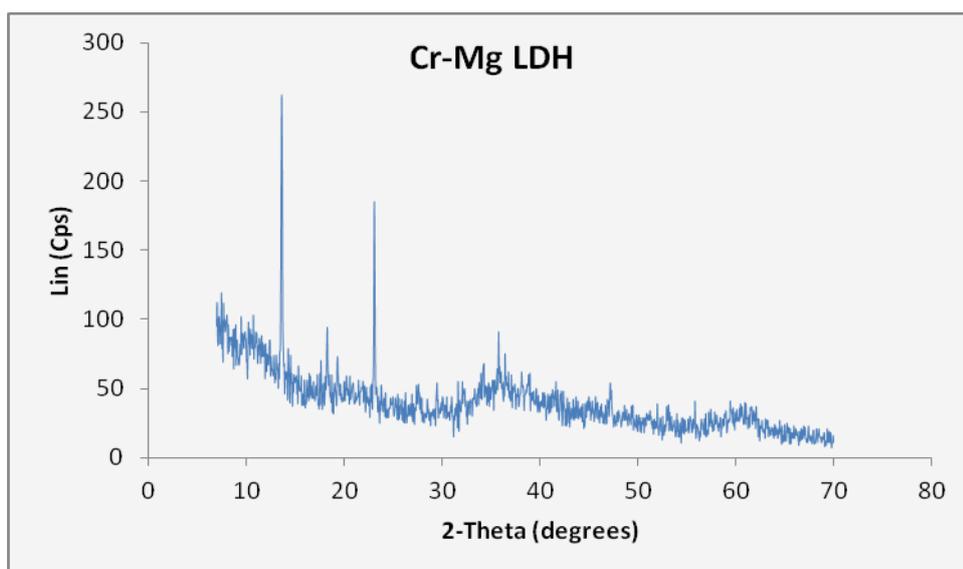
Attempt to replace 100% of Al with Cr
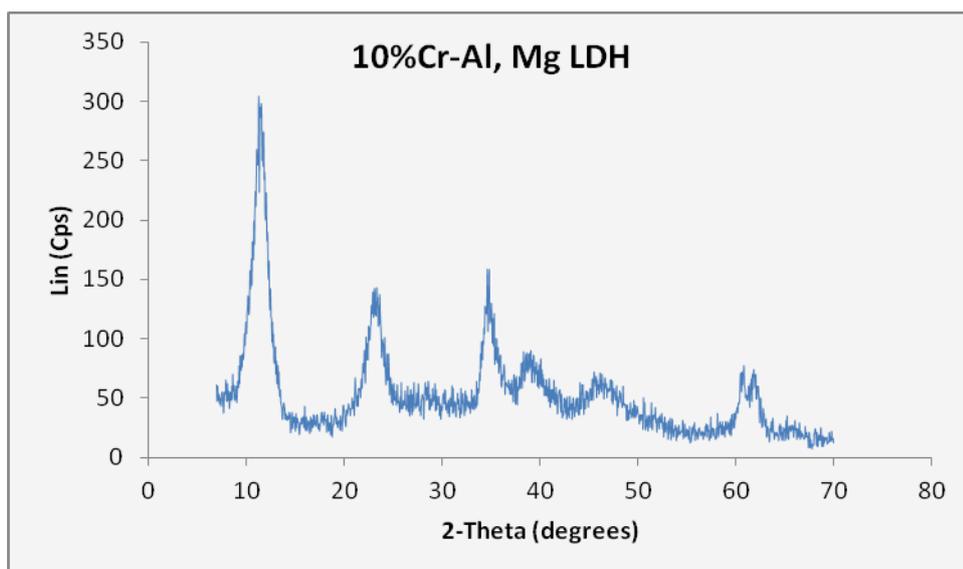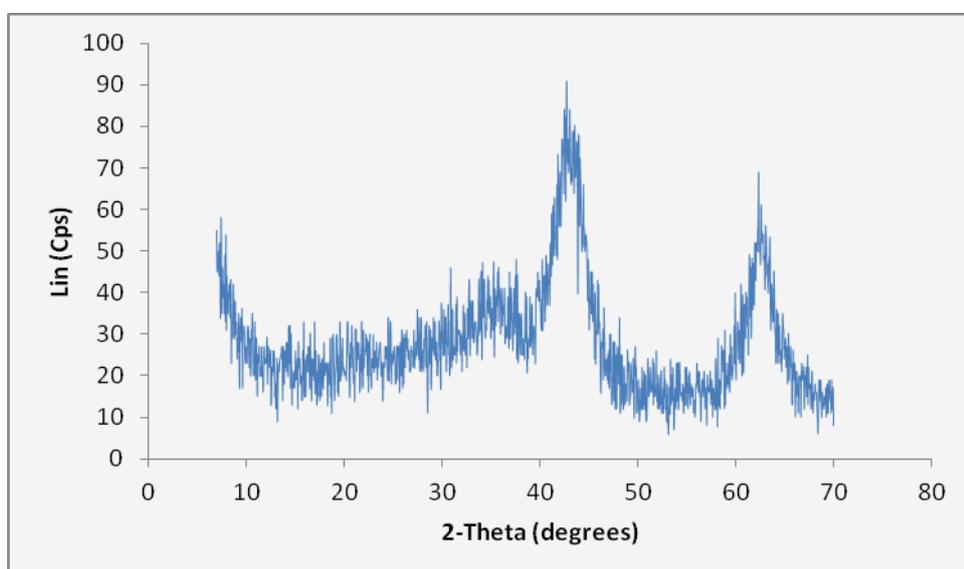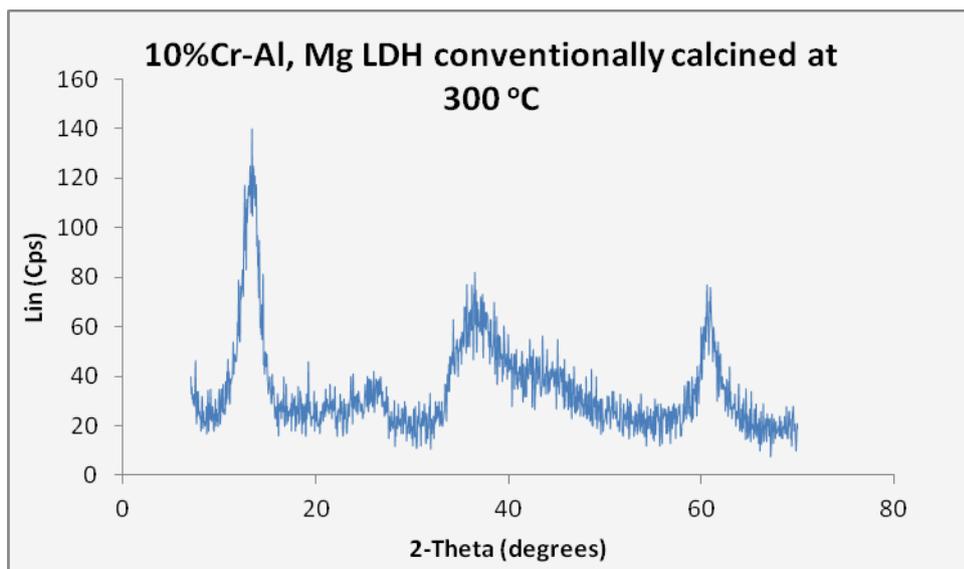
10%Cr-Al, Mg LDH conCal at 400 C

10%Cr-Al, Mg LDH conventionally calcined at 500 °C

10%Cr-Al, Mg LDH conventionally calcined at 700 °C